UNIVERSITI TEKNOLOGI MARA

OPTIMISING THE ACCURACY OF ENERGY DISPERSIVE X-RAY FLUORESCENT (EDXRF) METHOD FOR GOLD ALLOY PURITY MEASUREMENTS

ADLAN AKRAM BIN MOHAMAD MAZUKI

PhD

April 2026

UNIVERSITI TEKNOLOGI MARA

OPTIMISING THE ACCURACY OF ENERGY DISPERSIVE X-RAY FLUORESCENT (EDXRF) METHOD FOR GOLD ALLOY PURITY MEASUREMENTS

ADLAN AKRAM BIN MOHAMAD MAZUKI

Thesis submitted in fulfilment
of the requirements for the degree of
Doctor of Philosophy
(Science)

Faculty of Applied Sciences

April 2026

CONFIRMATION BY PANEL OF EXAMINERS

I certify that a Panel of Examiners has met on 20 January 2026 to conduct the final examination of Adlan Akram Bin Mohamad Mazuki on his Doctor of Philosophy thesis entitled "Optimising the Accuracy of Energy Dispersive X-Ray Fluorescent (EDXRF) Method for Gold Alloy Purity Measurements" in accordance with Universiti Teknologi MARA Act 1976 (Akta 173). The Panel of Examiners recommends that the student be awarded the relevant degree. The Panel of Examiners was as follows:

Noor Najmi Bonnia, PhD
Associate Professor
Faculty of Applied Sciences
Universiti Teknologi MARA
(Chairman)

Ahmad Taufek Abdul Rahman, PhD
Professor
Faculty of Applied Sciences
Universiti Teknologi MARA
(Internal Examiner)

Abu Bakar Sulong, PhD
Professor
Faculty of Engineering and Built Environment,
Universiti Kebangsaan Malaysia
(External Examiner)

PROF DR HJH ZURAEDA IBRAHIM
Dean
Institute of Postgraduates Studies
Universiti Teknologi MARA

Date: 30 April 2026

AUTHOR'S DECLARATION

I declare that the work in this thesis was carried out in accordance with the regulations of Universiti Teknologi MARA. It is original and is the result of my own work, unless otherwise indicated or acknowledged as referenced work. This thesis has not been submitted to any other academic institution or non-academic institution for any degree or qualification.

I, hereby, acknowledge that I have been supplied with the Academic Rules and Regulations for Postgraduate, Universiti Teknologi MARA, regulating the conduct of my study and research.

Name of Student	:	Adlan Akram Bin Mohamad Mazuki
Student ID. No.	:	2019857878
Programme	:	Doctor of Philosophy (Science) – AS 950
Faculty	:	Applied Sciences
Thesis Title	:	Optimising the Accuracy of Energy Dispersive X-Ray Fluorescent (EDXRF) Method for Gold Alloy Purity Measurements
Signature of Student	:	……..
Date	:	April 2026

ABSTRACT

The demand for gold-based transaction products is increasing, driven by the need for faster and more efficient analytical solutions. Conventional methods for determining gold alloy purity, such as fire assay, are destructive, time-consuming, and require complex laboratory-based analysis. The Energy-Dispersive X-Ray Fluorescent (EDXRF) offers a modern, non-destructive alternative to traditional fire assay methods, requiring minimal sample preparation while delivering rapid results. This research examines the role of matrix-specific corrections in enhancing the accuracy of EDXRF analysis for gold alloys. A hybrid approach combining empirical calibration with standardless Fundamental Parameter (FP) methods was employed to enhance the quantification of gold (Au), silver (Ag), and copper (Cu) across a purity range of 75.00 wt.% to 99.99 wt.%. Key challenges addressed include matrix effects (interelement interference), spectral overlaps, and irregular sample geometry, which contribute to measurement inaccuracies. The methodology involved optimizing instrument parameters, refining calibration conditions, standardizing sample preparation, and applying matrix-effect correction factors. To validate the robustness of the optimized EDXRF method, results were compared with fire assay analyses using Certified Reference Materials (CRMs) and commercial gold alloy samples. The study successfully improved EDXRF precision and accuracy through targeted matrix corrections, achieving a near-perfect regression coefficient ($r^2 \approx 0.9999$) for gold calibration curves across all tested metals. Measurement errors were minimized to <0.1% relative error, while relative standard deviations (%*rsd*) were reduced to <0.11% for pure Au, 0.16% for binary Au-Ag/Au-Cu alloys, and <0.20% for ternary Au-Ag-Cu alloys. A Student's t-test confirmed the null hypothesis, demonstrating statistical equivalence between EDXRF and fire assay mean values. Overall, this study has successfully established a robust and optimised EDXRF analytical framework for accurate gold alloy purity measurement, offering a reliable non-destructive alternative to conventional destructive analytical techniques.

ACKNOWLEDGEMENT

All praises are due to Allah the most Gracious and most Merciful. I praise Him and seek for His forgiveness and guidance.

The work presented here would not have been possible without the support, encouragement, teaching, and friendship of many people. Firstly, I would like to express my sincere gratitude to all my supervisors Associate Professor Dr. Mohd Muzamir Mahat, for his continuous support of my Ph.D study, motivation, and immense knowledge. He has not only guided me and encouraged me to carry on through these years and has contributed to this thesis with a major impact but also emotionally through the rough road to finishing this thesis. Thank you as well for guiding me, often with big doses of patience, through the subtleties of scientific writing. I could not have imagined having a better supervisor and mentor for my Ph.D study as well as for my life.

I would like to extend my gratitude to co-supervisor Prof. Dr. Saifollah Haji Abdullah and Associate Professor Dr Rosmamuhamadani Ramli for the stimulating discussions and guidance. Also, I thank all the to Muzamir group members who have always been there, offered me wisdom, and encouraged me; Dr. Faiz, Nazreen, Ayu, Dr. Dania, Ain, Hidayah, Syifa, Anis, Zatul, Arif, Dr. Zharfan. and many more for many helps throughout my PhD.

My sincere thanks go to NMIM & SIRIM Berhad for granting me a scholarship.

Finally, I would like to thank my family, especially my father (Mohamad Mazuki Ariffin), my mother ([redacted]), my father-in-law (Che Ab Malek), my late mother-in-law ([redacted]), my beloved wife (Siti Khadijah Che Ab Malek), my twin daughters (Khairunnisa Busyra & Khairunnisa Badzlin), and my son (Muhammad Umar), who were always at my side, supporting me throughout this Ph.D. journey. I could not thank you enough for your sacrifices, understanding, and unconditional love. I am profoundly grateful for the enduring impact they have had on my life and academic pursuits. They are the driving force behind my achievements, and I dedicate this thesis to them with love and appreciation. To myself, thank you for the resilience and determination that kept me moving forward when circumstances seemed to conspire against my progress. Thank you for the perseverance that endured through setbacks and uncertainties. They remembered me in their prayers for this ultimate success. They are my motivation and keep me stronger in any situation. I consider myself nothing without them. They gave me enough moral support, encouragement, and motivation to accomplish my PhD and my life. This piece of victory is dedicated to both of you. Alhamdulillah's.

TABLE OF CONTENTS

LIST OF TABLES

LIST OF FIGURES

LIST OF SYMBOLS

Symbols

rsd	Residual Standard Deviation
m	The Slope
c	The Intercept of the Y-Axis (C)
y_o	The Observed Response for the Unknown Samples
$\widehat{y_i}$	The Predicted Response for Each Calibration Sample
N	The Number of Measurements of the Response of the Unknown (y_o)
n	The Number of Points in the Calibration Line
z'	Z-Score
wt%	Weight Percentages

LIST OF ABBREVIATIONS

Abbreviations

BAM	Bundesanstalt fuer Materialforschung und -pruefung
CM	Calibration Material
CRM	Certified Reference Material
EDXRF	Energy Dispersive X-ray Fluorescent
FWHM	Full Width Half Maximum
ICP-OES	Inductively Coupled Plasma Optical Emission Spectroscopy
ILC	Interlaboratory Comparison
IMBIH	Institute of Metrology of Bosnia and Herzegovina
KPDN	Ministry of Domestic Trade and Consumer Affairs
LA-ICPMS	Laser Ablation Inductively Coupled Plasma Mass Spectroscopy
LIBS	Laser-Induced Breakdown Spectroscopy
NIST	National Institute of Standards and Technology
NMIM	National Metrology Institute of Malaysia
PT	Proficiency Testing
SIRIM	Standard and Industrial Research Institute of Malaysia

CHAPTER 1
INTRODUCTION

1.1 Research Background

The demand for gold-based transaction products is rising, driven by the need for faster and more efficient solutions. Investing in these products caters to market preferences and enhances transaction speed and reliability (Zhavoronkova et al., 2021). The lasting attraction of gold can be attributed to its intrinsic value, investment potential, and cultural significance. There is a wide variety of gold products available to suit different preferences, desires, and budgets, including gold bars, coins, wafers, and jewelry (Majid & Abdullah, 2019). The recent increase in gold prices has highlighted its value, making it a worthwhile consideration for individuals seeking both investment opportunities and elegant jewelry options (Nordin et al., 2015). For over a century, consumers have recognized that the price of jewelry reflects the true value of its purity, and the quality of the precious metal used. Investing in jewelry means understanding its worth and choosing pieces that will endure in value over time (Nor et al., 2020).

The issue of gold counterfeiting has emerged as a critical concern for researchers, regulatory bodies, and organizations around the globe that are dedicated to fighting fraud in the gold market. This illegal practice can appear in numerous forms, such as jewelry, coins, bars, and other gold products, making it increasingly challenging for consumers and investors to discern authentic gold from its counterfeit counterparts (Nor et al., 2020). Furthermore, counterfeiters may utilize alloys that closely resemble gold in colour and weight, further complicating efforts to identify fakes. The implications of counterfeit gold extend beyond individual transactions and can undermine trust in the gold market. As a result, heightened vigilance and the implementation of advanced detection technologies are essential in safeguarding against these fraudulent practices and ensuring the integrity of investments in gold. The Ministry of Domestic Trade and Consumer Affairs (KPDN) has thoroughly identified separate cases of deceptive activities related to the authenticity of precious metals (KPDN, 2021). Additionally, a bank has reported a loss of RM 72 million because of fraudulent gold collateral. These occurrences underscore a rising concern in the sector, highlighting the need for

heightened awareness to safeguard consumer interests and uphold the standards of precious metals (Nor & Ismail, 2019)

To protect buyers, regulations require legislation that verifies the gold purity of the precious metal in one thousand weight units of the alloy, and this must be marked on the article as hallmarking (Nordin et al., 2015). In Malaysia, the Trade Description Act 2011 (Act 730) plays a crucial role in ensuring quality control and promoting fair trade practices for gold items. This legislation establishes clear standards for the purity of precious metal articles, defining what constitutes authentic gold. It also regulates the terminology and descriptions used during commercial transactions, ensuring that consumers can trust the representations made about these items. By adhering to the standards set by this Act, businesses contribute to a transparent marketplace where customers can make informed decisions based on accurate information about the purity of their gold purchases (Trade Description Act 2011, 2016).

Gold assaying is a crucial procedure in the precious metals industry, aimed at determining the purity and composition of gold samples. This process is essential for evaluating the quality and value of gold, which can significantly affect pricing in the market (Zhitenko, 2013). There are several methods utilized for gold assaying, each suited to different situations and resources. The two most widely recognized and established techniques are fire assay and Inductively Coupled Plasma Optical Emission Spectrometry (ICP-OES) (Mazuki et al., 2021).

Fire assay is considered the gold standard for accurately determining gold content. It involves heating a sample to high temperatures, allowing for the separation of gold from other metals and impurities. This method is renowned for its precision and reliability, making it a preferred choice for many professionals in the industry (Kumar et al., 2018). On the other hand, ICP-OES is a more modern analytical method that provides rapid and detailed information about the composition of the gold sample. By using plasma to excite atoms, this technique measures the emitted light to ascertain the concentration of various elements, including gold. ICP-OES is particularly useful for determining trace elements and provides high-throughput analysis (Chandra Sekhar et al., 2004). Both methods have demonstrated exceptional accuracy in measuring gold purity, making them invaluable tools for jewelers, miners, and assayers alike (Zhitenko, 2013). Depending on the specific requirements of the analysis and available resources, one method may be favoured over the other. However, despite their widespread use, both methods entail inherent disadvantages, such as their destructive nature, reliance on

chemicals, and time-consuming process (Silveira & Falcade, 2022). It will interfere with the integrity of a product and is also impractical for destructive appraisal performed at the place of business where gold transactions in such items are conducted, especially heritage gold and unique samples. (Zhou et al., 2021).

1.2 Motivation of This Work

The demand for non-destructive testing methods, specifically Energy Dispersive X-ray Fluorescent (EDXRF) spectrometry, has significantly increased in various industries, especially within jewellery shops and pawn shops. The International Organization for Standardization (ISO) has recognized the potential of this technique for years. In 2021, the jewellery and precious metals committee (ISO/TC 174) completed standard ISO 23345:2021, which outlines the configuration, calibration, and assay measurement of precious items using bench-top EDXRF instruments, the most common type in this field. These establishments rely on quick and accurate gold transactions to maintain efficiency and profitability. Verifying the authenticity of gold items is vital to prevent losses from counterfeit products (Mazuki et al., 2023)

Furthermore, the EDXRF method produces results rapidly and requires minimal sample preparation. (Navas et al., 2016). This cutting-edge technology is more significant and relevant because it can analyze the various materials used to create completed gold objects and their purity, design, and cultural significance (Bonizzoni, 2015). Silveira & Falcade, 2022 have reviewed the potential of the EDXRF technique in metallic cultural heritage studies. The investigation of historical heritage pieces provides a variety of information that helps historians and archaeologists to identify and catalog the items, and stipulate conditions for storage, conservation, and restoration of the works without damaged samples.

Therefore, this study aims to improve the application of non-destructive testing using the EDXRF method. The goal is to achieve a level of accuracy in measuring the purity of gold alloys that competes with the traditional fire assay method. By exploring the integration of EDXRF with other non-destructive techniques, this research addresses the significant issue of counterfeit gold samples, which can undermine trust in the jewelry market. To achieve these objectives, the study carefully optimized the instrument setup to ensure precise measurements. A major focus has been placed on enhancing the correction for matrix effects (inter-element interactions) that can cause

substantial errors in gold analysis. Through these improvements, the research has successfully established a reliable traceability link between EDXRF technology and the gravimetric method, thereby solidifying the credibility of its findings (Gallhofer & Lottermoser, 2018).

1.3 Problem Statements

Determining the purity of gold alloys is essential in industries such as manufacturing, hallmarking, and precious metal trading. Traditionally, methods like fire assay, Inductively Coupled Plasma Optical Emission Spectroscopy (ICPOES), and other wet chemical analyses have been used for this purpose. While these techniques are well-established, they are inherently destructive, as they require the physical removal, melting, or dissolution of gold samples for laboratory analysis. This means that valuable items can be permanently damaged during testing, which is particularly problematic for high-value or exclusive items (Ghosh et al., 2015). Additionally, conventional methods can be time-consuming and resource intensive. Samples must be sent to specialized laboratories, analysed by skilled personnel, and often involve the use of hazardous chemicals. This not only increases operational costs but also delays decision-making in industrial or commercial settings where rapid verification of gold purity is crucial (Navas et al., 2016).

These limitations underscore the need for an alternative method that is non-destructive, rapid, and reliable. Energy Dispersive X-Ray Fluorescent (EDXRF) has emerged as a promising solution, allowing for in-situ analysis without physically altering or destroying the sample. By providing immediate and accurate measurements of gold alloy composition, EDXRF overcomes the shortcomings of traditional methods and offers significant advantages in terms of sample preservation, cost efficiency, and operational practicality (Silveira & Falcade, 2022).

A critical challenge has been identified based on the current review of the EDXRF analysis regarding the accuracy of gold purity measurement. Despite being widespread among companies, EDXRF is still not used for fineness measures in ordinary jewellery companies, and is routinely used to qualitatively check the composition of unknown samples (Zhitenko, 2013). This analysis technique is viewed with suspicion by quality control operators because it is considered unreliable or

inaccurate compared to the more traditional fire assay. It is often used to monitor the produced items, but is always accompanied by control measurements performed by cupellation (Jotanović et al., 2012). A share of this uncertainty can certainly be attributed to the relatively recent development of these faster instrumentations capable of performing delicate fineness measurements, but also to the scarcity of studies and procedures describing the correct approach for this measurement method, despite some exceptions (Gallhofer & Lottermoser, 2018).

According to ISO 23445 for jewellery and precious metals - non-destructive precious metal fineness confirmation by ED-XRF, before conducting each batch analysis, a verification procedure shall be performed by analysing the certified reference material (CRM). The CRM should be analysed at a minimum of five different positions. The analysis time for each replicate must not exceed the time used for calibration. Validation by comparing the purity measured for the CRM (based on the mean value of the analyses) with its certificate value. The difference (Δ) between these two values should not exceed 0.12 wt% of the main element and will be considered in the uncertainty evaluation of the method. If the differences of the measurements between the purity measured for the CRM and its certified value falls outside the specified tolerances, the method of calibration should be repeated. The CRM should also be analysed at regular intervals to monitor the stability of the instrument under consistent conditions (ISO 23345, 2021).

Furthermore, the lack of traceability raises concerns about the reliability of the EDXRF method, especially in gold purity measurement analysis. Without established benchmarks, the EDXRF cannot be properly validated, leading to measurement inconsistencies. This can undermine regulatory compliance, quality control, and consumer trust. To enhance the credibility of EDXRF methods, it is crucial to develop specific matrix calibration materials that provide a reliable analysis baseline.

Therefore, addressing these calibration dependencies is crucial for enhancing the reliability of EDXRF as a method for evaluating gold purity (Conrey et al., 2014). The intensity of the measured fluorescence signal is influenced by several factors. While the concentration of the analyte is a primary determinant, other elements within the sample matrix can also play a significant role. Additionally, the physical form of the sample, the methods used in sample preparation, and the specific conditions under which the measurements are conducted further impact the fluorescence signal. Understanding these contributing factors is essential for accurate analysis and interpretation of results

(Artyukh et al., 2018). Adapting the tuning of the equipment setup and applying the optimum matrix effect correction to analyze the data is one method for obtaining accurate results (Mazuki et al., 2023)

1.4 Research Objectives

The primary objective of the study is to enhance the accuracy of gold alloy purity measurement by optimising the Energy Dispersive X-Ray Fluorescent (EDXRF), serving as a viable alternative to conventional destructive fire assay methods. The specific objectives are:

a. To fabricate a series of gold-silver-copper calibration materials for EDXRF accuracy measurement.
b. To optimise the tuning configuration of the EDXRF method for higher accuracy of gold alloy analysis.
c. To validate the tuned EDXRF method through interlaboratory comparison (ILC).
d. To establish the reliability of the EDXRF method for gold alloy purity analysis.

1.5 Research Questions

i. What are the main sources of error in EDXRF when measuring the purity of gold alloys, and how can these errors be minimized?
ii. How does the choice of calibration model (e.g., standard addition, external calibration) affect the accuracy of gold alloy purity measurements using EDXRF?
iii. What is the impact of matrix effects (such as sample composition and thickness) on the accuracy of EDXRF measurements for determining the purity of gold alloys?
iv. How can the use of Certified Reference Materials (CRMs) and traceability to international standards improve the reliability and accuracy of EDXRF measurements for gold alloy purity?

1.6 Research Hypotheses

a. Optimized calibration using specific matrix gold calibration materials will significantly improve the accuracy and precision of EDXRF measurements for gold alloy purity across various compositions.
b. Implementing matrix correction methods will effectively minimize the interference effects of other alloying elements (e.g., silver, copper) in gold alloys, thereby enhancing the reliability of EDXRF purity measurements.
c. Optimising surface preparation techniques will reduce measurement variability in EDXRF analysis of gold alloys, particularly for samples with surface irregularities or coatings.
d. Controlling environmental conditions (such as temperature and humidity) will reduce variability in EDXRF gold purity measurements, particularly in portable and field applications.
e. Enhancing the calibration method and matrix correction will yield gold purity measurements comparable in accuracy to traditional methods like fire assay

1.7 Scope and Limitations of Study

The study will focus on enhancing the accuracy of the EDXRF method for measuring the purity of gold alloys. The scope includes evaluating various factors that can impact the accuracy of gold purity measurements using the EDXRF method, such as calibration methods, instrument settings, sample preparation, matrix effects, and potential interference from other metals in the alloy. It will also evaluate the performance-enhanced method and the impact of calibration techniques on the reliability of the results. Due to the high cost of the materials and lack of sources of the certified reference materials, this study has set a limit to the common yellow gold alloy matrix, consisting of an Au-Ag-Cu mixture with gold purity ranging from 75.00 wt.% to 99.99 wt.%, which will be used as the study material. The parameters of the EDXRF method that will be adjusted include optimisation of collimator beam sizes and peak spectrum selection.

1.8 Significance of the Study

This study is significant to establish an optimized Energy Dispersive X-ray Fluorescent (EDXRF) method as a fast, accurate, and efficient tool for measuring the purity of gold alloys. By overcoming the limitations of conventional destructive methods, this approach reduces analysis time from at least three hours to just a few seconds while delivering measurement accuracy comparable to the fire assay method, with a deviation of less than 0.1 wt%. Importantly, it preserves the integrity of valuable samples. The findings provide a reliable, cost-effective, and sustainable solution for industries such as jewellery stores, pawn finance agencies, and government regulatory bodies, enabling faster quality assurance and compliance processes. Additionally, this study seeks to establish the traceability and reliability of EDXRF measurements according to the International System of Units (SI), which supports fair trade and enhances confidence in gold transactions. Beyond the gold industry, the innovations from this research have applications in fields such as archaeology and heritage artifact analysis, where accurate, non-destructive evaluation is critical for preservation. Overall, this study not only addresses the immediate challenges of measuring gold purity but also lays the groundwork for broader applications of the EDXRF technique across multiple disciplines.

1.9 Thesis Outline

Chapter 1 discusses the importance of the EDXRF method in accurately measuring gold alloy purity, essential for industries like jewelry, pawn, and investment. It highlights challenges in achieving high accuracy and sets objectives to optimize the EDXRF method for better precision in gold analysis. The chapter also outlines key research questions and emphasizes the study's practical applications and significance.

Chapter 2 reviews the fundamentals of the EDXRF method, highlighting its principles, advantages, and limitations in elemental analysis. It specifically examines EDXRF's application in precious metal analysis, comparing it to other alloy composition methods. The chapter discusses factors affecting the EDXRF method accuracy, including instrumental and environmental influences, as well as existing calibration techniques. It concludes by identifying gaps in current research, indicating opportunities for improving EDXRF accuracy in gold alloy measurements.

Chapter 3 describes the research design, detailing the experimental setup and materials of gold alloy samples. It focuses on calibration techniques to improve the EDXRF method accuracy while minimizing errors. The chapter also discusses the optimization of hardware, software, and environmental controls, along with data collection methods and statistical analysis procedures to assess accuracy improvements. Additionally, it evaluates the optimized EDXRF results against other methods used for measuring gold purity, providing reliability and ensuring traceability assessment of performance.

Chapter 4 reported the results related to the research objectives, focusing on how tuning techniques affect the EDXRF method accuracy. We discuss the practical implications of these findings for industrial applications requiring reliable gold purity measurements. We also acknowledge study limitations and suggest ways to address them in future research, along with recommendations for enhancing the EDXRF method accuracy through technological and methodological advancements.

Chapter 5 concludes the current findings and provides suggestions for future work required to further advance the performance of the EDXRF method.

CHAPTER 2
LITERATURE REVIEW

2.1 Gold

Gold, silver, platinum, and palladium are types of precious metals. However, gold is one of the world's most precious commodities, and gold remains a secure investment (Nordin et al., 2015). Gold is a chemical element in the periodic table with the symbol Au for Aurum in Latin. The atomic number is 79, with a density of 19.0 g/ml. For centuries, it continued to be a safe investment for most people. Gold plays a dominant role in the jewelry market. This is largely due to the intrinsic value of gold, its beauty, and its unique resistance to stains and corrosion (Majid & Abdullah, 2019). The design of rust gold alloy is studied not only for high purity gold exceeding 22 Karat but today, lower grades such as 18 Karat gold is gaining popularity because of its yellow cluster, versatility, and value for a mortgage. (Klotz et al., 2017).

Pure gold or 24K gold means that the 24 parts of the gold are pure gold. While gold with 916 or 22K gold means that 22 parts of the gold are pure gold and the remaining parts are possibly some other metal, such as copper, silver, zinc, nickel, and palladium (Zhitenko, 2013). Purity can also be determined in weight percentages (wt %). Pure gold or gold 999 consists of 100 wt % pure gold (practically 99.9 wt %). Therefore, for gold 916 out of 100, only 91.67 wt % of pure gold, and the balance possibly consists of 2 or more elements in the metal alloys. The calculation will also be applied to the lower grade of gold. Karat is the unit of measurement for the proportion or percentage of gold in an alloy, with the abbreviation K or kt. It is based on the ratio of the pure gold to the total metal present by weight but divides the total present into 24 parts. Thus, each karat is 1/24 of the whole. The reduced Karat number represents the reduced percentage of pure gold (Mohamed et al., 2016). Table 2.1 shows typical Karat values and their equivalent measures in part gold to alloy, percentages, fineness, normal European Stamping, and normal American Stamping.

Table 2.1
Gold Purity/Karat Information Chart

Karat Gold	Percentage gold	Fineness	Normal European Stamping	Normal American Stamping
9K	37.50 wt %	375	375	-
10K	41.67 wt %	417	416	10K
12K	50.00 wt %	500	500	-
14K	58.33 wt %	583	582 or 585	14K
18K	75.00 wt %	750	750	18K
22K	91.67 wt %	916	917	-
24K	99.9 wt %	999 or 9999	999 or 99999	24K

Pure gold is inherently too soft for jewellery, so it is alloyed with other metals to enhance its strength and durability for daily use. This combination of alloys can yield a variety of colours, including yellow, white, red, rose, etc. (Corti, 2004)(Ortega-Feliu et al., 2007). In Malaysia, most items accepted by pawnshops are jewellery with gold purities of 18 karats, 22 karats, and 24 karats (Azizah Othman, 2013). Additionally, gold bars and coins represent popular investment options in the country (Yaacob, 2012). A gold bar, often referred to as gold bullion or a gold ingot, consists of a quantity of refined gold shaped according to established standards, complete with proper labelling and record-keeping. Figure 2.1 shows a certificate of a gold bar, which typically features markings that indicate its purity, weight, serial number, and the manufacturer's name. The Trade Descriptions Act 2011 (Act 730), established in Malaysia, aims to promote fair trade practices by prohibiting false trade descriptions and misleading statements in the supply of goods and services. Furthermore, all gold products in Malaysia must undergo analytical testing to ascertain their purity, helping to combat counterfeit gold in the market, which possesses a high acceptance rate for leasing by pawnshops.

Figure 2.1 Gold Bar with a Certificate of 999.9 Fineness

2.2 Silver

Silver is a chemical element with the atomic number 47 and the symbol Ag. The transition metals group of the periodic table contains this white, glossy metal. Due to its appealing look, malleability, and superior electrical and thermal conductivity, silver has been known to humans for thousands of years and has been employed in various products. Silver has a shining, white colour and is a soft, pliable metal. Although it is resistant to oxidation and corrosion, exposure to air and some chemicals can cause tarnish over time. Silver is utilized in a wide range of fields and industries. Due to its aesthetic appeal, it is most frequently used in jewellery and ornamental products (Mozgai et al., 2021).

Figure 2.2 Pure Silver (Ag) with 999.9 Fineness

Throughout history, silver has been used as a store of value and a type of currency. It is regarded as a valuable metal. Some individuals still think of it as a valuable investment. On commodities markets, silver coins and bars are exchanged and sought by investors and collectors. Silver alloys are frequently used to improve the characteristics of silver. For instance, the alloy of sterling silver has 92.5% silver and 7.5% copper. Because it offers endurance and strength while preserving the appealing look of silver, this alloy is frequently used in jewellery and silverware. Additionally, silver may be alloyed with other metals to provide specialty materials for use. Figure 2.2 shows a pure silver (Ag) bar 999.9 fineness produced by the Royal Canadian Mint.

2.3 Copper

Copper has the chemical symbol Cu and the atomic number 29. It is a soft, malleable, and ductile metal that belongs to the transition metals group of the periodic table. Because of its superior electrical and thermal conductivity, as well as its corrosion resistance and appealing look, copper has been utilised by humans for thousands of years. Copper has a reddish-orange colour with a vivid metallic luster. It is a soft metal that is very malleable and ductile, which allows it to be readily molded and formed into wires. It is also corrosion resistant, particularly when exposed to air and moisture, and develops a protective greenish patina over time. Copper is popularly used as a mixture in the manufacturing of jewelry products (Kraut & Stern, 2000).

Figure 2.3 Pure Copper (Cu) with 999 Fineness

Copper is frequently alloyed with other metals to improve its qualities or to produce new materials. Bronze, for example, is a copper-tin alloy noted for its strength, corrosion resistance, and historical importance. Brass is another popular copper alloy that combines copper and zinc. Brass is praised for its visual appeal, low-friction qualities, and corrosion resistance. Copper alloys are used in a variety of applications, including musical instruments, electrical connections, and maritime applications (Buccolieri et al., 2021). Copper is a very valuable metal with a wide range of practical uses across sectors due to its outstanding conductivity, corrosion resistance, and adaptability. Its historical relevance, health advantages, and aesthetic appeal add to its prominence in human civilization. Figure 2.3 shows a pure copper (Cu) with 999 fineness.

2.4 Gold Alloy

Gold alloy products have enchanted people for thousands of years. Hues and colours are only variations of the same artistic theme of beauty and brilliance. Gold will always be distinctive due to its unique yellow colour, but the need for diversity and originality will cause some of the coloured gold alloys to remain in fashion. New designs and ideas will certainly arise, and with today's knowledge and technologies, new solutions will most likely be found for the challenges posed by some of the coloured gold alloys. Table 2.2 shows a comparison of the properties of gold (Au), silver (Ag), and copper (Cu).

Table 2.2

Comparison of the Properties of Gold, Silver, and Copper

Properties	Gold (Au)	Silver (Ag)	Copper (Cu)
Density (g/cm³)	19.32	10.49	8.96
Melting Point (°C)	1,064	961.8	1,085
Boiling Point (°C)	2,856	2,162	2,567
Electrical Conductivity (S/m)	Very High (45.2×10^6)	High (63.0×10^6)	Very High (59.6×10^6)
Thermal Conductivity (W/m·K)	315	429	398
Hardness (Mohs Scale)	2.5	2.5	3.0
Color	Yellow	White/Gray	Reddish-Brown
Corrosion Resistance	Excellent	Moderate	Moderate
Tensile Strength (MPa)	120–190	170	210–250

The three materials which gold (Au), silver (Ag), and copper (Cu) exhibit closely aligned melting points, which makes them particularly compatible for blending into a gold alloy. This alloying capability enhances their physical properties, such as durability and color, making it ideal for various applications. The Au-Ag-Cu system is widely recognized as one of the most prevalent formulations in the creation of gold jewelry and dental alloys used in modern practices. Remarkably, this combination has a rich history that spans several millennia, tracing back to ancient civilizations that recognized the aesthetic and functional benefits of alloying gold with silver and copper. This longstanding tradition highlights the enduring appeal of these materials in both decorative and practical applications.(Kraut & Stern, 2000). Colour variations of yellow, red, and green can be obtained by different ratios of Au-Ag-Cu. Alloying additions to this system are also used to improve properties like castability and hardness. A multitude of hues and colours can be obtained in the Au-Ag-Cu system alone by variation of composition as shown in the ternary phase diagram in Figure 2.4. Additions of copper give a reddish tint to the alloy, and additions of silver make the alloy greenish (Cretu & Van Der Lingen, 1999).

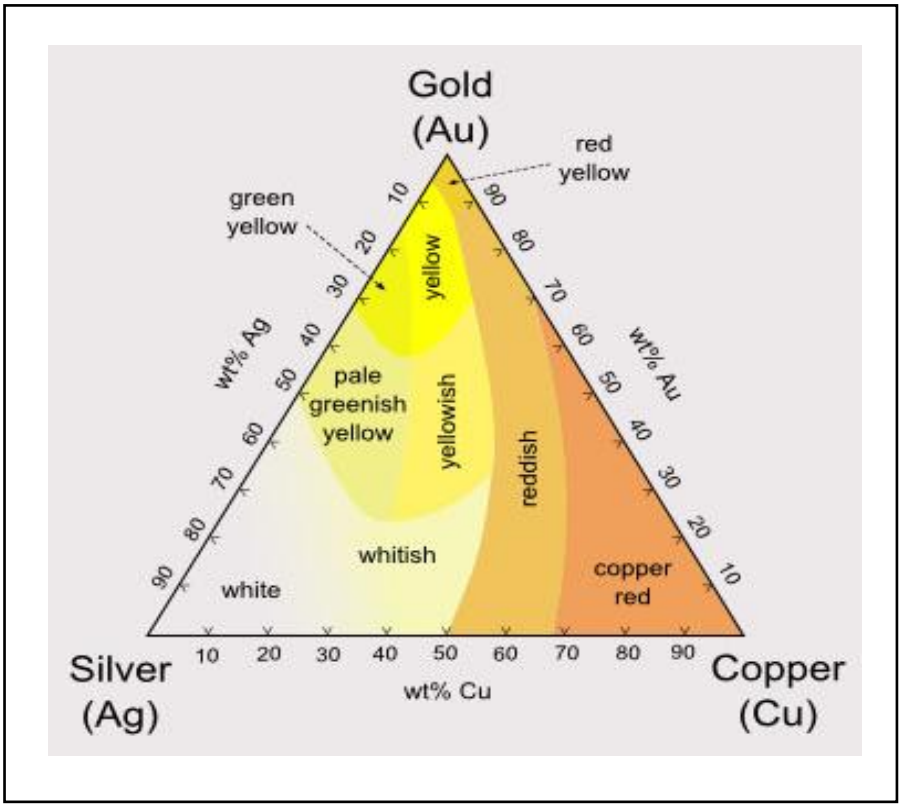

Figure 2.4 Relationship between Colour and Composition in the Au-Ag-Cu System

As well as affecting physical properties, alloying gold generally increases its strength and hardness, with some reduction in malleability/ductility. The silver atom is slightly larger than that of gold, so alloying gold with silver gives a moderate improvement in strength and hardness. The copper atom is significantly smaller than that of gold, and so it has a greater effect on strengthening gold than silver, as it distorts the gold crystal lattice more (Corti, 2004). Thus, reducing karat (K) from 24 karats to 22 karats, down to 18 karat gold, results in stronger and harder alloys. However, at any given mixture, the actual gold content values (karat) vary according to the relative silver and copper contents. Therefore, the accuracy in determining the other alloys in the mixture is well considered (Artyukh et al., 2018).

2.5 Gold Purity Measurement Method

Inaccurate gold purity measurement increases the risk of counterfeiting and fraud, which can lead to financial losses and harm the economy. There are several methods available for determining the purity of gold, and these can be broadly divided into two categories: destructive and non-destructive techniques. Each method presents unique benefits and drawbacks, and the selection of the most appropriate technique often depends on the specific requirements of the analysis being conducted. A comparison of various analytical methods for assessing gold purity can be found in Table 2.3, which summarizes findings from previous studies.

Destructive methods such as fire assay, ICP-OES, and potentiometric titration yield highly accurate results for high-purity gold but require sample destruction and complex procedures, making them suitable for scenarios where precision is critical. In contrast, non-destructive methods such as EDXRF, LIBS, and LA-ICPMS preserve sample integrity and are useful for rapid, on-site testing, although they generally have higher uncertainties, especially with lower-purity alloys. EDXRF is the most used non-destructive method due to its ability to accommodate a wide range of purities and maintain relatively low uncertainty with empirical calibration, although it requires numerous standards that closely match real samples (Mazuki et al., 2023).

Table 2.3
Comparison of analytical methods for gold purity measurements

	Method	Au Content wt.%	Expanded uncertainty, u wt.% (k=2)	References
Destructive method	Fire Assay (Cupellation)	33.3 - 99.0 (yellow gold)	0.05	Jotanović et al., 2012
	ICP-OES	99.9 and higher	0.02	Manchanda, 2011
	Potentiometric titration	38.5 - 91.7	0.008	Caporali et al., 2010
Non-Destructive method	LA-ICPMS	60 - 80	0.8–4.1	Zhitenko, 2013
	LIBS	75 - 99.8	0.8	Anggraini et al., 2020
	EDXRF	40 – 60 Fundamental Parameter (FP-standardless)	0.8 – 2.5	Silveira & Falcade, 2022
		33 – 98 Empirical (with standard)	0.31	Artyukh et al., 2018

2.5.1 Fire Assay (Cupellation) Method

Conventionally, the purity of gold alloy articles is appraised using the fire assay (cupellation method) as follows, according to the international standard method ISO 11426 (Jotanović et al., 2012). The assay chemically separates gold content through cupellation from the whole material. The second step requires the application of a high accuracy weighing scale to determine the percentage of gold content. Due to its unparalleled accuracy, Artyukh et al., (2018) stated that the fire assay method is popular among the member countries of the International Convention. Battaini et al. (2014) echoed the same statement by adding that the fire assay method is still practiced among goldsmiths. Despite its widespread use, the fire assay method comes with a few inherent disadvantages, such as its destructive nature (Jotanović et al., 2012), reliance on chemicals (Artyukh et al., 2018), and time-consuming process (Li et al., 2015). Table 2.4 shows the high accuracy of cupellation methods on the determination of gold content (Zhitenko, 2013).

Table 2.4
An Existing International Standard for Fire Assay Methods

Standard	Method	Principle	Au Content, wt %	U, wt % ($k = 2$)
ASTM E1335-08, 2017	Standard test methods for determination of gold in bullion by cupellation	Fire assay (cupellation)	20.0–99.8	0.05–0.08
			98.9–99.8	0.053
ISO 11426, 2021	Determination of gold in gold jewellery alloys–Cupellation method (fire assay)	Fire assay (cupellation)	33.3–99.0 (yellow and red gold)	0.05
			58.5–75.0 (white gold)	0.10
			99.0 and higher	0.02

Figure 2.5 A process of cupellation in the furnace to melt the gold alloy samples

Figure 2.5 shown a fire assay method performed at a temperature of 1050°C in a furnace and a cupel furnace area, to melt the gold alloy sample. This high temperature was specifically selected to ensure the homogeneous melting of gold and its alloying elements, particularly silver and copper. Tightly controlled furnace temperature is required for the various metals in the alloy to be melted simultaneously, so they're mixed uniformly (Zhitenko, 2013). An overview of each step in the cupellation method is shown in Figure 2.6 outlining the processes that need to be taken to get the best results for extracting pure gold from its alloys.

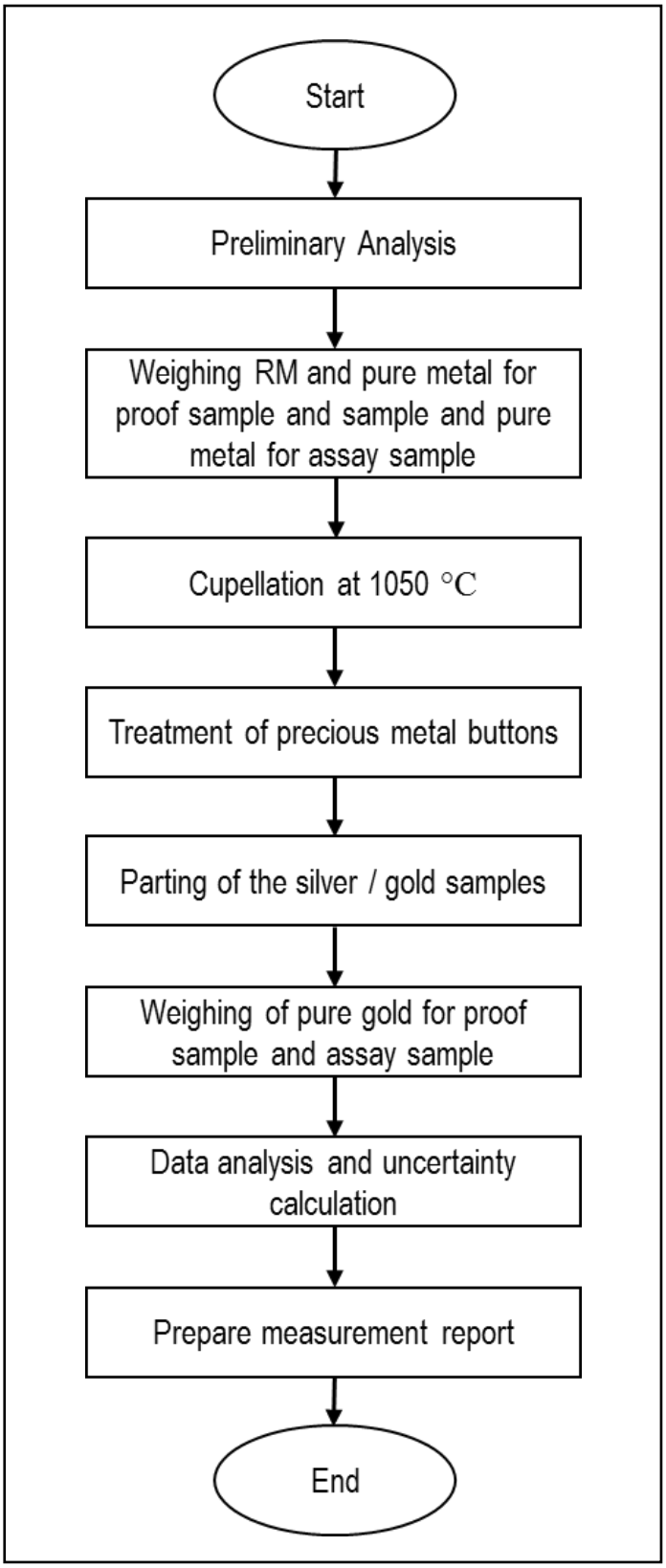

Figure 2.6 Flow chart on the procedure for the determination of gold content by the fire assay method

2.5.2 Inductive Coupled Plasma Optical Emission Spectroscopy

The purity of precious metals is the main factor for their monetary value. Therefore, it needs to be most accurately determined when trading precious metal products, whereby contents of up to 99.99 wt% are determined with Inductive Coupled Plasma Optical Emission Spectroscopy (ICP-OES) following the international standard method (ISO 15093:2020). Figure 2.7 shows an ICP-OES spectrometer. The ICP-OES method can be perfectly used for the analysis of impurities in precious metals, and the purity of the precious metal is calculated by subtraction of all measured impurities. Due to its multi-element capability, large linear dynamic range, and high sensitivity. It is the recommended analytical procedure for the analysis of contamination traces in high-purity gold. Table 2.5 shows the international standard ICP-OES methods in determining precious metal (Zhitenko, 2013).

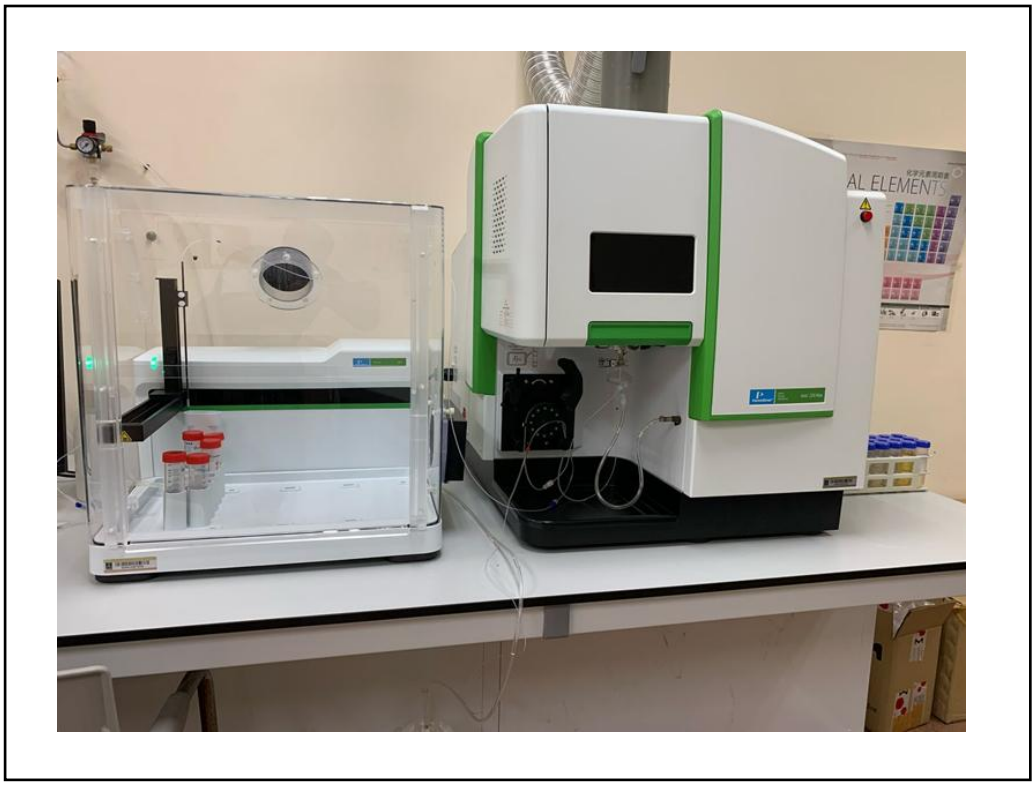

Figure 2.7 The ICP-OES Spectroscopy

Table 2.5
An International Standard for ICP-OES Methods for Precious Metals

Standard	Method	Principle	Precious Metal Content, wt %	U, wt % (k = 2)
ISO 15093, 2020	Jewellery–Determination of precious metals in 999 ‰ gold, platinum, and palladium jewelry alloys–Difference method using inductively coupled plasma optical emission spectroscopy (ICP-OES)	The samples of the precious metal alloy are weighed and dissolved in aqua regia to prepare a 10 g/l solution. The impurities are determined by inductively coupled plasma optical emission spectroscopy (ICP-OES), and the precious metal content is obtained by subtraction of the total content of impurities in the sample from 1 000 ‰	Au, Pt, Pd 99.9	0.02
ISO 15096, 2020	Jewellery - Determination of Silver In 999 0/00 Silver Jewellery Alloys - Difference Method Using Inductively Coupled Plasma Optical Emission Spectroscopy (ICP-OES)	The samples of the silver alloys are weighed and dissolved in nitric acid to prepare a 10 g/l solution. Hydrochloric acid is added to precipitate the silver. The solutions are filtered to separate the silver chloride. The impurities are determined in the filtrate by inductively coupled plasma optical emission spectroscopy (ICP-OES), and the silver content is obtained by subtraction of the total content of impurities in the sample from 1 000 ‰	Ag 99.9	0.02

The principle of the ICP-OES method is determining the impurities, and the precious metal content is obtained by subtraction of the total content of impurities in the sample from 100 %. Limit for high purity, and not suitable for gold alloy. The Figure 2.8 show a flow chart of determination of elements in liquid and solid sample using standard addition ICP-OES. Due to the nature of ICP-OES is destructive method, and involved a tidies chemical preparation, the non-destructive X-ray Fluorescent (XRF) method has been popular as an alternative to determine gold purity (Shah & Yaacob, 2018).

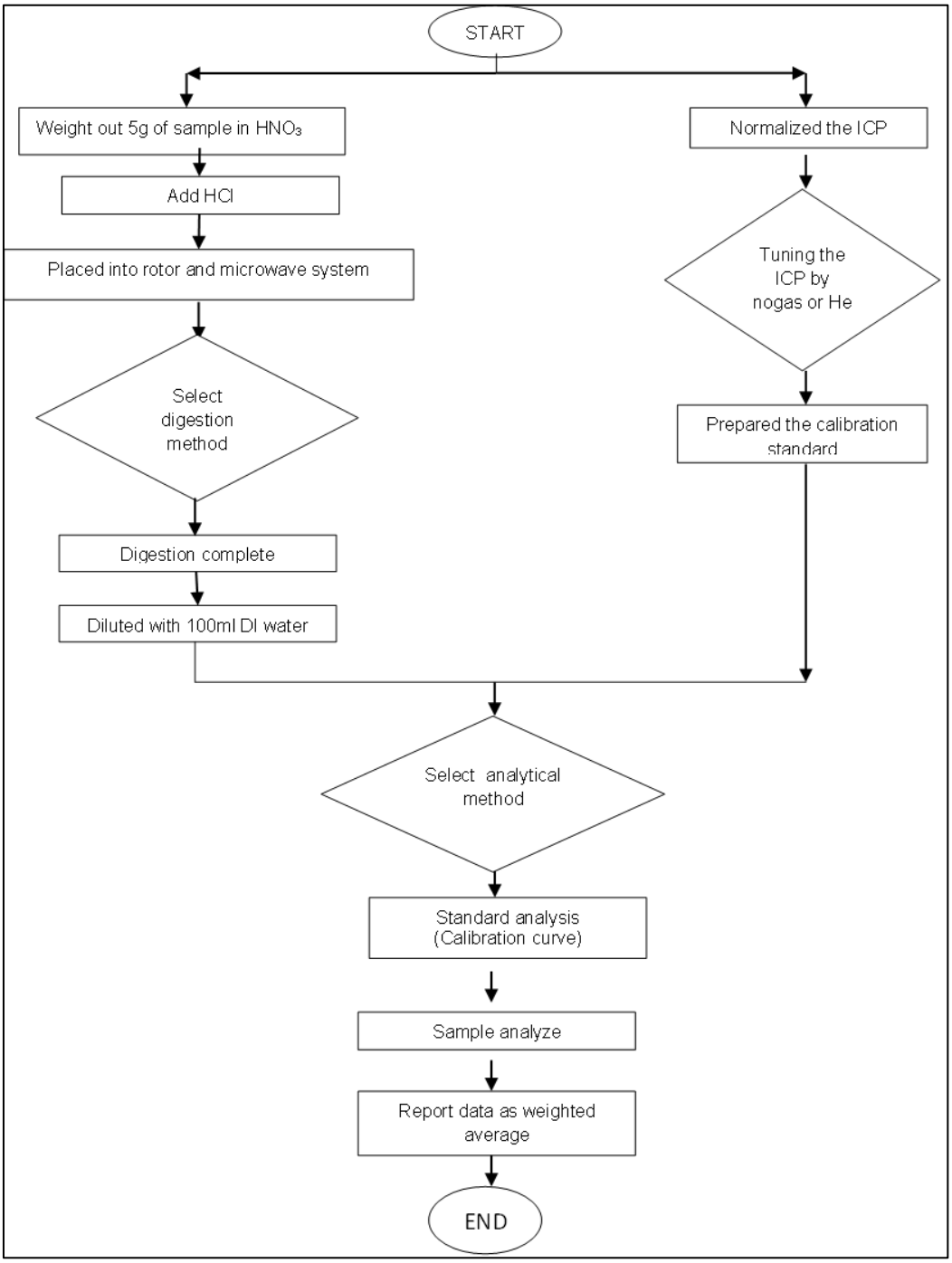

Figure 2.8 Flow Chart of the Determination of Elements in Liquid and Solid Samples Using the Standard Addition of the ICP-OES Method

2.5.3 X-Ray Fluorescent (XRF) Spectrometer

X-ray Fluorescent (XRF) has become the best alternative to the traditional fire assay procedure due to its good accuracy of less than 0.5 wt % error. In the last few

years, the performance of this method has increased (Zhitenko, 2013). There are also a method that finds service in jewelry manufacturing and gold assaying laboratories for anti-fraud control (Abdullah et al., 2015). The ability to rapidly test results, non-destructive methods, easier sample preparation, and full scan of precious metals content in a variety of sample materials make it a valuable and popular tool for gold buyback organizations and pawnbrokers (Navas et al., 2016). XRF is a technique based on the photoelectric effect. Figure 2.9 shows a benchtop type of XRF spectrometer used on the market to determine gold purity.

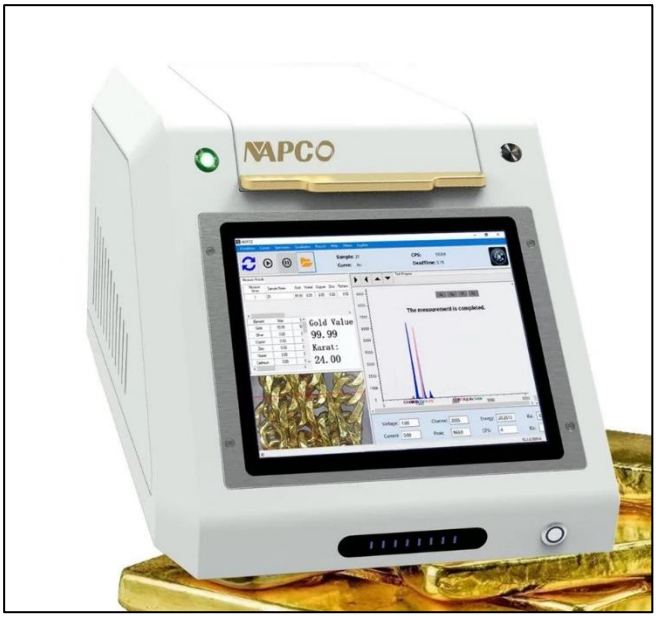

Figure 2.9 A Type of Benchtop XRF Spectrometer on the Market

The commissions within the International Organization for Standardization (ISO) have long acknowledged the potential of this approach, and in 2021, the technical committee for jewelry and precious metals (ISO/TC 174) finalized the development of standard ISO 23345:2021, which specifically addresses how to set up, calibrate, and perform assay measurements on precious items using a bench-top energy dispersive X-ray fluorescent (ED-XRF) instrument, the most common type of instrument utilizing this analytical method (ISO 23345, 2021).

2.5.3.1 Fundamental Principle of XRF Spectrometer

The fundamental principle of XRF spectrometry is based on the interaction of high-energy X-rays with matter, leading to the emission of secondary X-rays (fluorescence) from the sample, shown in Figure 2.10. a) An electron in the K shell is ejected from the atom due to an external primary excitation X-ray, resulting in a vacancy. b) An electron from the L or M shell fills the vacancy and, in the process, emits a characteristic X-ray specific to the element, creating a new vacancy in the L or M shell. c) When a vacancy is formed in the L shell, either from the primary excitation X-ray or from the preceding event, an electron from the M or N shell occupies the vacancy. This action also results in the emission of a characteristic X-ray unique to the element and creates a vacancy in the M or N shell. d) The excitation energy from the inner atom is transferred to an outer electron, leading to its ejection from the atom. This secondary radiation is then detected and quantified. Each element emits unique characteristic secondary X-rays, and the energy of these X-rays correlates with the concentration of the analyte, the sample matrix, and the conditions under which excitation and detection occur (Wolff, 2006).

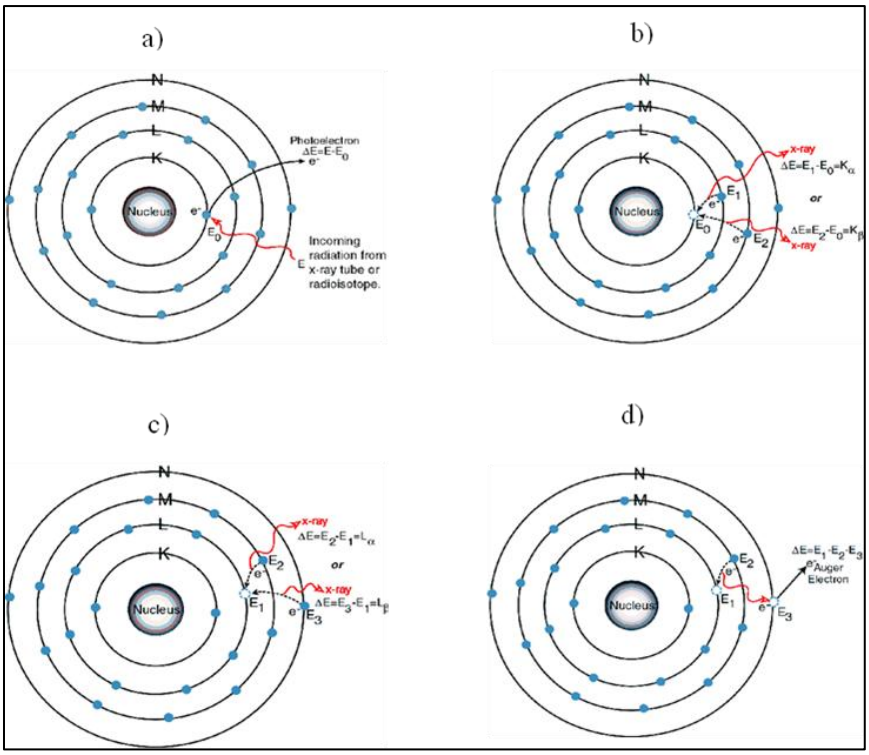

Figure 2.10 Illustration of the Fundamental Principle of X-Ray Fluorescence

There are two primary methods for collecting X-ray fluorescence emission: measuring either the wavelength dispersion or the energy dispersion spectra. Wavelength Dispersive X-ray Fluorescent (WDXRF) requires a crystal to separate the wavelengths of different sample elements. For each angle of incident radiation, only the wavelength that meets Bragg's law is reflected to the detector. The elements being analyzed are selected by adjusting the crystal angle. The intensity of the spectral peaks is highly dependent on the sample, influenced by the interfering X-ray lines of matrix elements and the mechanical preparation of the sample. Therefore, quantitative analysis necessitates calibration with standards that closely match the composition of the sample and have a similar surface finish. For highly accurate gold analysis, a mirror finish is essential. Under these conditions, this method allows for determining the gold fineness in a gold alloy with a level of accuracy comparable to that achieved by cupellation, typically around 0.3 *wt%.* WDXRF spectrometers require high-voltage generators, high-energy X-ray sources, efficient water-cooling systems, and advanced analyzing crystals. As a result, these instruments are expensive, demanding significant installation requirements and incurring high operational costs. Additionally, limitations within the sample chamber make WDXRF unsuitable for assaying many finished gold jewelry pieces.

In contrast, the EDXRF method utilizes less powerful X-ray sources than those used in wavelength dispersion systems. This reduces the need for water cooling, resulting in substantial cost savings. Consequently, the EDXRF method is more affordable and smaller than its WDXRF counterparts, while still achieving highly accurate analytical results, typically around 0.5 *wt%*. Recent technological advancements have enabled the development of a completely portable, small-sized EDXRF method for in-situ analysis, broadening the application of this technique to various fields, including archaeometry, environmental analysis, and even in vivo determinations of toxic elements. The advantages of using EDXRF over WDXRF have been well documented, particularly regarding the analysis of precious metals in jewellery. In most studies discussed in this review, the EDXRF method has been the technique of choice. Table 2.6 summarizes a comparison of EDXRF and WDXRF for metal analysis.

Table 2.6
Comparison of the features of EDXRF and WDXRF for metal analysis

Feature	EDXRF	WDXRF
Resolution	<160 eV FWHM at Mn Kα (5.9 keV)	<5 eV FWHM
Sensitivity	Moderate	High
Speed of Analysis	Fast (seconds to minutes)	Slow (minutes to hours)
Sample Preparation	Minimal	Extensive (especially for solids)
Matrix Effects	Higher	Lower
Element Detection Range	Na to U (suitable for most metals)	Na to U (better at low Z elements)
Cost	Lower	Higher
Detection Limit	ppm range	Sub-ppm range
Complexity of Data Analysis	Simple	Complex
Applications	Industrial, bulk analysis	High-precision, research, trace elements

In summary, the EDXRF method is better for quick, high-throughput analyses and is suitable for larger samples and less stringent resolution requirements. It is more cost-effective and less complex to operate, but its sensitivity and resolution are not as high as WDXRF. On the other hand, WDXRF may provide superior resolution, sensitivity, and lower detection limits, making it ideal for precise analysis of trace elements and complex materials; however, it is not practical in metal analysis applications due to being more expensive and slower compared to EDXRF. The EDXRF is often chosen for routine industrial and field applications, while WDXRF is used in laboratory settings requiring high precision and detailed analysis, particularly for trace elements and complex alloys. Since then, the latest commercial EDXRF method has been equipped with advanced, accurate solid-state detectors for high-resolution X-ray spectroscopy. These devices effectively separate electron energies into distinct elemental components and collect energy (which is proportional to the incoming radiation) in the form of an electrical signal. This signal is then translated into qualitative or quantitative elemental data in a word-processor format. User-friendly PC menu assistance ensures easy operation, yielding accurate results even for less experienced operators.

2.5.3.2 Application of Non-Destructive EDXRF Method

Analysing a sample typically involves the destruction of at least a portion of it. However, in the case of certain valuable items, such as unique pieces of jewellery or significant works of art, it is crucial to employ non-destructive techniques. This approach safeguards the integrity of these irreplaceable objects while still providing valuable analytical insights. The information derived from the analysis of these valuable samples can serve a variety of purposes, which can differ based on the type of sample being examined. For jewellery, for instance, the primary objective is often to ascertain the precious metal content or fineness of the alloy from which the piece was made. This information is vital for preventing economic fraud, as it helps determine the actual value of the jewellery. Additionally, it addresses potential health risks associated with harmful metals that could be present in the alloy, substances that can lead to skin conditions such as dermatitis. In such cases, the analysis of the major and minor constituents of the alloy typically suffices, as more detailed trace analysis is not usually required.

Conversely, the analysis of archaeological or artistic metallic objects presents a more intricate challenge. In these situations, the analysis must provide answers regarding the object's provenance—where it originated—and the manufacturing methods that were used to create it. This type of investigation can yield significant historical insights into the societies that produced these items, including their industrial capabilities and economic conditions. To conduct a thorough study, researchers must not only analyse the major and minor components of the object but also identify trace elements. These trace elements can be instrumental in linking the object to a specific geographical location, for instance, by correlating the metal composition of a coin to its ore source. Furthermore, scientific methods may be applied to assess the conservation state of the material, which is critical for guiding the most appropriate restoration techniques to preserve the object for future generations.

According to Conrey et al., 2014, an ideal method for analysing objects of artistic, historic, or archaeological significance should exhibit several key characteristics:

i. Non-destructive: The method must prioritize the preservation of the physical integrity of the material or object being analysed. This is especially important for items of cultural significance, where any alteration or damage could diminish their historical value.

ii. Fast: The analysis should be expeditious, allowing for the assessment of numerous similar objects efficiently, or enabling the investigation of multiple locations on a single object's surface. This is crucial for researchers working within time constraints or dealing with large collections.

iii. Universal: A single analytical instrument should be capable of assessing a wide range of materials and objects of varying shapes and dimensions, with minimal preparation required for the samples. This versatility is important for researchers who handle a diverse array of artifacts.

iv. Versatile: The method should facilitate the extraction of both average compositional information and localized data from small areas of heterogeneous materials. This dual capability is particularly useful for analysing materials that might have undergone complex manufacturing processes or have been affected by environmental factors.

v. Sensitive: The analysis must be sensitive enough to support provenance studies and object classification, not only through major element analysis but also by detecting trace elements and unique fingerprints of materials. This sensitivity enables researchers to draw connections between various artifacts and their origins.

vi. Multielement: The analytical technique should allow for the simultaneous measurement of multiple elements, including those that may not have been anticipated. This capability ensures a comprehensive understanding of the object's composition, which can yield unexpected insights into its history or production methods.

The EDXRF method has emerged as a widely utilized technique that meets many of these essential requirements. Due to its non-destructive nature, rapid analysis capability, and aptitude for multi-elemental detection, the EDXRF method is particularly advantageous for qualitative and semi-quantitative assessments of valuable materials (Sitko & Zawisz, 2012). In recent advances, XRF has also become proficient in delivering accurate quantitative analyses, greatly enhancing its utility in the field of artistic, historical, and archaeological studies (Rousseau, 2006). The EDXRF method is a technique that can be applied to almost all elements in the periodic table, except for the first two, hydrogen (H) and helium (He). It covers an energy range from approximately 50 eV to 100 keV. However, measuring many light elements can be challenging and often requires advanced instrumentation. This limitation typically confines practical applications to elements with atomic numbers between 13

(Aluminium, Al) and 92 (Uranium, U). Additionally, factors such as equipment cost and the complexities of radiation protection at high photon energies mean that L lines, rather than K lines, are generally analysed for elements with atomic numbers over 50 (Tin, Sn). As a result, the fluorescent photon energies usually fall between 1 and 25 keV, with excitation voltages of less than 50 kV. This energy range is significant not only for analytical purposes but also for assessing potential radiation hazards.

Metals are particularly well-suited for the EDXRF method analysis. Their high atomic numbers and densities help produce strong secondary X-ray lines, even when using low-intensity sources. In the case of metal alloys, the emission lines of the individual elements can also be detected. Quantitative XRF analysis is conducted using the fundamental parameters method, which is an atomic physics algorithm that theoretically describes the interaction between the EDXRF method and the sample (Silveira & Falcade, 2022). This method interprets the processed X-ray spectra to identify the elemental composition, considering the physical parameters of the spectrometer, which include the generation of primary X-rays from the X-ray tube, secondary fluorescence production in the sample, inter-element matrix effects, and the detection of X-rays. When analysing precious metal alloys, the accuracy of the fundamental parameters method varies depending on the alloy composition. For instance, determining gold content in an alloy that contains copper may result in an overestimation of 0.5% to 1% due to overlapping emission bands.

Conversely, the analysis of silver-copper alloys tends to be very accurate, as their spectral bands are well-separated (Klotz et al., 2017). To ensure accurate analysis, the objects being examined should be homogeneous and possess a flat surface. This is crucial for optimal positioning during the incidence of the primary beam and for the effective collection of the secondary beam by the detector. However, this requirement poses a challenge when dealing with jewelry items, given their diverse sizes and shapes. Routine methods typically involve sampling, which includes cutting the object and polishing the samples to achieve the proper surface for precise analysis. However, these methods are not suitable for valuable items, so it is essential to select the flattest available surface for examination (Ridolfi, 2012).

2.6 Evaluation of the EDXRF Method for Analysing Gold Alloy Artifacts

Most manufacturers have taken the opportunity to offer a less expensive special class of resolution for the EDXRF method that is pre-calibrated for the simultaneous analysis of precious alloy constituents. Due to the factors of low cost, compact, lightweight, low voltage, and easy mobility (portability), the EDXRF method has been most popular among Ar Rahnu to determine the gold purity from the borrower. Nowadays, there are more than 200 units of the EDXRF method in the Ar-Rahnu in Malaysia (Shah & Yaacob, 2018). Other researchers claimed that the low resolution of the EDXRF method is a technique used in historical studies of coins, providing information about their provenance, authenticity, manufacturing technologies, chronological identification, or some political or economic trends in ancient societies. They affirm that the EDXRF method can be an alternative to routine analysis in numismatic studies and that it provides an outstanding tool (Navas et al., 2016). Figure 2.11 shows several types of commercial EDXRF methods for precious alloy constituents in the market.

Figure 2.11 Several Types of Commercial EDXRF in the Market

2.6.1 EDXRF Measurement Principle

The EDXRF method is founded on the fundamental principle of X-ray fluorescent spectroscopy, whereby atoms in each sample are stimulated by X-rays, resulting in the emission of distinctive X-rays that can be identified and evaluated. The present discourse provides a synopsis of the fundamental principles and operational mechanisms of the EDXRF method. The process of exciting the sample in the EDXRF method involves subjecting it to high-energy X-rays, which are usually produced by an

X-ray tube. The X-rays possess adequate energy to expel electrons from the innermost shells of the atoms present in the specimen, thereby leading to the formation of vacancies. X-ray emission occurs because of the removal of an inner shell electron, which subsequently prompts an electron from an outer shell to occupy the newly vacated position, thereby releasing energy in the form of X-rays. The X-rays that are released possess distinctive properties that are indicative of the constituent elements within the specimen. Distinct energies are exhibited by the characteristic X-rays of each element. The process of detecting emitted X-rays involves the utilization of a detector system, which is commonly a solid-state detector like a silicon drift detector (SDD) or a germanium detector in energy dispersive detection. The X-ray detector quantifies both the wavelength and intensity of the X-rays (Wolff, 2006).

The process of spectrum analysis involves the conversion of detected X-rays into electrical signals, followed by the analysis of their energy. The production of a spectrum is initiated, which exhibits discernible X-ray peaks that are representative of the distinct elements that are contained within the specimen. The spectral peaks' placement corresponds to the energy level of the X-rays that are emitted, thereby facilitating the identification of the constituent elements. In quantitative analysis, it is observed that the intensity of X-ray peaks exhibits a direct proportionality with the concentration of the corresponding elements present in the sample. Through the utilization of known standards and the comparison of characteristic peak intensities, a quantitative analysis may be conducted to ascertain the elemental composition and concentration of the given sample. To achieve accurate quantitative analysis, the utilisation of a calibration curve or calibration standards is imperative. The standards comprise predetermined concentrations of elements that are deemed significant, and their respective X-ray intensities are subsequently assessed. The concentration of elements in a sample can be ascertained through a comparison between the intensities of the sample and those of the standards. The utilization of the EDXRF method presents numerous benefits, such as non-invasive examination, concurrent multi-element analysis, and the capability to measure solids, liquids, and thin films. The technique is extensively employed across diverse domains, including but not limited to environmental analysis, mining, geology, materials science, and quality control in industrial settings (Markowicz, 2011).

The EDXRF method is a qualitative and quantitative elemental analysis method based on the detection of distinctive X-rays of the elements present in the investigated sample. Although the approach could be utilized for lighter elements when utilizing sophisticated instrumentation, it is primarily suitable for atoms with an atomic number of more than around 13 (Aluminum). The fundamental principle of the approach is the incidence of X-ray radiation on a sample. When light photons collide with atoms in the sample, they may transfer some of their energy to electrons orbiting the inner shells of these atoms. If the incident radiation has higher energy than the electrons' binding energy, the electrons are ejected, leaving holes in their orbitals. The ejected electron is known as a photoelectron, and the phenomenon is known as the photoelectric effect. The atom becomes unstable, and there may be two ways for it to return to its lowest energy state. One example is the emission of Auger electrons. The other is fluorescence. It consists of the decay of an electron from a higher energy level to provide the electron vacancy in the lower energy level. This action causes the emission of photons with an energy proportional to the electronic transition, which is characteristic of each element present in the sample. Moseley's law describes the link between the frequency of a typical X-ray photon, v, and an element's atomic number Z, where C is a constant with a different value for each spectral series and is known as the shielding constant (Shackley, 2011).

Direct excitation is a process by which atoms in a specimen are excited by primary photons from external sources, such as an X-ray tube, radioactive source, and synchrotron beam, to produce primary fluorescence. An alternative process is indirect excitation, in which the observed fluorescence is produced as a secondary process by photons or particles (electrons) originating from direct excitation or other secondary processes within the specimen. X-ray is an electromagnetic radiation generated by high-energy particles bombarding atoms. This radiation has wave-particle duality. The EDXRF method uses primary X-ray photons or other microscopic particles to excite the atoms in the test material to produce secondary X-rays for material composition analysis and chemical state research. Qualitative analysis of X-ray spectroscopy is based on Moseley's law, and the energy Equation 2.1 is as follows:

$$E_x = -Rhc\,(Z-\sigma)^2\left(\frac{1}{n_1^2}-\frac{1}{n_2^2}\right) \tag{2.1}$$

where E_x is the characteristic X-ray energy, R is Rydberg constant (R_∞ =1.09737 × 10^7 m^{-1}), h is Planck's constant (h =6.6262 × 10−34 J·s), and C is the speed of photons, 3 × 10^8 m·s^{-1}. Z is the atomic number, σ is the Shielding constant, and n_1 and n_2 are energy series. For the spectrum of $K\alpha_1$ shielding constant σ = 1, n_i =1 (K-shell), and n_i =2 (L-shell). The law reveals the relationship between the X-ray energy and atomic number. This law is the theoretical basis for the qualitative analysis of material composition using XRF. A positive relationship exists between the count rate of the characteristic X-ray and the content of an element of the tested sample, as follows:

$$I_k = \frac{KI_0}{\mu_0 + \mu_k} W_k \tag{2.2}$$

where I_k and I_0 are the K shell characteristics of the X-rays of the measured elements and the count rates of the incident X-rays, respectively. Moreover, μ_0 and μ_k are the absorption coefficients of the tested substance to the incident X-ray and the tested element to the layer K characteristic X-rays, respectively. K is the constant related to the specific measurement device and should be determined by the calibration instrument $KI_0 / (\mu_0 + \mu_k)$. W_k is the measure of the content elements. Quantitative analysis of the measured elements using XRF is theoretically based on Equation 2.2.

2.6.2 EDXRF Components

The EDXRF method system is designed in Figure 2.12. The spectrometer consists of a power supply, a light path subsystem, a control circuit, and a personal computer (PC). High-voltage power is supplied to the X-ray tube to emit a primary X-ray, which irradiates the sample. The sample is then stimulated to emit X-rays, which are received by an EDXRF detector. The detector classifies the received photons according to energy and counts the number of photons that correspond to different energy levels. The detector then sends the results to the PC, which completes the qualitative and quantitative analyses.

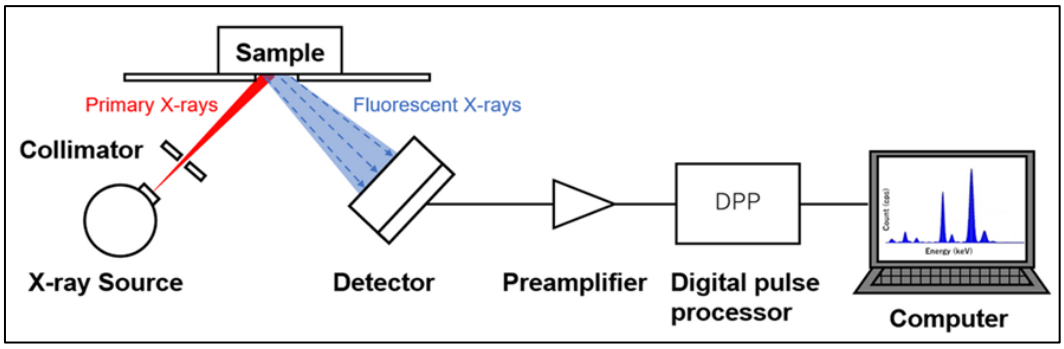

Figure 2.12 Structural Diagram of the EDXRF Method

The light path subsystem includes the X-ray tube, filter, collimator, detector, and a camera. The light path subsystem is responsible for emitting, receiving, and counting the XRF photons. Its operation is as follows. A high-voltage power supply provides high-voltage energy to the X-ray tube, which is stimulated to emit primary X-rays. The primary X-ray passes through the Be window, filter, and collimator, finally irradiating the sample. The sample is stimulated to emit X-ray that can be recognized by the detector. The received X-rays is transformed into a low-voltage pulse by the preamplifier. The pulse amplitude that is strictly proportional to the energy of the received X-rays is further amplified by the main amplifier. The analog-to-digital converter then transforms the amplified voltage into a digital signal. The digital signal is further shaped, sorted, and transformed into a pulse counter with amplitude information. This information is stored in a multichannel analyser according to its amplitude and finally formatted into an X-ray spectral line. The detector transmits spectral information to the PC through a USB hub in the control circuit for qualitative and quantitative analyses.

2.6.2.1 EDXRF Tube

The X-ray tube in the light path subsystem (example: Variant X-ray tube), as depicted in Figure 2.13, is a main component that plays a key role in generating X-rays for the spectrometer system, particularly for the EDXRF method. This tube operates under specific conditions, including a high voltage of 50 kV and a low current of 0.8 mA, which are optimized for producing X-rays with sufficient energy for material analysis while maintaining low power consumption and minimizing the potential for

damage to the system components. The combination of high voltage (50 kV) and low current (0.8 mA) is crucial in determining the characteristics of the X-rays generated by the tube. High voltage increases the energy of the electrons that are accelerated toward the anode, leading to the production of X-rays when these electrons strike the target material (anode). The low current helps ensure that the tube remains energy-efficient while preventing excessive heating that could affect the tube's lifespan and performance. This combination also provides a stable, controlled X-ray output that is consistent over time.

Figure 2.13 The EDXRF Tube Excitation Source Shines X-Rays from Below Up onto the Sample

One of the most important features of this X-ray tube is its high stability. It is designed to maintain low errors, with a remarkable relative standard deviation of 0.2 *%rsd* over 4 hours. This stability is critical for precise measurements in the EDXRF method, where accuracy and consistency are essential for reliable data. The low error rate ensures that the X-ray tube produces consistent X-ray flux over extended periods, minimizing variability that could lead to erroneous results in analytical applications. The ability to maintain stable operation for up to 4 hours without significant fluctuations

means that the system can perform long-duration tests without requiring recalibration or adjustments, enhancing efficiency and reliability.

The X-ray tube is equipped with a small focal spot size of just 0.4 mm × 0.4 mm, which is a significant advantage in terms of precision and resolution. A smaller focal spot enables the X-ray beam to be highly focused on a small area of the sample, allowing for more detailed and localized analysis. This is particularly beneficial when working with small or complex samples, where a larger focal spot would spread the X-ray beam too widely, potentially reducing the accuracy of the measurements. The small focal spot size ensures that the X-ray radiation is concentrated and directed effectively, improving the resolution of the resulting spectrometric data.

2.6.2.2 Silicon Drift Detector (SDD)

The silicon drift detector (SDD) technology is known for its superior energy resolution and fast response times compared to traditional detectors. In SDD, the silicon material is used to convert incoming X-ray photons into electron-hole pairs. When an X-ray photon strikes the detector, it ionizes the silicon, creating these electron-hole pairs. The electric field within the drift region causes the electrons to move toward the anode, creating an electrical pulse. The energy of this pulse is proportional to the energy of the incoming X-ray photon. The detectors are fitted with a thin window, which is an essential feature for improving the sensitivity of the detector, especially for low-energy X-rays.

A thin window reduces the X-ray absorption in the material before the X-rays enter the detector, allowing more photons to reach the active area of the detector. This is particularly important for the EDXRF method, as it allows the detector to capture a wider range of X-ray energies, including those in the lower energy spectrum. The thin window material is typically beryllium (Be) or a similar light material that offers minimal absorption for low-energy X-rays while maintaining structural integrity. This design ensures that the detector can measure X-rays across a wide energy range with minimal loss of signal. An example of an SDD detector is shown in Figure 2.14, with model Vortex-60EX.

Figure 2.14 Vortex-60EX X-Ray Detector

One of the standout characteristics of the SDD detector is its energy resolution, which is less than 160 eV full width at half maximum (FWHM) at the Mn Kα line (5.9 keV) as shown in Figure 2.15. Energy resolution refers to the ability of the detector to distinguish between different X-ray energies. The Mn Kα line is a standard calibration point used in the EDXRF method, and a resolution of <160 eV at 5.9 keV means the detector can accurately differentiate between X-ray peaks that are close in energy. The high energy resolution is crucial for elemental analysis in the EDXRF method, as it allows for precise identification and quantification of elements in a sample. The smaller the FWHM value, the sharper and more distinct the peaks in the X-ray spectrum, leading to improved accuracy in determining the elemental composition of the sample (Conrey et al., 2014).

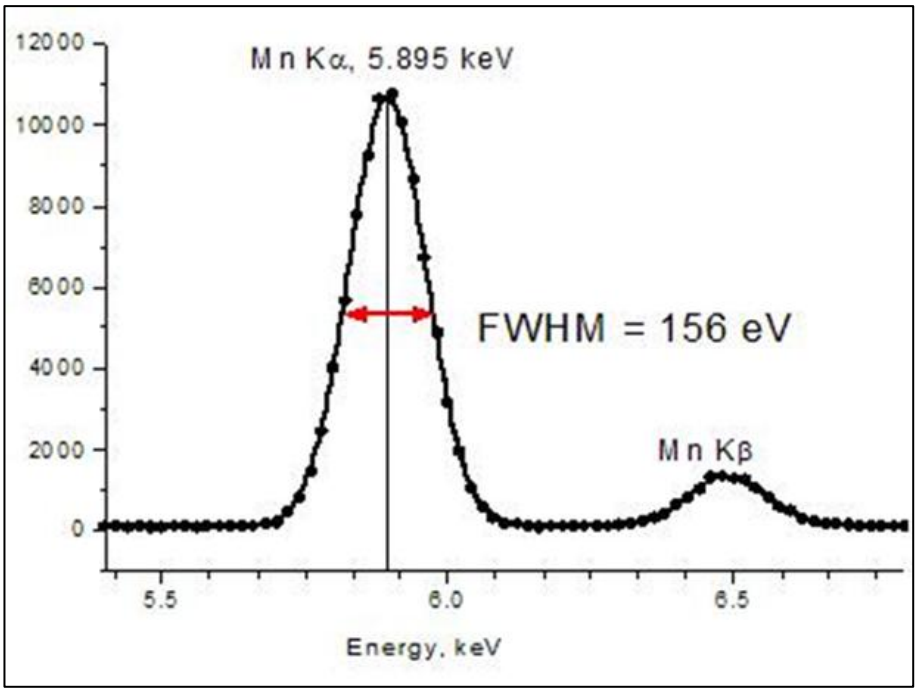

Figure 2.15 Full width at half maximum (FWHM) at the Mn Kα line (5.9 keV) (West et.al, 2017)

2.6.3 Qualitative Analysis of the EDXRF Method

Qualitative analysis is the basis of quantitative analysis. Existing element types can be determined using the former analysis. Qualitative analysis is generally divided into three steps.

i. *Peak Location.* The uncertainty of a large peak is approximately ±10 keV, whereas that of a small peak is up to ±50 eV. Small peaks can be neglected when they overlap with a large peak, particularly when its energy level is below 12 keV. Spectral overlap and interference frequently occur in the *K* line (where the atomic number is between 22 and 35) and the *L* line (where the atomic number is between 56 and 96). All aforementioned factors hamper an accurate qualitative analysis.

ii. *Peak Recognition*. The uncertainty of the peak position generally increases the difficulty of peak recognition. More than one peak corresponds to the energy peak in the spectrum in several cases. Accumulated, escape, and scattering peaks can also interfere with recognition.

iii. *Element Determination*. Except for light elements, such as Na, Mg, Al, Si, P, and S, identifying an element typically requires more than two characteristic spectral peaks. When the voltage of the X-ray tube is over 30 keV for atomic numbers ^{19}Z

to ^{42}Z, the spectral peaks $K\alpha$ and $K\beta$ appear simultaneously. Furthermore, relative intensities in different spectral peaks should also be considered.

The characteristic peak area of the relative element in the qualitative analysis is calculated. This area corresponds to the photon number of the relative energy. The intensity of the characteristic peak can then be achieved. However, interference peaks should be considered in calculating the peak area. The peak in the peak location, which is an interference peak to the main peak, is called a pseudo peak. Such peaks include accumulated, escape, and scattering peaks. The accumulated peak is also called the sum peak, which is a phenomenon of peak hyperplasia resulting from the accumulation of signal pulses while counting at a high rate. In a sum peak, the peak position does not correspond to the characteristic energy but to the sum of two independent peaks.

When the energy of an X-ray photon is higher than the detection limit, some energy of the characteristic X-ray can escape because of its high transparency. The escaped energy forms an escape peak in the low-energy position. The energy difference between the main and escape peaks is equal to that of the energy of the characteristic X-ray photons, which is recognized by the detector. The software automatically integrates the peaks for each element and produces intensity data in the units of counts/second/mA. Every element has its unique peaks. Figure 2.16 shows the characteristic X-ray spectrum obtained from EDXRF for gold jewellery samples. Peaks of Aurum (Au) lie at 9.711 keV and 11.439 for AuLα and AuLβ, respectively. Peaks of the Copper (CuKα) will be observed at 8.041 keV and CuKβ at 8.907 keV, while the peaks detected at higher energy values are connected to the presence of the Ag Kα peak will be at 22.104 keV and 24.987 keV. The energy scale is determined and expressed in units of kiloelectron Volt (keV) (Majcen et al., 2002).

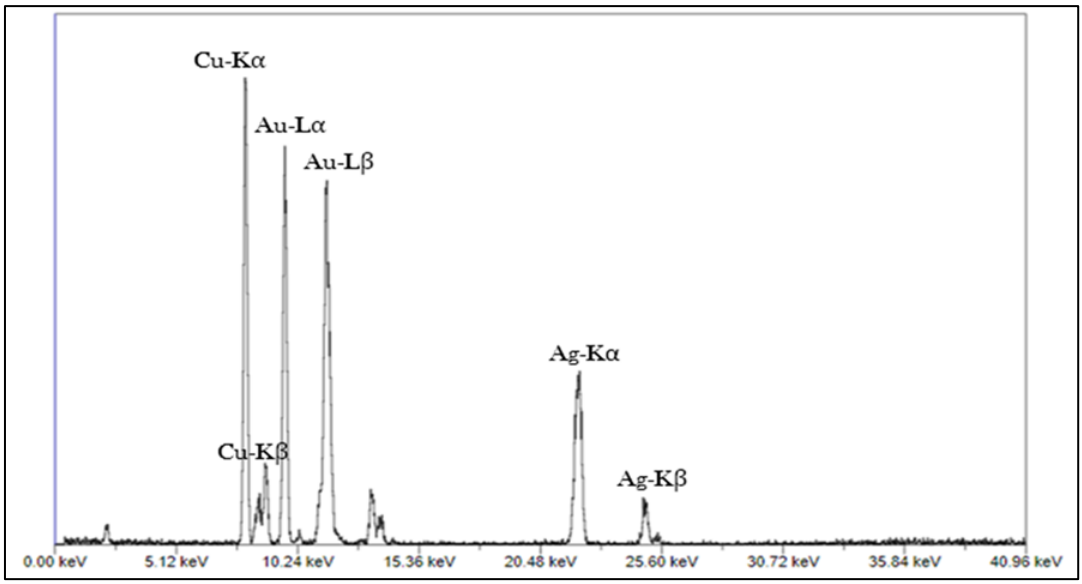

Figure 2.16 The Characteristic X-ray Spectrum Obtained from EDXRF for the Common Yellow Gold Alloy Mixture Samples (Mazuki et al., 2023)

2.6.4 Quantitative Analysis of the EDXRF Method

Quantitative analysis in the EDXRF method is primarily based on the standard calibration curve. The standard calibration curve allows the spectrometer to convert the measured intensity of X-ray fluorescence emitted from a sample into the concentration of the elements present in that sample. The accuracy and reliability of this method depend on the quality of the standard samples and how similar the conditions are between the standard samples and the unknown samples being measured. To perform quantitative analysis using the EDXRF method, standard samples with known concentrations of specific elements are required. These standards are crucial because they help establish a reference for the relationship between the X-ray fluorescence signal (intensity) and the elemental concentration in the sample. The detailed steps are illustrated in Figure 2.17.

Quantification of the EDXRF method is being conducted on precious metal artifacts at a rate that would have been unimaginable 20 years ago, and the pace is accelerating. The ease with which quantitative results may be obtained using manufacturers' software may seem to suggest that the EDXRF method is a simple and straightforward technique (Rousseau, 2009).

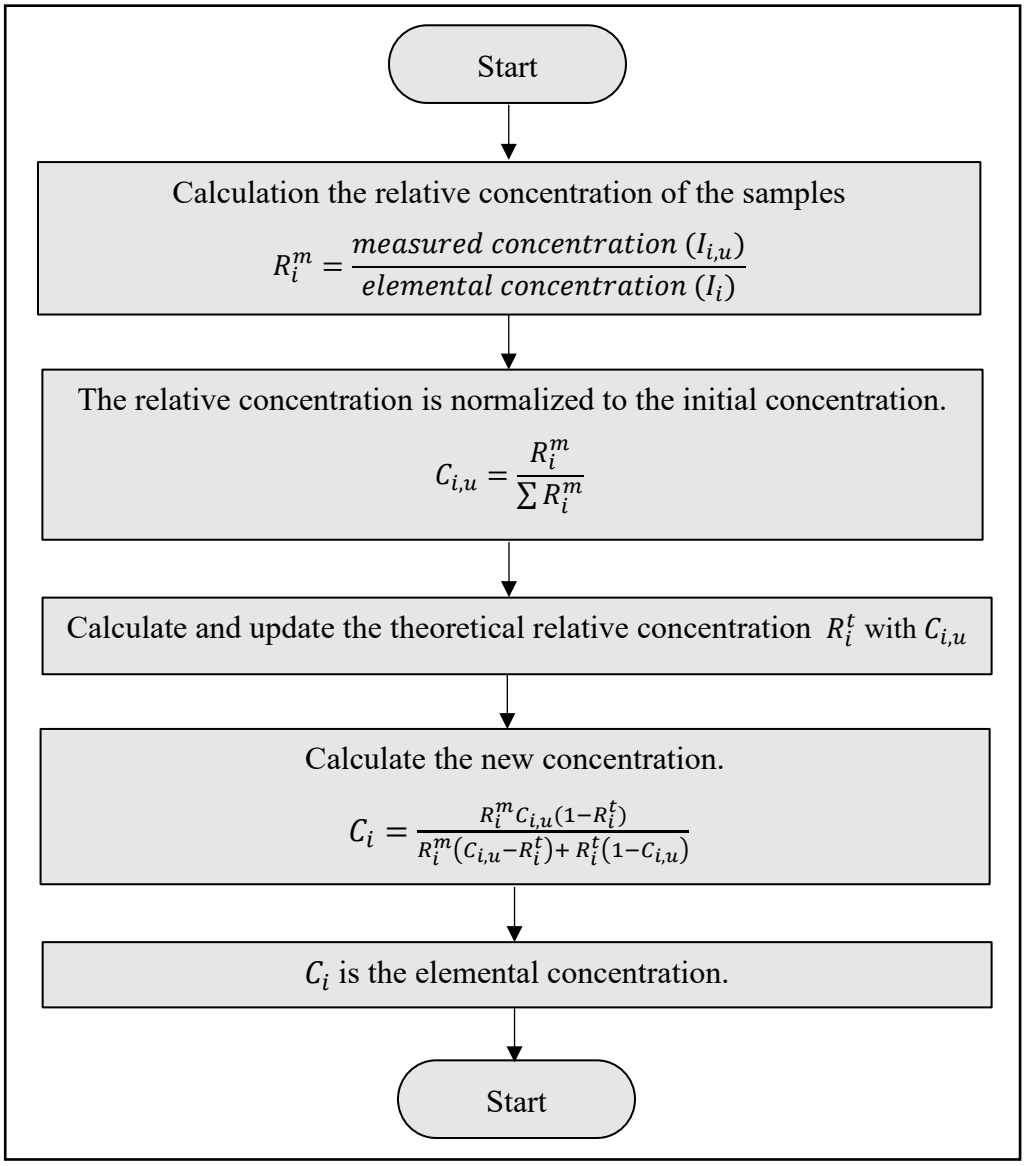

Figure 2.17 Steps of Quantitative Analysis, where *m* is the Measured Value, and *t* is the Calculated Value (Rousseau, 2009)

A remarkably complex and tortuous series of physical interactions can occur between the emission of an X-ray from its source and the detection of fluorescent radiation by the instrument's detector. Particularly for dense samples such as metals, these interactions are highly dependent on the composition and structure of the sample material, or matrix, and as a result, the detector response is inherently nonlinear. For this and many other reasons, discussed by many researchers, the conversion of an XRF spectrum to an accurate quantitative result is, by nature, a complicated and challenging undertaking (Conrey et al., 2014).

2.6.5 Pre-calibration Method of the EDXRF Method

The accuracy of the analytical data has been debated for a long time. In the early seventies, the EDXRF method analysts were confronted with the problem of choosing the most appropriate calibration method for calculating the composition of the samples to be analysed (Rousseau, 2009). Some researchers have claimed that the existing pre-calibrations of this commercial EDXRF method fail to fully utilize the method's capabilities due to the manufacturer's control over the instruments. The factory pre-calibration provided is not quantitatively well-suited to complex precious metals (Marucco, 2004)(Conrey et al., 2014). It varies widely in gold product properties, such as a variety of other metal alloy compositions (matrix), sizes, shapes, impurities, etc., which often pose a considerable analytical challenge (Bonizzoni et al., 2006; Artyukh et al., 2018). The summary list of pre-calibration methods of the EDXRF method has been outlined in Table 2.7 (Conrey et al., 2014).

Table 2.7
Summary List of Pre-Calibration Methods of the EDXRF

Method	Advantages	Disadvantages
Fundamental Parameters Standard-less	Analysis of any material using fundamental X-ray physics	1. Require full X-ray spectrum due to normalizing results. 2. Not the most accurate for materials; requires considerable computing power
Empirical Influence Coefficient	Most Accurate Method for Materials	1. Require many standards. 2. Inaccurate if compositions exceed calibration ranges
Compton rationing	Helps correct for analysis of irregular surfaces, useful for analysis of medium to heavy Z elements with simple matrices	1. Approximate correction for absorbance only, not enhancement. 2. Difficult to apply to light elements

With the limited numbers, an appropriate specific matrix of calibration standards is always critical, especially to achieve better accuracy on the complexity of gold bullion and jewellery products (Stankiewicz et al., 1998). The matrix interference effect between the element, overlapping peaks, and irregular shape of gold samples will affect the accuracy of the EDXRF method (Conrey et al., 2014; Bonizzoni et al., 2006). Over the last years, several developments have taken place in the methodology for quantitative analysis of the EDXRF method using this technique to enhance the quality

and reliability of the results and to extend the range of its applications on the other hand. The EDXRF method shall be calibrated so that the chemical data generated may be reliably compared with that obtained using more standard analytical methods (Rousseau, 2009)(Gallhofer & Lottermoser, 2018). The selection of the calibration method has often been discussed, especially in the consideration of the correction of the matrix effect. The EDXRF correction for the elements present in addition to the target analyst is referred to as the 'correction matrix' (Artyukh et al., 2018).

2.6.6 Factors Affecting the Accuracy of EDXRF Measurement

A variety of sample types, purity, and design adversely influence the accuracy of the EDXRF method measurements of gold contents in gold alloy samples. This can lead to challenges in accurately determining the exact composition of the sample. One common issue is the presence of other elements in the alloy, such as copper or silver, which can interfere with the detection of gold. Additionally, variations in the sample's surface finish or thickness can also impact the results obtained from the EDXRF method (Mazuki et al., 2021). Such discrepancies can cause significant differences in the resulting levels of gold measured by the EDXRF method if the alloy is not carefully calibrated and characterized. Several factors can affect the accuracy of the EDXRF method in gold measurement. To achieve both reproducible and accurate measurements of gold in precious metal alloys, all these factors must be understood and compensated for. Proper calibration and characterization of the alloy are essential to ensure accurate results in the EDXRF analysis of gold. Additionally, maintaining consistency in sample preparation and measurement conditions can help minimize discrepancies and improve the reliability of the measurements (Mazuki et al., 2023).

2.6.6.1 Absorption and Enhancement Impact (Matrix Effects)

The presence of additional elements in a gold alloy has a significant impact on the analysis conducted through the EDXRF method (González et al., 2024). Analysing these alloys can pose challenges due to the absorption characteristics of X-rays emitted from gold, which can be interfered with by the introduction of other metallic elements. For instance, certain elements like copper, especially when present in high

concentrations, can absorb specific portions of the X-ray spectrum associated with gold. This absorption phenomenon occurs primarily because the energy levels of copper's characteristic X-rays, particularly the Cu Kα peak at 8.041 keV and the Cu Kβ peak at 8.907 keV, are lower than the corresponding X-ray energies for gold, which includes the Au Lα peak at 9.711 keV and the Au Lβ peak at 11.439 keV. When this absorption occurs, it results in an underrepresentation of the actual gold content in the alloy, leading to potentially inaccurate assay results that could misguide further processing or valuation.

Conversely, other alloying elements may enhance the fluorescence signal of gold, thereby complicating the assay results. Silver serves as a prime example of such an element; its presence may promote increased scattering and the emission of secondary radiation, effectively elevating the detected signal for gold. The characteristic peaks for silver are notably higher, with the Ag Kα identified at 22.104 keV and the Ag Kβ peak at 24.987 keV. If these contributions from elements like silver are not appropriately accounted for during analysis, there is a risk that the gold content could be overestimated, especially if the analytical method is not properly calibrated to recognize the influence of these enhancements.

When conducting the EDXRF method of gold alloys, matrix effects emerge as a crucial consideration. The different elemental compositions present in the alloy can lead to spectral interferences that manifest as absorption or enhancement effects, presenting significant calibration challenges. These effects complicate the interpretation of gold content, leading to possible overestimation or underestimation of the assay results. Several best practices should be employed to alleviate the impact of these matrix effects and improve the accuracy of the assays. Utilizing matrix-matched standards can ensure that the calibration reflects the actual composition of the alloy being analysed, while optimizing the EDXRF method settings specific to the sample can improve precision. Moreover, applying advanced software corrections can help to further adjust for these interferences, ultimately resulting in more accurate, reliable, and trustworthy gold assay outcomes. Figure 2.18 shows an example of the mechanism of matrix effect (interelement) in the metal alloy samples (Rousseau, 2006).

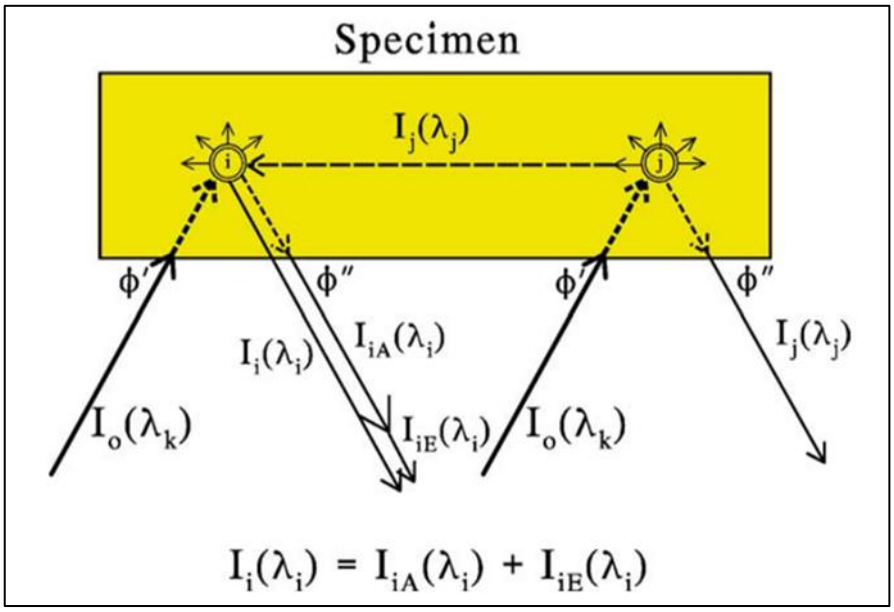

Figure 2.18 Primary Excitation of the Analyte *i* and Enhancement of '*i*' by '*j*' in an *i*–*j* Binary Specimen. A Practical Example Would be *i*=Fe and *j*=Ni in a Fe–Ni Alloy (Rousseau, 2006)

Figure 2.19 shows a significant optimization of the calibration method, especially in the consideration of the correction of the matrix effect (Conrey et al., 2014). The graphs depict the relationship between concentration (ppm) and net intensity (cps) for each element, showing that as concentration increases, the net intensity also increases, reflecting the typical behavior in X-ray fluorescence analysis. The influence coefficients may refer to the calibration adjustments made to account for specific variations in the XRF data for each element: (a) Yttrium, Y, and (b) Barium, Ba, in obsidian and flint. The EDXRF correction for the elements present in addition to the target analyst is referred to as the 'correction matrix'. This is crucial in almost all EDXRF method because the intensity measured by the element depends on how much X-ray is absorbed or enhanced by the other elements present in the sample (González et al., 2024).

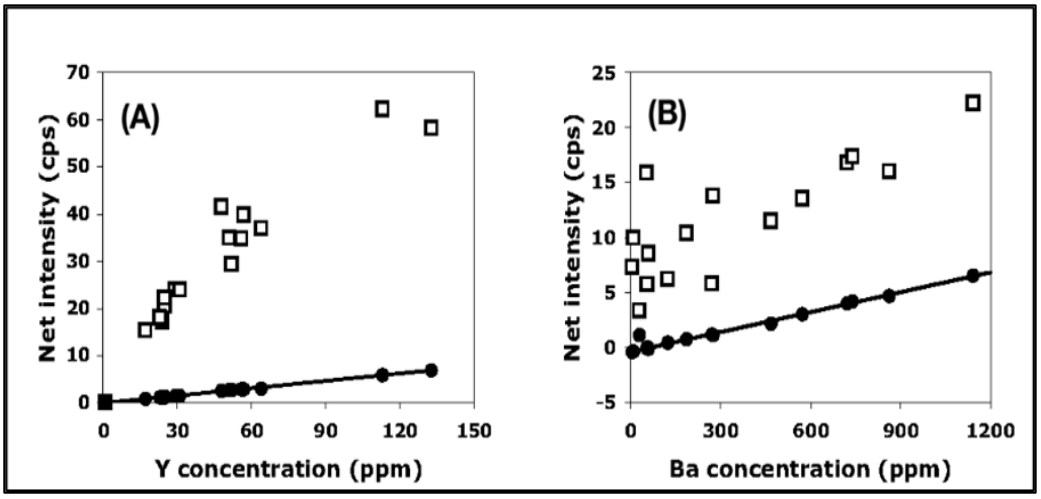

Figure 2.19 XRF Calibration with Influence Coefficients. Raw Net Intensities (open squares) and Matrix-Corrected Intensities (dots) for (a) Y and (b) Ba in Obsidian and Flint. Matrix Effects from Other Elements are Corrected in Both Cases (Conrey et al., 2014)

Černohorský et al. (2006) stated that the EDXRF method, based on empirical calibration curves, provides very good results if the composition of reference materials used as calibration standards corresponds to that of the sample under study. The large set of calibration standards is, in general, necessary for the calculation of coefficients for matrix effects correction (Rousseau, 2009). However, the accuracy of this method is in addition strongly dependent on the correspondence matrix match between samples and standards (Shackley, 2011). Alternatively, excellent results may be accomplished with the application of Fundamental Parameter (FP) calculation modelling, which is based on calculating results for all elements, not just the main element, i.e., gold (Au), silver (Ag), but also all the elements of the matrix (Jalas et al., 2002). However, accuracy complicates some practical FP applications in the analysis of precious metals (Jurado-López et al., 2006). Therefore, the introduction of the algorithm for the FP in combination with specific gold matrix calibration standards can considerably improve the accuracy of precious metals analysis.

2.6.6.2 Overlapping Peaks in the Measured X-Ray Spectrum

Gallhofer & Lottermoser (2018) explained in their study that the factor of overlapping peaks (interferences) in the measured X-ray spectrum can reduce the accuracy significantly. Due to the low resolution of commercial EDXRF, peak overlapping potentially occurs when the energies of spectrum lines of two or more elements are close to each other. In practice, if two peaks are closer than 400 eV to each other, the overlapping may affect the analysis result. This is the case, particularly, which has been in wide use in low-cost XRF analysers earlier. Today, commercial semiconductor-based detectors offer an affordable solution with energy resolution, expressed in Full Width Half Maximum (FWHM) of a peak well below 150 – 300 eV (6). However, peak overlapping can still be a problem. For example, where the concentration of one element is over 90% weight and the other below 3%, the accuracy can be affected. The critical elements may be determined in common geological materials when pronounced peaks occur in the spectra, and the matrix-match of standards and samples is essential. Hence, EDXRF spectra should be routinely reviewed to identify erroneous quantification due to spectral interferences.

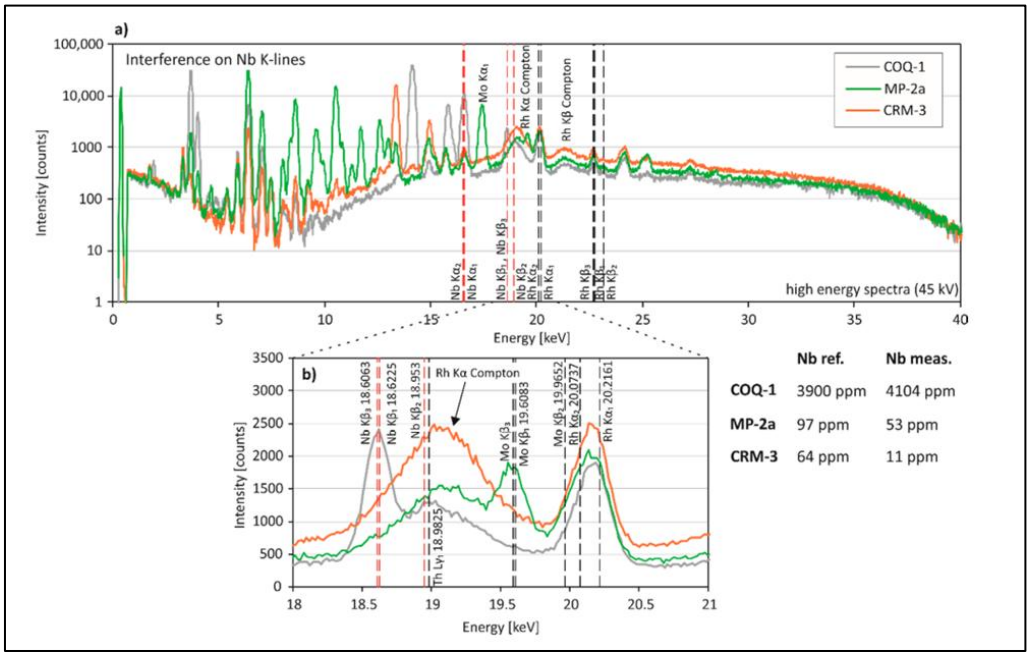

Figure 2.20 Overlapping Peaks on Nb in XRF Spectra. (a) Full Range (0–40 keV) and (b) Zoomed-in View Showing Nb K-lines (red) with Mo and Rh Interferences. 45 kV Excitation (Gallhofer & Lottermoser, 2018)

Figure 2.20 shows an example of peak overlapping on Niobium (Nb) elements. This graph shows the high-energy spectra obtained from the portable XRF measurements at 45 kV excitation energy for three different samples: COQ-1 (green), MP-2a (orange), and CRM-3 (grey). The Nb K-lines are marked with red vertical lines. These K-lines correspond to the characteristic X-ray emissions of niobium (Nb), specifically the Kα and Kβ lines. The chart illustrates how peaks for each sample (COQ-1, MP-2a, and CRM-3) vary in intensity across the energy spectrum. Several interferences are present, most notably the Mo Kα and Mo Kβ peaks near the 17–18 keV region, and the Rh Kα Compton peak around 20 keV. These elements cause overlapping signals, complicating the measurement of Nb in the sample. The tail of one peak overlaps the centre of an adjacent element to increase the intensity of this peak, which then overestimates the concentration. Accounting for this phenomenon requires standards to determine the real element contribution, and alternatively, use secondary emission lines on the spectrum where there is no overlap (González et al., 2024). Modern EDXRF method employs the Fundamental Parameter (FP) as a calculation routine; most of the individual spectrum peaks need to be reasonably separate from each other to get unambiguous information about the spectrum. However, due to the result of FP being always normalized to 100 %, the accurate determination of other elements in the gold alloys is significant. The improvised FP calibration method with corrects spectral interference must be considered in this study.

2.6.6.3 Influence of Gold Alloy Sample Sizes

Quantitative analysis of the EDXRF method for gold alloys, such as jewellery, can be obtained by using the general fundamental parameter method based on the comparison of X-Ray fluorescence signals with those obtained from reference standards in identical experimental conditions. The FP calculation modelling is usually less dependent on the sample size. Bonizzoni et al. (2006), in their study, state that the FP calculation method can result in better statistical precision, namely for irregular samples such as gold rings or some archaeological artifacts, than the empirical calibration curve method. When analysing a real object with irregular size, or at least no shape, geometry, and/or incorrect positioning, an additional correction factor for X-ray fluorescence line intensities must be entered. The problem of the contributions to the error specific to an irregular surface or incorrect positioning intrinsic to the FP method, in the more

enlarged context of considering a real experimental setup in which irradiation and detection angles are not exactly constant, as assumed in the fundamental parameter method (Trojek & Trojková, 2023).

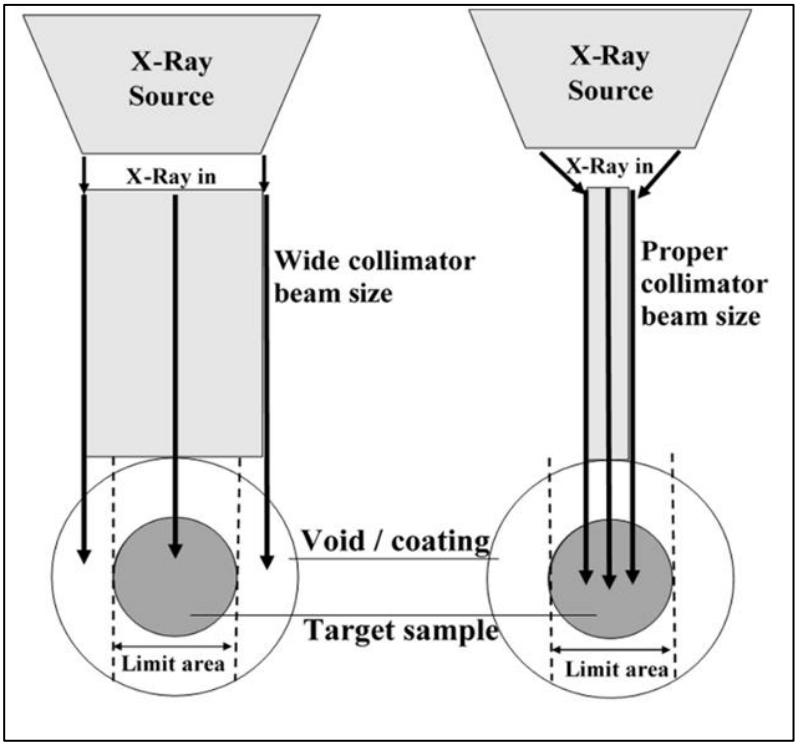

Figure 2.21 Influence of the Sample Size of the Sample on X-Ray Signal (Mazuki et al., 2021)

To reduce the size of the analysed target area of the jewellery samples to avoid other impurities, the usage of smaller collimators is always applied, as shown in Figure 2.21 (Mazuki et al., 2021). However, the EDXRF detector could only capture a low fluorescent signal due to the narrower X-ray beam on the sample target. This minimal fluorescent signal led to poor spectral distribution (Sitko et al., 2009). Furthermore, the presence of more dominant elements in the sample could have contributed to this low fluorescent signal observation. This required a prolonged counting time to achieve a higher fluorescent signal. The factors of the corrective irregular shape are considered. The effectiveness of the collimator size on the real gold sample, such as jewellery, will be evaluated

2.7 Metrological Traceability of the EDXRF Method

For measurement results to be considered reliable, they must align with recognized international convention calibrators with calibration certificates of metrological traceability of the embodied quantity value. Traceability, therefore, refers to the process of establishing procedures that ensure the quantitative results of an analytical measurement can be traced back to the International System of Units (SI). According to the International Vocabulary of Basic and General Terms in Metrology, traceability is defined as "the property of a measurement result or standard value that allows it to be connected to stated references, typically national or international standards, through an unbroken chain of comparisons, each with defined uncertainties (VIM, 2021). Figure 2.22 shows a hierarchy of the traceability chain of embodied quantity value in analytical analysis (de Bièvre et al., 2011).

Therefore, establishing traceability for linking the EDXRF method to stated references includes analysing certified reference materials (CRM) and comparing results with those obtained using alternative methods recognized as reference methods. The expression of results should include specified uncertainties, derived from a thorough inspection of an uncertainty budget that encompasses the main stages of sample preparation, calibration, measurements, and the quantification model used. Measurement conditions, calibration procedures, and calculations must be clearly defined in operational procedures. Additionally, implementing an internal quality control practice, along with participation in proficiency tests, is necessary to ensure the traceability of analytical results (ISO 17025, 2017).

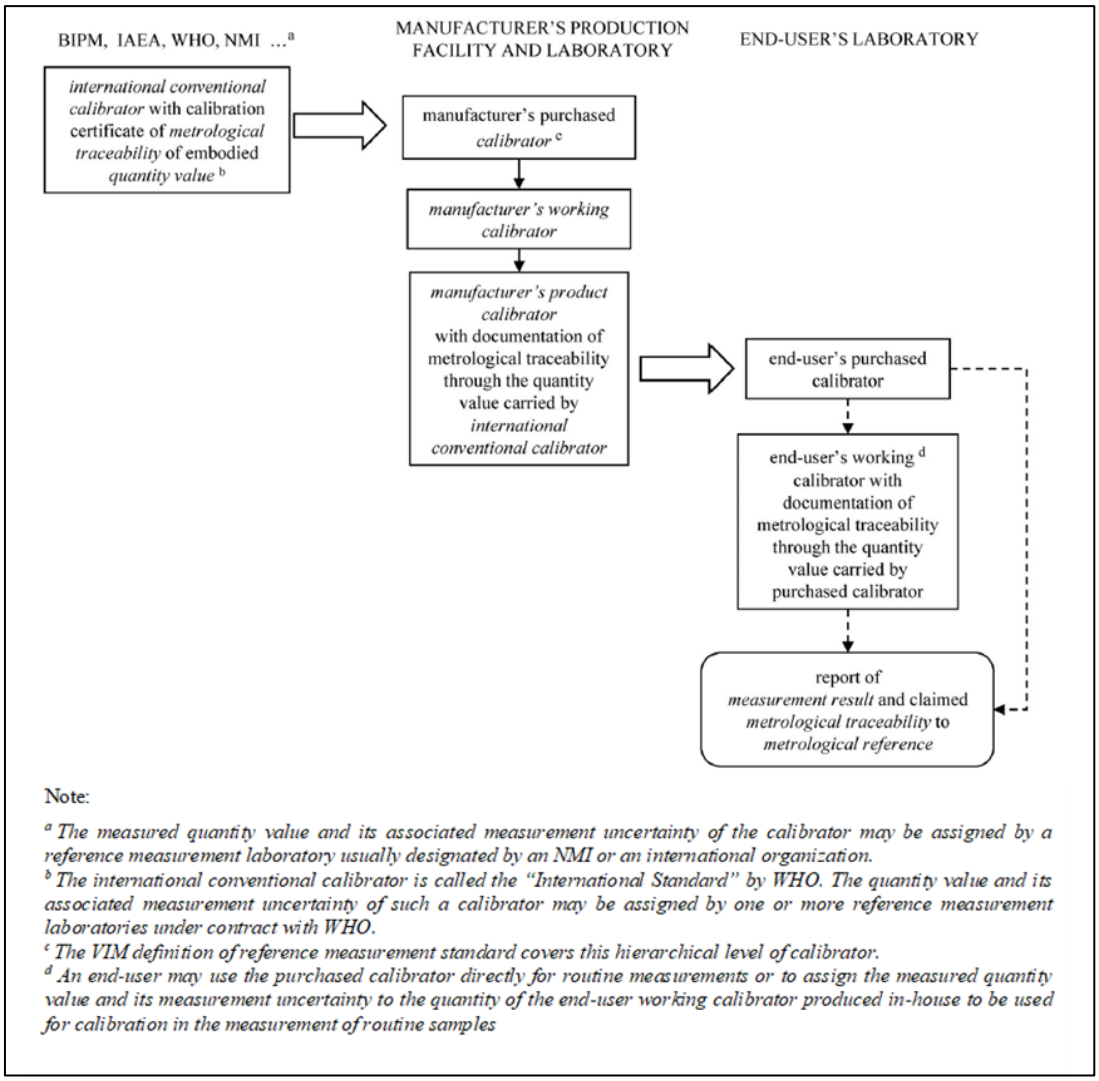

Figure 2.22 A Hierarchy of Calibrators Starts with "an International Conventional Calibrator with a Calibration Certificate of Metrological Traceability of Embodied Quantity Value".

2.8 Method Validation of the EDXRF Method

For results to be comparable, they must all be traceable to an SI Unit (De Bièvre & Taylor, 1997). Although direct traceability to the SI unit is the ideal goal, achieving this connection is not straightforward and is not the typical approach in the EDXRF method. The measurand, usually expressed as a mass fraction, is linked indirectly to a measurement procedure. It needs to be defined as a function of the measurement parameter, which is the fluorescence characteristic radiation count rate. This involves creating a working equation that models the experimental measurements and conditions

and assigning results to the measurement. Subsequently, the validity of the working equation (method specification) is evaluated based on its ability to accurately represent the real situation. This assessment is carried out through validation processes and uncertainty evaluations. A general scheme illustrating the main steps for the EDXRF method validation and quality management activities is provided in Figure 2.23 (Markowicz et al., 2007).

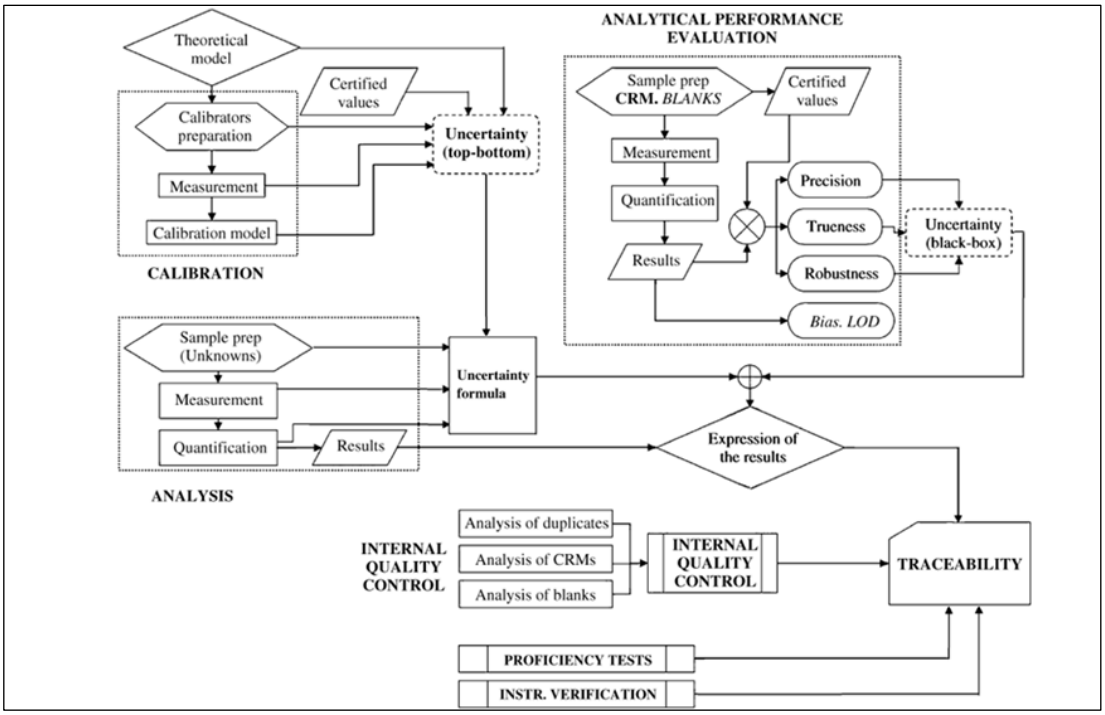

Figure 2.23 Flow Chart for Method Implementation and Quality Management in the EDXRF Method

Method validation is a critical process that ensures the accuracy and reliability of analytical measurements. This validation is achieved through two primary approaches: performing measurements on suitable certified reference materials (CRMs) or comparing the results obtained from a given method with those produced by reliable independent methods. The rationale behind these approaches is grounded in the fact that the certified values provided by reference materials have a higher metrological level compared to the results generated by individual laboratories, which can often vary due to a range of factors (Thompson, 1997).

Certified reference materials can be classified into two categories: pure reference materials and matrix reference materials. Among these, matrix reference materials are predominantly utilized in practical applications. Matrix reference materials are chosen based on their ability to closely resemble the composition and properties of the samples being analysed, which enhances the relevance and applicability of the validation process. When assessing the suitability of a matrix reference material for a specific analytical method, it is essential to evaluate several key factors. Firstly, the alignment of the elemental mass fraction range of the reference material should closely match that of the target samples. This ensures that the validation reflects the actual conditions under which the analytical method will be used (Sargent, 2020) .

Matrix compatibility is equally important, as discrepancies between the matrix of the reference material and that of the sample could lead to erroneous results (Trapmann et al., 2017). Potential interferences that could arise during the analysis should also be considered, as these can significantly impact measurement outcomes. Other practical considerations include the size of the sample; a larger sample may provide more homogenous results, but it must still be manageable for analysis. Homogeneity of the reference material is crucial, as it ensures that each portion taken for analysis is representative of the whole. Stability over time is another vital factor, as the reference material must maintain its properties under various storage and handling conditions.

Furthermore, the uncertainty values associated with the reference materials should be minimal to promote confidence in the validity of the measurements. Detailed certification procedures that delineate how the certification was conducted are also essential to affirm the reliability of the reference material. A key component of any certified reference material is its accompanying certificate, which must include a traceability statement. This statement provides transparency by outlining the principles and procedures employed to determine the property values and their associated uncertainties. The certificate is also instrumental in establishing the reference material as a common basis for comparison, serving as a universal measurement scale to which all results derived from different analytical methods can be referred. In this context, the reference material not only enhances the accuracy of measurements but also establishes a vital link through the issuing laboratory, promoting trust in the analytical results produced (Krummenauer et al., 2021).

2.9 Method Calibration of the EDXRF Method

Calibration is a crucial method for establishing traceability linkage. It involves comparing the unknown value of the sample with known values (standards) for various purposes. In the EDXRF method practice, the main calibration procedures include: (1) ensuring the proper functioning of the equipment (equipment calibration), (2) establishing the energy-channel relationship for analyte identification (energy calibration), and (3) establishing the count rate-concentration relationship for analyte quantification (sensitivity calibration). As previously mentioned, the accuracy of the chosen working equation for a given calibration model is of utmost importance. Significant uncertainty could arise if a working equation based on simplifications for monochromatic excitation is used with polychromatic excitation. For example, sensitivity should be defined as an independent factor for any sample type (e.g., intermediate or infinite thickness) only when monochromatic excitation is used. In cases of polychromatic excitation, it is more appropriate to determine geometric factors for calibration, as sensitivities for thin reference samples differ from those for intermediate-thickness samples. Additionally, improper adjustments in setup parameters when performing calibration and measurements can introduce further uncertainty to the results (Mazuki et al., 2023).

The quality of calibration of the EDXRF method is critical in determining the uncertainty of analytical results. Proper calibration ensures that the measurements are accurate and reliable, minimizing errors in the final data. Using certified reference materials (CRM) for sensitivity calibration in straightforward quantification models is often an effective approach, as these materials have well-established and certified values that can serve as a reliable benchmark for calibration. A certificate issued for this CRM is critical to maintaining the integrity of the traceability chain (Trapmann et al., 2017).

2.10 Working Range and Linearity

In the EDXRF method, the count rate measured of the characteristic radiation and the mass fraction of an element depend on both the experimental conditions and the composition of the sample. Experimental conditions include the type of radiation used for analysis, the energy distribution of this radiation, the efficiency of the detector, and

the design of the setup. These factors affect both the production and detection of X-rays. Additionally, we need to make extra corrections for x-ray attenuation and secondary enhancement effects in the sample. This makes the relationship between the measured count and the elemental mass fraction usually non-linear. Ideally, we would need to know the composition of the sample beforehand to estimate these corrections, but that is often not possible. As a result, these corrections are typically calculated during an iterative process (Markowicz et al., 2007).

Most of the EDXRF method simplifies the general relationship between elemental composition, the intensity of excitation flux, and the measured fluorescence and scattered radiation. By carefully selecting sample preparation and excitation conditions, we can make this relationship more linear. In other cases, empirical or theoretical methods help estimate corrections for sample attenuation and enhancement effects. The effective working range or linearity of the EDXRF method depends on the theoretical model used. For example, normalizing the count rates of measured fluorescent to scattered radiation can compensate for differences in attenuation. However, this is only valid if there are no significant changes in the total sample's attenuation coefficient between the energies of the characteristic and scattered radiation (Sitko & Zawisz, 2012).

2.11 Precision and Bias

The concept of precision refers to how closely results agree with each other. This is measured as the variation in results from repeated analyses. The standard deviation of a set of repeated measurements from one sample mainly shows this precision and is often called repeatability. The main causes of this variation include counting statistics and the quality of spectrum analysis done by the analyst. Random errors that occur in other steps, like sample preparation and quantification, also affect precision. To truly assess precision, it’s important to look at the variation in results from several replicates, each involving all steps of the analytical procedure. This helps capture all sources of uncertainty in terms of reproducibility. Meanwhile, the trueness measures how close the average of many test results is to the correct or accepted reference value (Frahm, 2013).

In the EDXRF method, there are two main sources of bias: first, interference from the blank, and second, errors in the quantification process. Excitation of elements

in the spectrometer or detector can create spectral interferences, often referred to as instrumental background. This excitation can occur from both direct radiation from the source and scattered radiation from the sample. This makes correction difficult and adds uncertainty to the results, which may lower the limits of detection (Conrey et al., 2014).

2.12 Statistical Analysis of Student's t-test in Analytical Method Evaluation

Statistical evaluation is a crucial component in analytical method evaluation, ensuring the reliability, accuracy, and comparability of measurement results. Among inferential statistical tools, Student's *t*-test is widely employed to assess whether a statistically significant difference exists between the mean values obtained from two analytical methods or between experimental results and certified reference values (Ellison & Willians, 2019). In analytical chemistry, the *t*-test is extensively applied to evaluate method accuracy, trueness, and equivalence, particularly when alternative techniques are proposed as replacements for established reference methods (Mishra et al., 2019).

The *t*-test assumes of normally distributed data and is especially suitable for small sample sizes, which are common in analytical method validation studies. For paired measurements, the test statistic is defined as Equation 2.3:

$$t = \frac{\bar{d}}{s_d/\sqrt{n}} \tag{2.3}$$

where $\bar{d}$represents the mean difference between paired measurements, $s_d$is the standard deviation of the differences, and $n$is the number of observations. The calculated *t* value is evaluated against the critical *t* value (t_{crit}) obtained from the *t*-distribution at a selected confidence level, typically 95%, and degrees of freedom defined as $v = n - 1$. If the absolute value of the calculated *t-statistic* does not exceed t_{crit}, the null hypothesis, indicating no statistically significant difference between the compared means, is accepted (Mazuki et al., 2023). In addition to hypothesis testing, confidence interval analysis provides further insight into method comparability by estimating the range within which the true mean difference lies. The confidence interval for the mean difference is expressed as Equation 2.4:

$$\bar{d} \pm t_{\text{crit}}\left(\frac{s_d}{\sqrt{n}}\right) \tag{2.4}$$

The inclusion of zero within this interval indicates statistical agreement between the two analytical methods being compared. This approach is particularly valuable in analytical method evaluation, as it allows both the magnitude and significance of potential systematic bias to be assessed quantitatively (Belouafa et al., 2017). By comparing experimental results with certified reference materials or established standard methods, the *t*-test enables objective, statistically defensible decision-making based on predefined confidence levels rather than subjective judgment. Numerous studies have demonstrated that the student's *t*-test is effective in detecting systematic bias, verifying method trueness, and confirming agreement between analytical techniques. Consequently, the *t*-test remains a fundamental statistical tool in analytical method validation, supporting the acceptance of new analytical approaches in both laboratory and industrial applications, in accordance with international guidelines for analytical quality assurance (Mishra et al., 2019).

2.13 Traceability of EDXRF Method

The traceability flow in the EDXRF method is a critical component in ensuring both the accuracy and credibility of assessments regarding gold purity. This traceability process involves linking each step of the analysis to internationally recognized standards and reference materials. This approach not only guarantees precise and reliable results but also enhances the confidence of various stakeholders in the integrity of the gold market, including investors, traders, and regulatory bodies. From previous discussions, it has been established that the EDXRF method has been successfully developed to provide accurate determinations of gold purity within precious metals. This is significant because the EDXRF method is renowned for being a non-destructive analytical method, allowing for the assessment of materials without altering their physical state. Consequently, it is widely employed in assigning values to CRM, which serve as benchmarks for quality assurance in analytical laboratories (de Bièvre et al., 2011).

Each CRM is assigned with reference value accompanied by an uncertainty measurement that reflects a stated level of confidence, providing further assurance of the data's reliability. CRMs are indispensable tools in achieving metrological traceability, linking measurement results directly to the SI (International System of

Units) unit known as the mole, which pertains to the quantity of substance. This connection ensures that measurements are both accurate and comparable over extended periods and across different geographical locations. Despite their importance, only a limited selection of CRMs currently exists within the precious metals sector. As a result, the usage of non-certified reference materials has become a more common practice among analysts and laboratories (Markowicz et al., 2007).

Considering these factors, the study has decided to focus on the development of a gold alloy as a certified reference material. This choice is justified by the availability of the alloy, broad demand across various markets, and high intrinsic value. Producing a gold alloy CRM may fill a gap in the existing market for certified materials in the precious metals, thus aiding in the standardization of purity assessments and contributing to greater transparency and trust in gold trading and valuation practices. Figure 2.24 shows a detailed flow chart to produce chemical reference material (CRM).

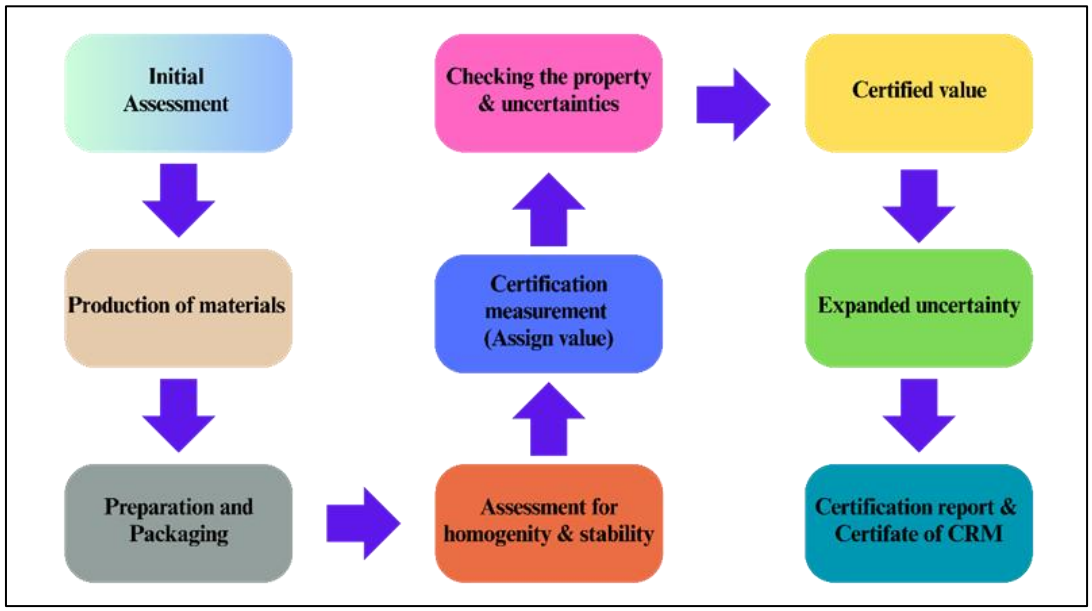

Figure 2.24 Flow Chart to Produce Certified Reference Material (CRM)

Therefore, in this study, due to increasing demand from the community for reliable certified analytical results, EDXRF laboratories face an urgent need for the implementation of quality management systems, especially those that meet the general requirements of ISO / IEC 17025 testing and calibration laboratory competencies standard document. Some specific features of the EDXRF method require a careful interpretation of some concepts related to method validation and quality control.

Measurement conditions, calibration procedures, and calculations must be clearly and adequately stated in operating procedures. Internal quality control practices complemented by participation in comparison tests are also required to ensure the effectiveness of the analysis results.

CHAPTER 3
RESEARCH METHODOLOGY

3.1 Introduction

This chapter provides comprehensive details of the sample preparation procedure and characterization. These include the experimental configuration applied to solve the matrix effect and optimization of the instrumentation, determination, and validation of the correction factor, and evaluation of the robustness of the proposed approach. The primary equipment utilized in this study is the EDXRF method. As depicted in Figure 3.1, a research roadmap is demonstrated during the method and managing the quality of the EDXRF method. The aim is to enhance the accuracy of measurements and provide traceability to the SI Unit. This study was structured into four distinct phases, according to the four (4) outlined objectives, each serving a specific purpose in the overall experimentation process, as discussed in detail in chapter 3.1.1.

3.1.1 Overview of the theoretical optimisation of the EDXRF

The initial phase concentrated on the preparation of gold calibration materials, a critical step that sets the foundation for accurate measurements in subsequent stages. The main objective of this phase was to create a high-quality matrix composition characterized by homogeneity. Such homogeneity is essential for developing an effective calibration model for the EDXRF method measurements. To achieve this, gold calibration materials were formulated to represent a variety of gold alloy matrices, specifically gold-silver-copper alloys. The gold content within these materials was varied systematically, covering a range from 75.00 wt.% to 99.99 wt.%.

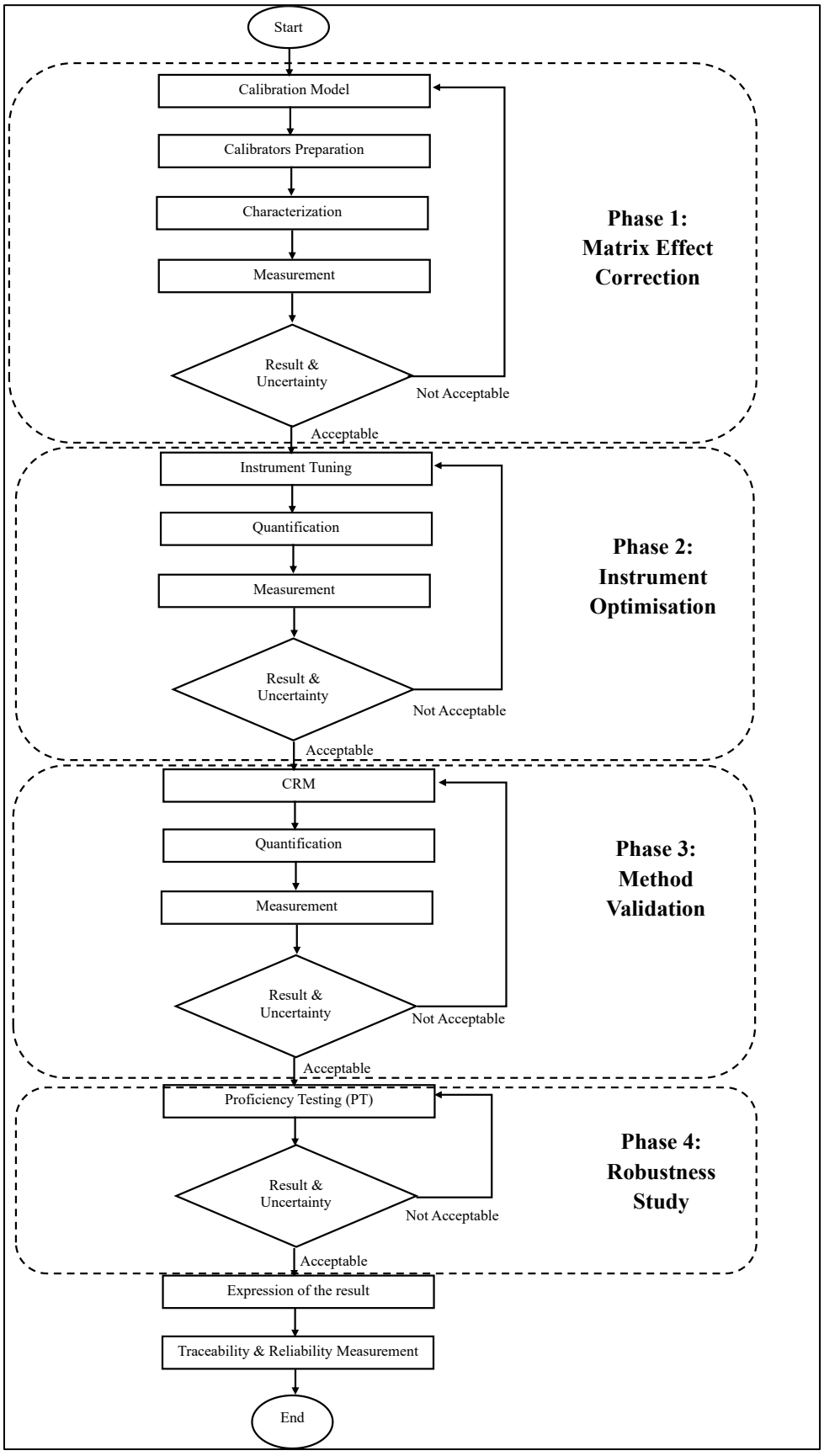

Figure 3.1 Research Roadmap Illustrating the Methodology and Quality Management of the EDXRF Method

The first phase aims to facilitate accurate measurements; the calibration materials were manufactured in the form of solid discs. Each disc was designed to be flat and free from any cavities or imperfections that could affect the measurement process. This attention to detail ensures that the calibration materials exhibit consistent characteristics across all samples. To evaluate the composition of these calibration materials, a combination of analytical techniques was employed. The fire assay method, also known as cupellation, was utilized to determine the gold content with high accuracy. Meanwhile, WDXRF was implemented for the analysis of silver and copper content within the alloys. An important aspect of this phase was the assessment of the repeatability of the gold content in each calibration material. This evaluation is crucial, as it establishes the reliability of the calibration standards. It was determined that the standard deviation for the gold content in the target materials remained ± 0.05 %wt., indicating a high level of precision and consistency in the preparation of the calibration materials. This level of repeatability is essential for ensuring the accuracy of the subsequent measurements in the overall study. Figure 3.2 shows the first phase of the preparation of gold calibration materials.

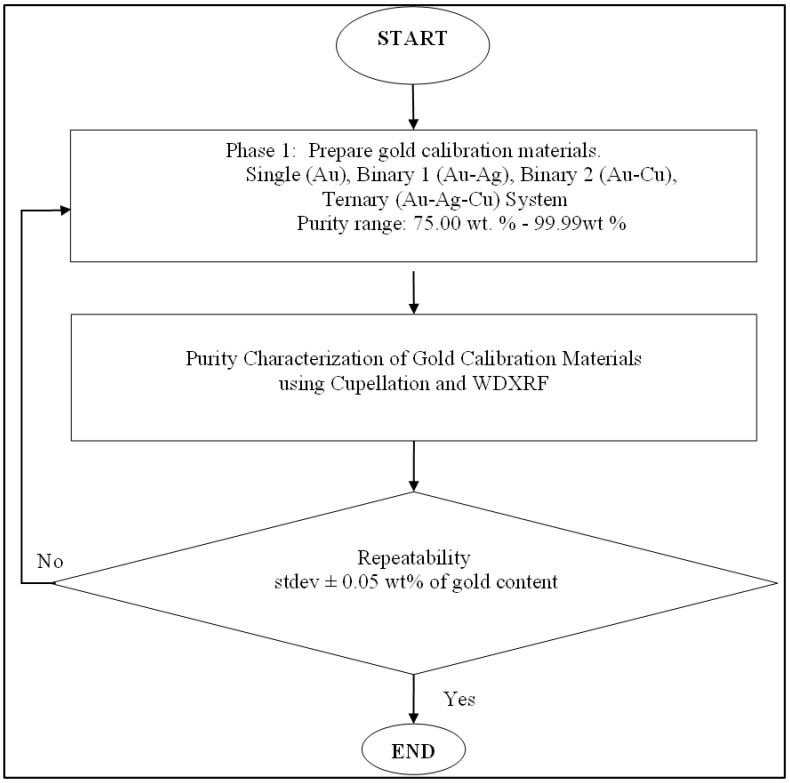

Figure 3.2 The First Phase of the Preparation of Gold Calibration Materials

The second phase of this comprehensive study is specifically designed to focus on the identification and optimization of the EDXRF method configuration. The primary objective in this phase is to enhance the accuracy of measurement analysis related to gold products. To achieve this, a careful examination of the selection process for spectral lines and the size of the collimator beam is underway. This assessment aims to minimize errors that arise from the intricate compositions and the irregular size of gold products. The selection of the Lα and Lβ peaks for gold was critical for accurate analysis. The higher-energy Kα and Kβ lines for gold were not used because the X-ray source (50 kV) was not powerful enough to effectively excite those peaks. Thus, the lower-energy L-lines of gold were chosen for analysis. Meanwhile, K-lines of copper and silver have been selected due to their relatively lower energy and sufficient to excite using an X-ray tube. Four (4) collimator beam sizes used in the experiment range, such as 1.0 mm, 2.0 mm, 3.5 mm, and 8.8 mm, to study the influence of collimator beam size on the XRF measurement accuracy and signal strength. By adjusting the beam size, it expected to optimize the balance between signal intensity and measurement precision, which is vital for achieving accurate results in elemental analysis using XRF.

In this phase, the research employs a combination of fundamental parameters (FP) algorithms alongside an empirical approach that utilizes gold calibration materials. This dual methodology is crucial in establishing the most accurate linear calibration curve, which correlates the measured values to the reference values. The latter are determined using the established cupellation method, also known as fire assay, specifically for measuring gold content. Additionally, the methodology for assessing silver and copper content draws on results obtained from the WDXRF method. The calibration curve not only reflects the relationship between measured and reference values but also aims to ensure a strong degree of linearity. The goal is to tune the calibration process to achieve regression values that fall within the narrow range of 0.990 to 1.010, denoted by the coefficient of determination, r^2. To provide a visual overview of the processes and steps involved in this phase, a flow chart has been created and is available for review in Figure 3.3.

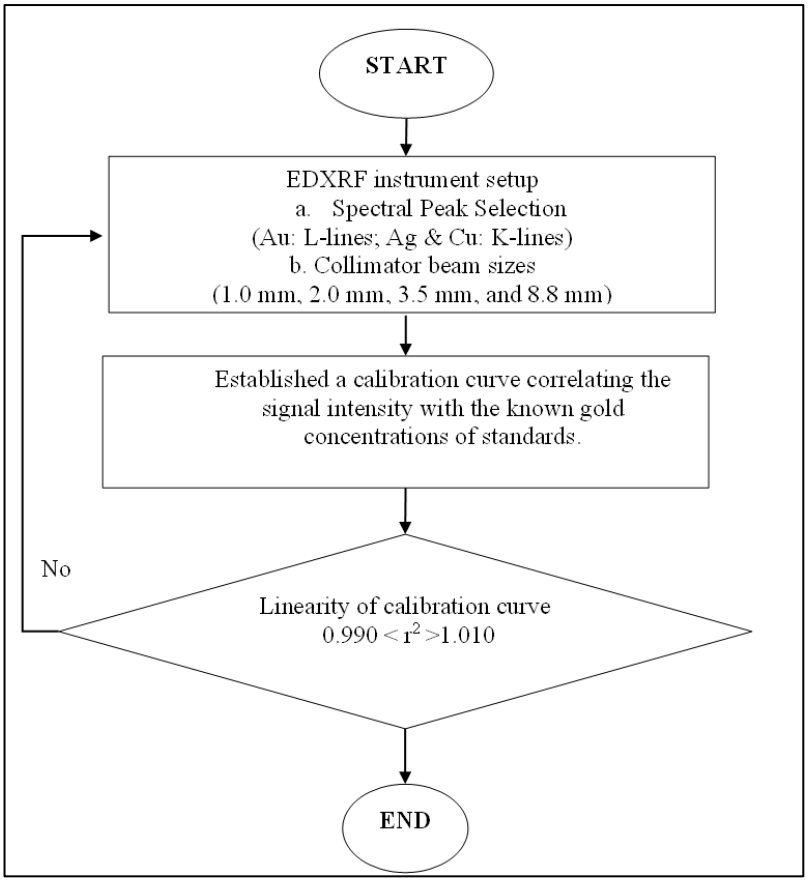

Figure 3.3 Optimisation of the EDXRF Method for Gold Purity Measurement

The third phase carried out in this study involves the meticulous determination of correction factors, commonly referred to as *k-factor* values. These values are essential for realigning the measurement instruments and calibrating the systematic deviations that occur with each specific alloy mixture. This calibration process is achieved by conducting comparisons between the measured values of the samples and well-defined certified reference materials that act as a reliable benchmark. Following this initial determination, the validity of the *k-factor* values was rigorously tested when applied to the computation of each analysed sample. This validation process is particularly important as it hinges on the similarity of the elemental composition within the gold mixtures being studied. Once the validation was completed, the unknown compositions of various commercial gold samples were accurately rectified using the established k-factor values. To facilitate a clear understanding of this methodology, a flow chart illustrating the steps taken to determine the correction *k-factor* values and to validate the overall method can be found in Figure 3.4.

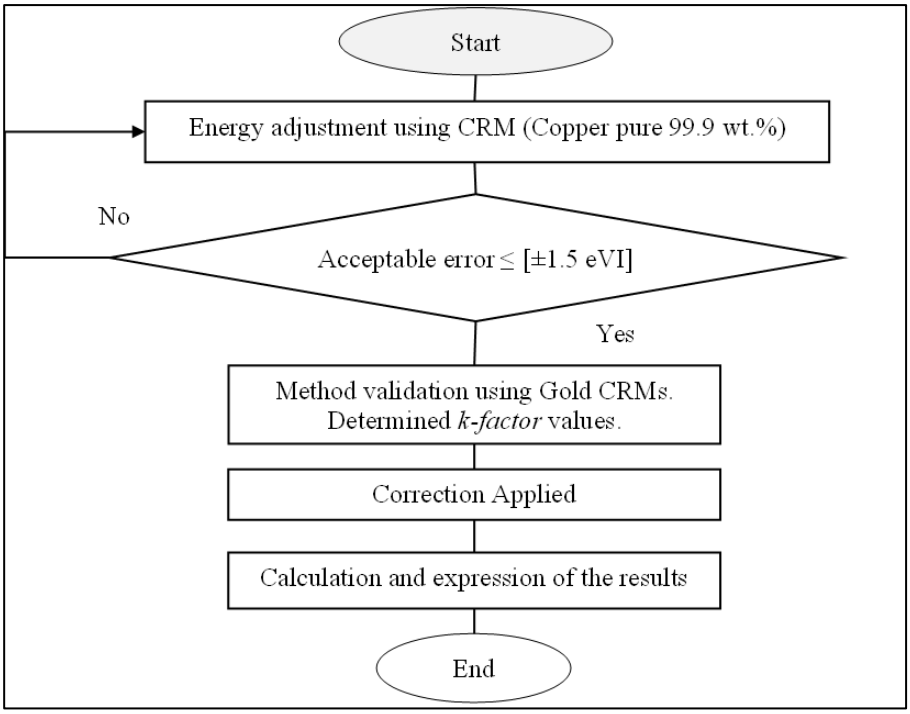

Figure 3.4 The Flow Chart for Determining Correction *k-factor* Values and Validation of the Method

To establish that results are both comparable and sufficiently robust to support claims of traceability, it is vital to effectively link the results obtained from the EDXRF method to recognized reference standards. This can be accomplished through a systematic comparison with results derived from alternative methods that are widely accepted as reference methodologies in the field. Traceability, in this context, refers to the comprehensive process of developing and implementing procedures that facilitate the ability to relate the quantitative outcomes of an analytical measurement back to an internationally recognized standard, specifically the International System of Units (SI). For the results to be meaningful and trustworthy, they must be presented alongside clearly stated uncertainties. These uncertainties should arise from a meticulous examination of an uncertainty budget that encompasses the principal stages involved in the analytical process. This budget should detail aspects such as sample preparation techniques, the calibration procedures employed, the measurement methodologies used, and the specific quantification models that are applied throughout the analysis. Moreover, it is essential to clearly articulate the measurement conditions alongside the operational steps taken during calibration, ensuring that calculations are fully

documented and replicable. This clarity in procedure is critical to maintaining the integrity of the results.

The final stage of this process emphasizes the importance of implementing rigorous internal quality control practices. These practices should be complemented by active participation in proficiency testing (PT), which serves as a benchmark to verify the traceability and accuracy of the analytical results produced. By adhering to these detailed protocols, laboratories can enhance the credibility of their findings and ensure compliance with established standards. International validation through interlaboratory comparisons is a valuable and necessary method for assessing the technical competence of laboratories. The Institute of Metrology of Bosnia and Herzegovina, specifically the Chemistry Department (IMBIH LH), has organized a Bilateral Interlaboratory Comparison (IMBIH.LH-B01.PT/20) focusing on gold alloys. This comparison aims to evaluate the technical competence of the NMIM laboratory and provide an objective review of its performance based on established methods. The laboratory has successfully demonstrated its testing capabilities at the international level, leading to the inclusion of its Calibration and Measurement Capabilities (CMC) for gold content in yellow gold alloys in the BIPM database. Competence in organizing interlaboratory comparisons (ILC) has been confirmed through accreditation following standard EN ISO/IEC 17043 requirements, specifically for gold mass fractions ranging from 33.30 wt% % to 99.99 wt %. A flow chart illustrating the process of the bilateral comparison can be found in Figure 3.5.

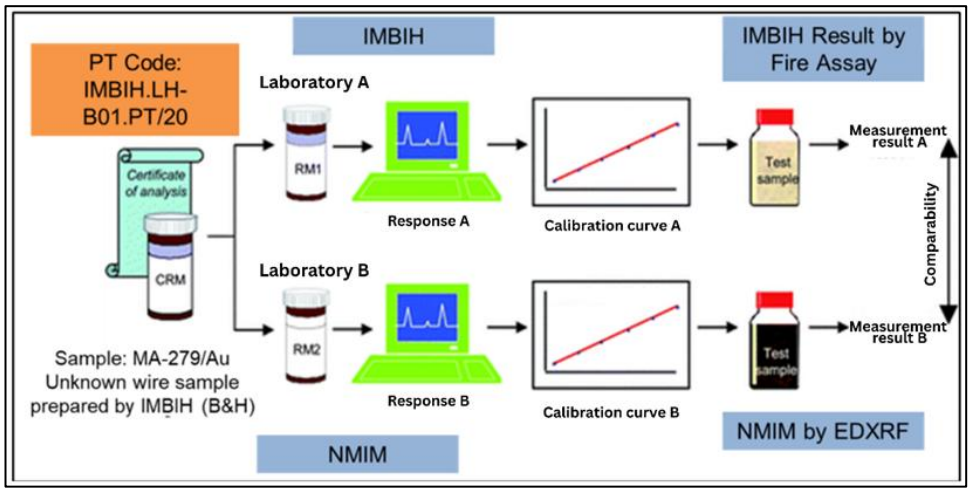

Figure 3.5 The Flow Chart of the Interlaboratory Comparison (ILC) Process

3.2 Environmental Condition

The study of the environmental laboratory is crucial to ensure that the EDXRF method is operated under optimized conditions. Prolonged exposure to high humidity can lead to corrosion and degradation of sensitive components within the EDXRF method. Additionally, the instrument detectors are sensitive to temperature variations. The detectors, particularly semiconductor-based detectors such as silicon drift detectors (SDDs), are highly sensitive to temperature fluctuations. Elevated temperatures can increase thermal noise in the detector electronics, reducing the signal-to-noise ratio and degrading energy resolution. This, in turn, affects the ability of the instrument to distinguish closely spaced spectral peaks, reducing sensitivity and potentially leading to inaccurate quantification of trace elements. Conversely, low or fluctuating temperatures may affect detector cooling systems, further impacting stability. These effects can compromise the stability and reliability of the measurements, leading to increased uncertainty.

In this study, the laboratory has controlled and monitored temperature and relative humidity using a thermohygrometer, maintaining conditions within 22°C ± 3°C and 65% ± 15%, respectively, as shown in Figure 3.6. All data has been transferred to a computer using HOBOware software, and a calibration certificate for the digital thermohygrometer can be found in Appendix A.

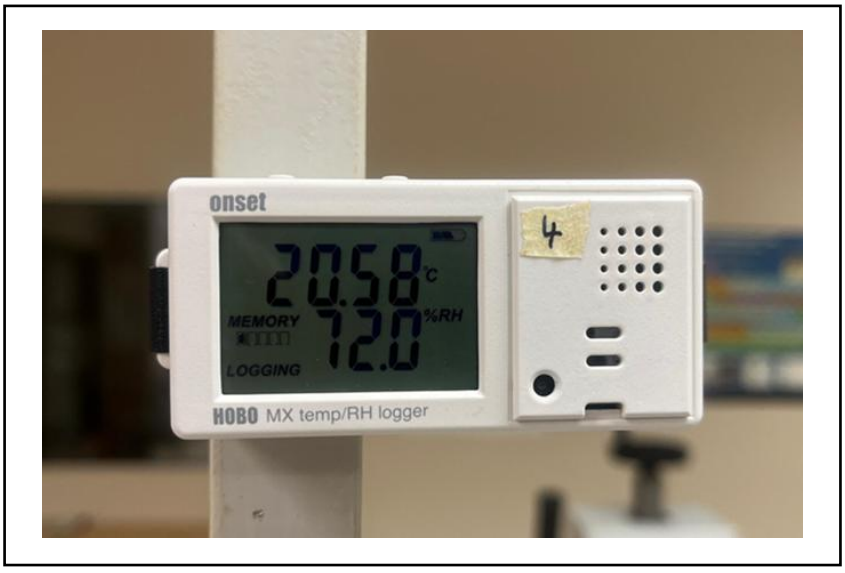

Figure 3.6 Digital Thermoghyrometer (Model: MX 1101)

3.3 Sample Preparations

3.3.1 Gold Calibration Materials (CM)

A series of carefully designed homogeneous gold materials was fabricated to closely resemble actual samples to develop calibration materials (CM). Homogeneity ensures the uniform distribution of gold and alloying elements throughout the material. This step is crucial, as inhomogeneous materials can compromise the accuracy, precision, and reproducibility of gold purity measurements. These materials were intended to optimize the EDXRF method by effectively correcting for matrix effects. The calibration materials comprised a precise weighing of the mixture of gold, silver, and copper, formulated to emulate the entire spectrum of yellow-gold alloys to give a total of approximately 5 grams. The mass fraction percentages of these alloys ranged from 75.00 *wt%* to 99.99 *wt%* gold content. The sample was then placed ceramic crucible for the melting process at 1050℃ in the furnace for 20-30 minutes. During the melting process, the samples are repeatedly stirred using a graphite rod to ensure homogeneity. A small amount of Borax (sodium borate), slowly added to the crucible to ensure it properly dissolves and forms the protective flux layer. This helps maintain the purity and prevents the formation of unwanted oxides. Once the gold is fully melted and impurities have been removed, the molten gold is carefully poured into a mould.

After pouring the gold into the mould, it is immediately quenched by immersing it in water or sometimes oil to cool it quickly. This rapid cooling solidifies the gold and preserves its shape. The mixture was subjected to a rolling process and subsequently cut into discs, each with a diameter of 12 mm. This fabrication process yielded discs with a surface area of approximately 113.10 mm^2, as depicted in Figure 3.7. The preparation stages for these calibration materials are thoroughly illustrated in Figure 3.8, showing each step of the process for clarity.

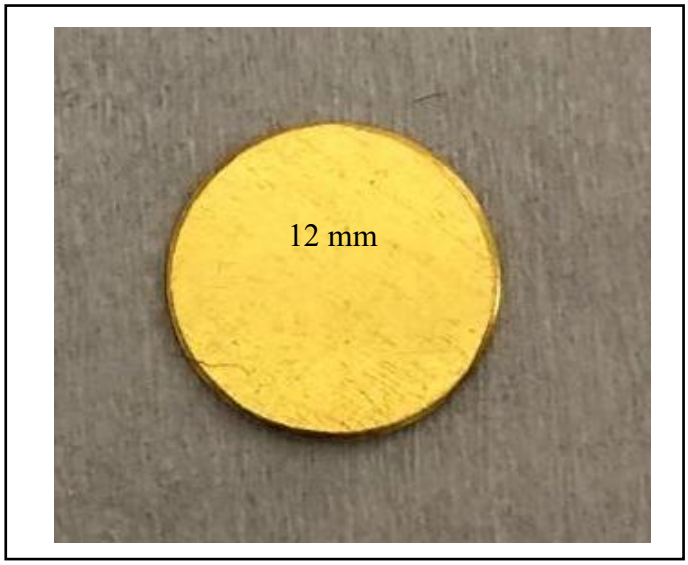

Figure 3.7 The calibration materials (CM) were rolled and cut into discs

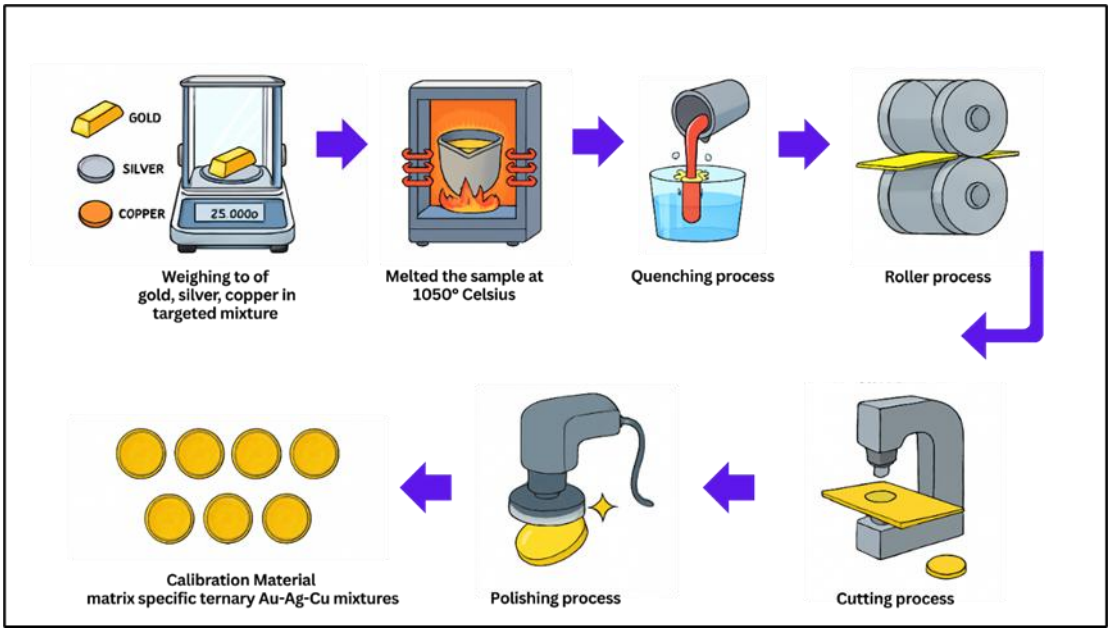

Figure 3.8 Preparation of Gold Calibration Material

The assessment of gold purity was conducted using the traditional fire assay method, which is well-known for its effectiveness in isolating gold from other metals. Alongside this, a WDXRF method was utilized to analyse and quantify the silver and copper content within the materials. The results of the element purity experiments revealed that the alloying elements were uniformly distributed throughout all the

calibration materials, leading to highly consistent outcomes. This uniformity also demonstrated repeatability in testing, with variations in gold content confined to within ± 0.05 *wt%.* For a comprehensive overview, Table 3.1 presents the detailed specifications of the calibration materials that reflect the various gold alloy compositions employed in this study.

Table 3.1

The Gold Matrix Composed of Au-Ag-Cu in the Range of 75.00 wt % to 99.99 wt%

Code of Calibration Materials	Composition in weight fraction of percent (%)		
	Au[a]	Ag[b]	Cu[b]
CM1	76.34 ± 0.05	23.66 ± 0.08	0.00 ± 0.00
CM2	75.85 ± 0.05	0.00 ± 0.00	24.15 ± 0.10
CM3	74.00 ± 0.05	15.00 ± 0.07	11.00 ± 0.07
CM4	91.89 ± 0.05	8.11 ± 0.0.5	0.00 ± 0.00
CM5	91.67 ± 0.05	4.72 ± 0.04	3.61 ± 0.04
CM6	92.02 ± 0.05	0.00 ± 0.00	7.98 ± 0.05
CM7	99.90 ± 0.04	0.00 ± 0.00	0.00 ± 0.00

[a] *Purity was evaluated with the fire assay method*

[b] *Purity was evaluated by WDXRF*

3.3.2 Gold Certified Reference Materials (CRM)

Figure 3.9 shows a set of certified gold reference materials (CRMs) selected based on their compositional similarities to the actual samples being analyzed. This selection process is crucial in ensuring that the reference materials accurately represent the gold alloys under investigation. As outlined in Table 3.2, the gold alloy compositions were rigorously certified, incorporating an expanded uncertainty figure that corresponds to a 95% confidence interval. This level of certification is vital for maintaining the integrity and reliability of the analyses performed using these reference materials. The meticulous selection of CRMs was essential for guaranteeing a homogenous distribution of gold within the samples, aligning with the guidelines established by ISO 17034. The diameter of each CRM sample is shown in the figure. To calculate the surface area of a gold disc using the formula πr^2, with π is approximately 3.14159 and r is the radius of the disc.

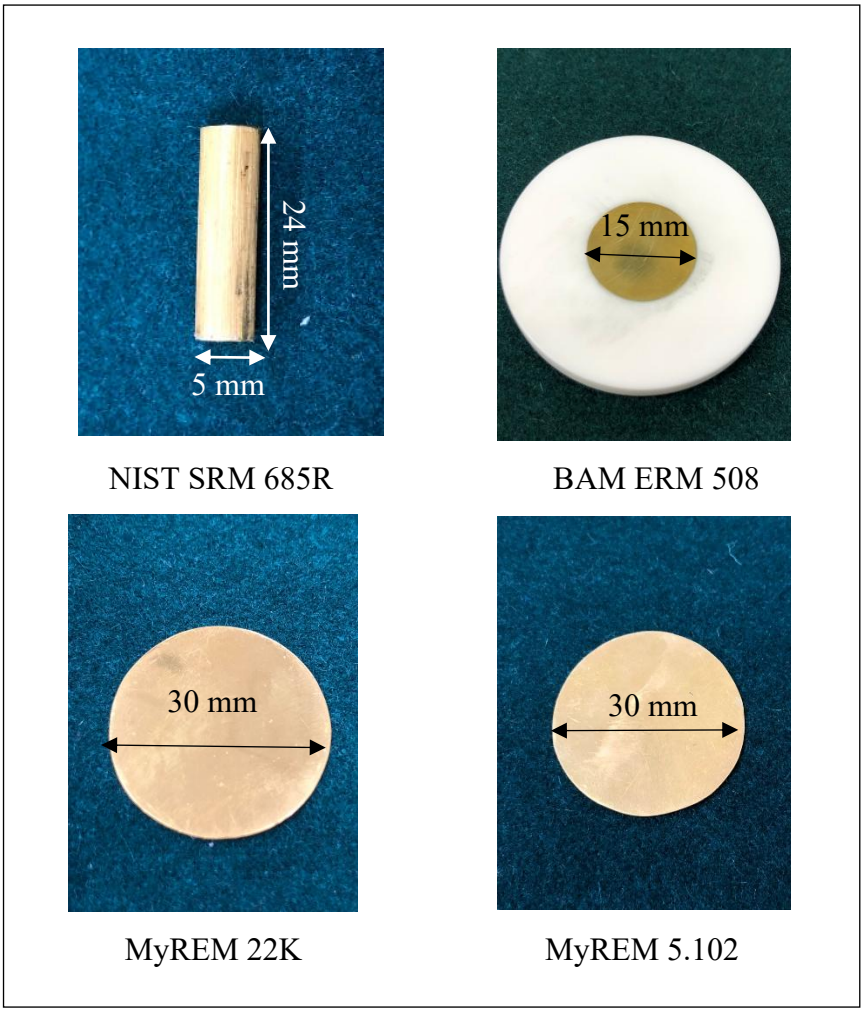

Figure 3.9 Sets of certified reference materials (CRMs)

Table 3.2
Gold Alloy Composition for Certified Reference Materials (CRMs)

Mixture	Code of CRMs	Composition in mass fraction of percent (wt%)			Sample Diameter (mm)	Calculated Surface Area πr^2 (mm^2)
		Au	Ag	Cu		
Au	SRM 685R	99.99 ± 0.05	-	-	5	19.64
Au-Ag	ERM 508	75.12 ± 0.11	24.90 ± 0.05	-	15	176.72
Au-Cu	MyREM 22K	91.80 ± 0.15	-	8.20 ± 0.05	30	706.86
Au-Ag-Cu	MyREM 5.102	92.14 ± 0.16	1.93 ± 0.05	5.96 ± 0.04	30	706.86

The SRM 685R, one of the CRMs utilized in this study, was sourced from the National Institute of Standards and Technology (NIST) in the United States. It is provided in rod form, featuring a cut surface with a diameter of 5.0 mm, resulting in a

total surface area of 19.64 mm². This specific form allows for efficient handling and uses in analytical procedures. In addition, the ERM 508 was obtained from the Bundesanstalt für Materialforschung und Prüfung (BAM) in Germany. This reference material comes in a disc form with a diameter of 15 mm, corresponding to a total surface area of 176.72 mm². The disc shape is advantageous for certain analytical techniques, providing an optimal surface for measurement. Furthermore, the National Metrology Institute of Malaysia has certified the compositions of MyREM 5.102 and MyREM 22 K. These reference materials are also offered in disc form, with a larger diameter of 30 mm, which results in a substantial surface area of 706.86 mm². This increased size allows for enhanced measurement precision and stability during analysis. Overall, the careful selection and certification of these gold reference materials are fundamental to ensuring the accuracy and reliability of the analyses conducted in this study.

3.3.3 Commercial Gold Alloy Samples

A total of sixteen (16) commercial gold alloy pieces were manufactured by Carbon Worldwide Sdn Bhd to validate the optimized EDXRF method. The real commercial sample was melted and cast to standardize it, ensuring a homogeneous composition. The samples were then cut, surface polished, and composed in several solid forms, which were designed into disc and rectangular shapes, illustrated in

Figure 3.10. These pieces share similar characteristics with commercially available gold matrix-specific materials, enabling a reliable assessment of the EDXRF method measurement technique employed in this study. Among the samples, eight were designed as round discs with a uniform diameter of 30 mm and 0.5 mm thickness, providing a consistent geometric shape for testing. In contrast, the other eight samples were rectangular, with 10 mm (width) x 18 mm (length) precise dimensions. Each sample maintained a thickness of approximately 0.3 mm, ensuring uniformity across all specimens.

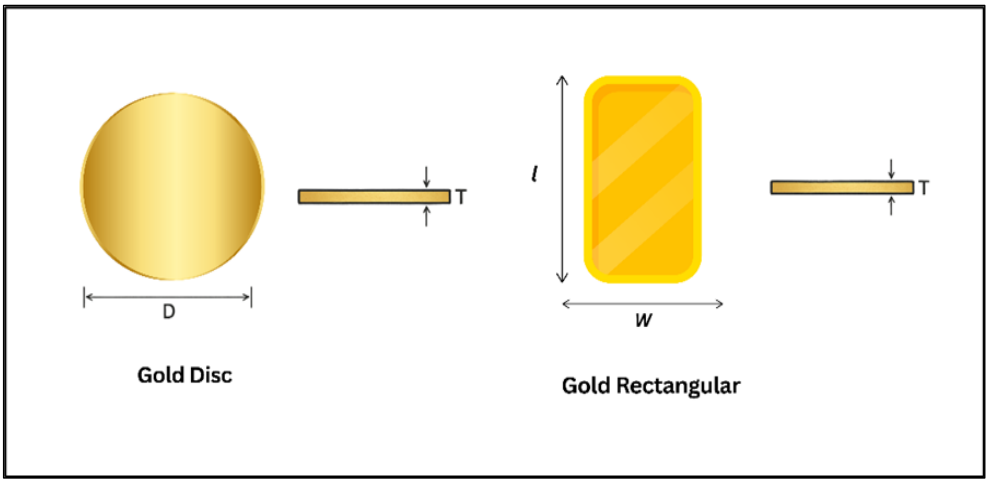

Figure 3.10 Illustrated are the Commercial-like Samples, Solid Gold Pieces, which were Designed into Disc and Rectangular Shapes

For the EDXRF analysis, each sample's surface was subjected to five separate measurements on each sample. The commercial samples exhibited a variety of compositions, predominantly featuring mixtures of gold (Au), gold-silver (Au-Ag), gold-copper (Au-Cu), and a combination of gold, silver, and copper (Au-Ag-Cu) matrices. These compositions were selected to reflect the types of materials typically found in commercial gold alloys. The sample has been labelled with code Au1 to Au16. The actual 16 samples are shown in Appendix 14. To clarify the purity levels of each sample, Table 3.3 presents a comprehensive overview of the sample codes, dimension sizes, and their respective purity assessments, which were determined using the fire assay method, a widely recognized and reliable technique for measuring metal content in precious metals.

Table 3.3
Lists Commercial Gold Alloy Materials, with Purity Measured by Fire Assay

Mixture	Sample code	Remarks	Gold Purity (wt%)	Expanded Uncertainty *(k=2)*	Sample Size (mm)
Au	AU1	Disc	99.9187	0.0459	30 (D*)* x 0.5 *(T)*
	AU2	Disc	99.9902	0.0452	30 *(D)* x 0.5 *(T)*
	AU3	Rectangular	99.9903	0.0450	10 *(W)* x 18 *(l)* x 0.3 *(T)*
	AU4	Rectangular	99.9901	0.0451	10 *(W)* x 18 *(l)* x 0.3 *(T)*
Au-Ag	AU5	Disc	83.5013	0.0482	30 (D*)* x 0.5 *(T)*
	AU6	Disc	91.7019	0.0473	30 *(D)* x 0.5 *(T)*
	AU7	Rectangular	87.5007	0.0484	10 *(W)* x 18 *(l)* x 0.3 *(T)*
	AU8	Rectangular	75.1002	0.0491	10 *(W)* x 18 *(l)* x 0.3 *(T)*
Au-Cu	AU9	Disc	91.8821	0.0480	30 (D*)* x 0.5 *(T)*
	AU10	Disc	91.9002	0.0471	30 *(D)* x 0.5 *(T)*
	AU11	Rectangular	76.1203	0.0492	10 *(W)* x 18 *(l)* x 0.3 *(T)*
	AU12	Rectangular	83.5801	0.0484	10 *(W)* x 18 *(l)* x 0.3 *(T)*
Au-Ag-Cu	AU13	Disc	91.8901	0.0490	30 (D*)* x 0.5 *(T)*
	AU14	Disc	76.3401	0.0494	30 *(D)* x 0.5 *(T)*
	AU15	Rectangular	75.1002	0.0489	10 *(W)* x 18 *(l)* x 0.3 *(T)*
	AU16	Rectangular	74.5500	0.0498	10 *(W)* x 18 *(l)* x 0.3 *(T))*

3.3.4 Interlaboratory Comparison (ILC) Samples

The 'blind' Interlaboratory Comparison (ILC) test sample is carefully prepared by the Institute of Metrology of Bosnia and Herzegovina (IMBIH) as the PT provider. The ILC test sample is created in the form of a wire that has a nominal composition of 75.0 *wt%* ± 2 *wt%* gold (Au). The precision of this composition ensures that the test sample is representative of gold alloys commonly encountered in industry and is suitable for testing various analytical methods used in gold content determination. The samples were then cut into equal pieces, each with a mass of approximately 1.0 grams and a diameter of 1.0 mm. These pieces are carefully selected to ensure that they have a consistent size and mass, which is crucial for accurate testing. Each ILC sample is identified and labelled with a specific sample identification number (MA-279/Au) as shown in Figure 3.11. To ensure that the samples remain anonymous, meaning that the participating laboratories cannot know the identity or composition of the sample in advance, which helps maintain the integrity of the ILC. The actual ILC samples are shown in Appendix 15.

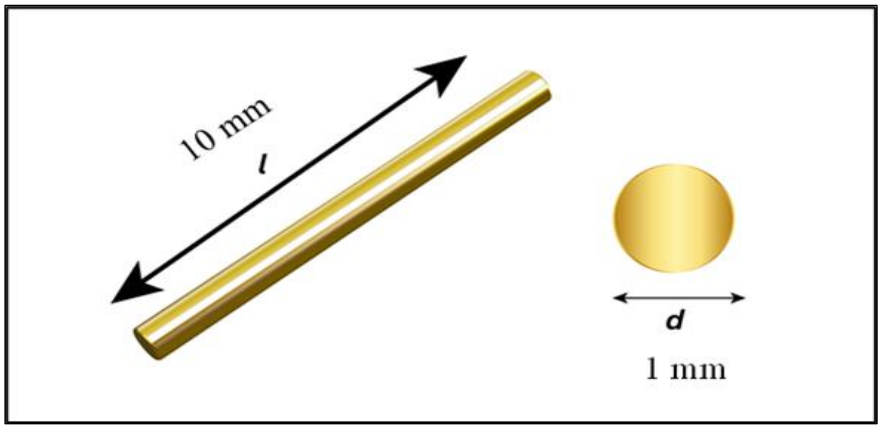

Figure 3.11 Illustration of the 'blind' ILC test sample in the form of a wire prepared by IMBIH

The assigned value of the test sample was determined by the ILC provider following ISO 13528:2015 (7.5 – Results from one laboratory). The IMBIH ensures the sample's composition is accurate, uniform, and well-documented, which helps maintain the integrity and reliability of the ILC. The use of the fire assay method to determine the assigned value is a time-tested technique for ensuring accuracy and precision, providing a reliable benchmark for gold content measurement across different laboratories.

3.4 Characterization Procedure

3.4.1 Fire Assay Method (Cupellation)

The fire assay method, also known as cupellation, was implemented in the NMIM laboratory following ISO 11426:2021 standards. This process was performed under a controlled oxidizing atmosphere in Orostudio muffle furnaces (MSC Model), as illustrated in Figure 3.12. Initially, each product was cut, and the required weight of the section being studied was measured using a semi-microbalance with an accuracy of 0.00001 grams, as shown in Figure 3.13. The samples were then rolled in mills and cut into fine strips, creating batches of the studied alloys. During the procedure, the furnace maintained a temperature of approximately 1050 °C. The temperature peaked toward the end of the cupellation when the ratio of lead to noble metals decreased significantly. The entire cupellation process lasted about 30 minutes, effectively removing all metals

except for the gold-silver alloy. Afterward, the lead button was rolled and immersed in nitric acid to eliminate the silver content. Finally, the pure gold cornet, depicted in Figure 3.14, was weighed to obtain the final weight. The weight ratio was multiplied by 100 to determine the fineness of the samples in mass fraction percent (wt%).

Figure 3.12 Orostudio Muffle Furnaces (MSC Model) that are Traceable to NMIM

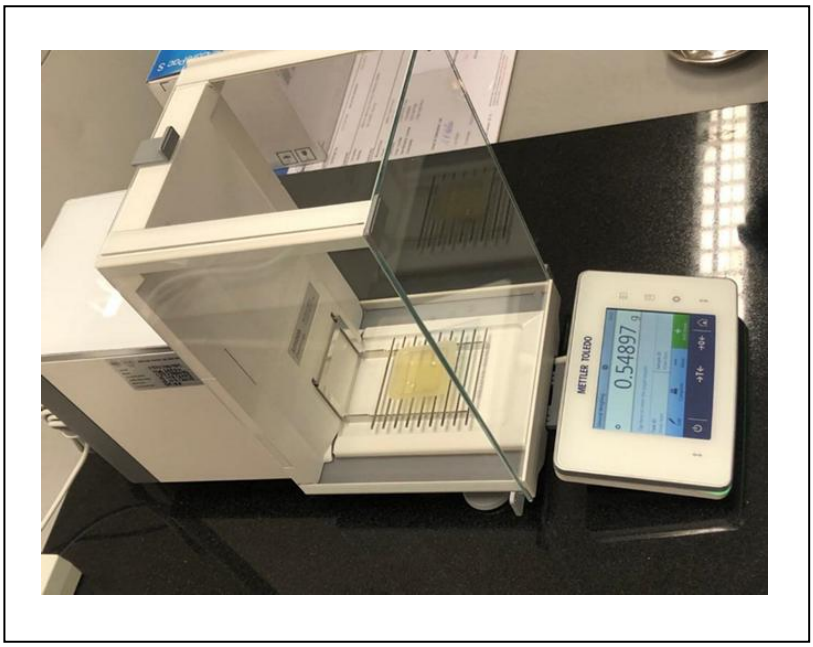

Figure 3.13 Semi-Microbalance from Mettler Toledo with Traceability to NMIM

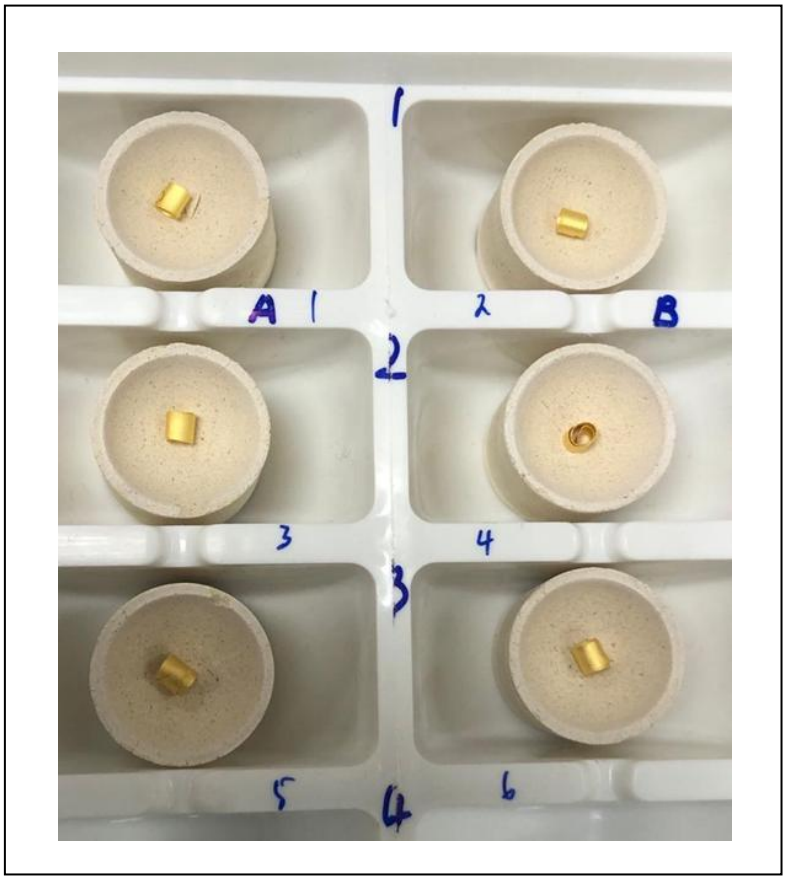

Figure 3.14 Gold Cornet After Immersed in Nitric Acid to Remove the Silver Content in Samples

3.4.2 Wavelength Dispersive X-ray Fluorescent Spectrometer

Figure 3.15 Wavelength-Dispersive X-ray Fluorescent Spectrometer

In this study, the determination of silver (Ag) and copper (Cu) content in the samples was conducted using the Thermo Scientific ARL PERFORM'X, a high-performance Wavelength Dispersive X-ray Fluorescent (WDXRF) system (Figure 3.15. The 1500W wavelength-dispersive XRF spectrometer with Rh x-ray (Rh 60 kV) tube quantitatively measures the elemental concentrations to a depth in a material, which is commonly 0.006 mm (6 micrometres) to about 1.5 mm deep, depending upon the density of the material and the energy of the characteristic x-ray emitted. XRF analysis has very low detection limits for these elements, measuring the lighter elements for concentrations greater than about 0.01 weight percent and the heavier elements to less than 10 ppm by weight. Our spectrometer also has a special crystal that provides analysis for carbon and nitrogen, though its usefulness is limited to low-density materials due to the very low energy of the characteristic carbon and nitrogen x-ray emission. It also has a small spot capability to compare the relative composition of spots of 0.5 or 3 mm in diameter.

The method applied in this study adheres to the guidelines outlined in ASTM E1621 −22, ensuring compliance with recognized standards for analytical procedures. To optimize the accuracy of the analysis, each sample underwent a meticulous polishing process, resulting in a clean and flat uniform surface that allowed for effective exposure to the X-ray beam. This preparation is critical to minimize any variances in readings that could arise from surface irregularities. Table 3.4 shows a setup parameter of WDXRF analysis.

Table 3.4
Set up the Parameters of WDXRF Analysis

Setup Parameter	Description
Tube Power	Rhodium (Rh) 60kV
Environmental Medium	Vacuum
Film Type	Mylar 6µm
Collimator Mask	3mm
Target element	Ag, Cu
Counting Times	300 seconds

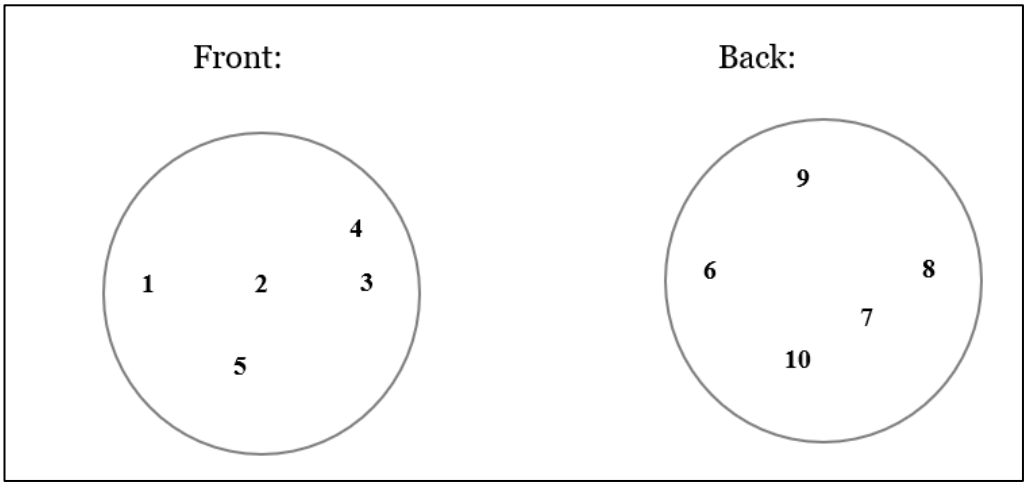

Figure 3.16 Summary for Tens (10) Location Spots Analysis of Calibration Materials Using a WDXRF Spectrometer

During the analysis, each sample was repeatedly analysed across at least ten different spot areas on both sides to ascertain the homogeneity of the material. This multi-point assessment, as depicted in Figure 3.16, ensures that the results obtained truly represent the composition of the entire sample and account for any potential variations in metal distribution. The rigorous approach taken in sample preparation and analysis contributes to the reliability and robustness of the findings in this study.

3.4.3 Energy Dispersive X-ray Fluorescent Spectrometer

3.4.3.1 Instrumentation and Experimental Setup

In this study, the Thermo ARL Quant EDXRF spectrometer, located at the National Metrology Institute of Malaysia (NMIM), served as the primary analytical instrument Figure 3.17. As illustrated in Figure 3.18, the spectrometer utilized a high flux 50 W rhodium anode X-ray tube, operating at an excitation voltage range of 4 to 50 kV and an anode current of 0.8 mA. This advanced instrument was equipped with a Silicon Drift Detector (SDD), featuring a narrow window designed to handle high count rates while achieving resolutions of less than 165 eV FWHM (Full Width at Half Maximum) at the Mn K-alpha peak. The SDD contributed to enhanced performance for the detection and analysis of elements across the periodic table, from light to heavy elements.

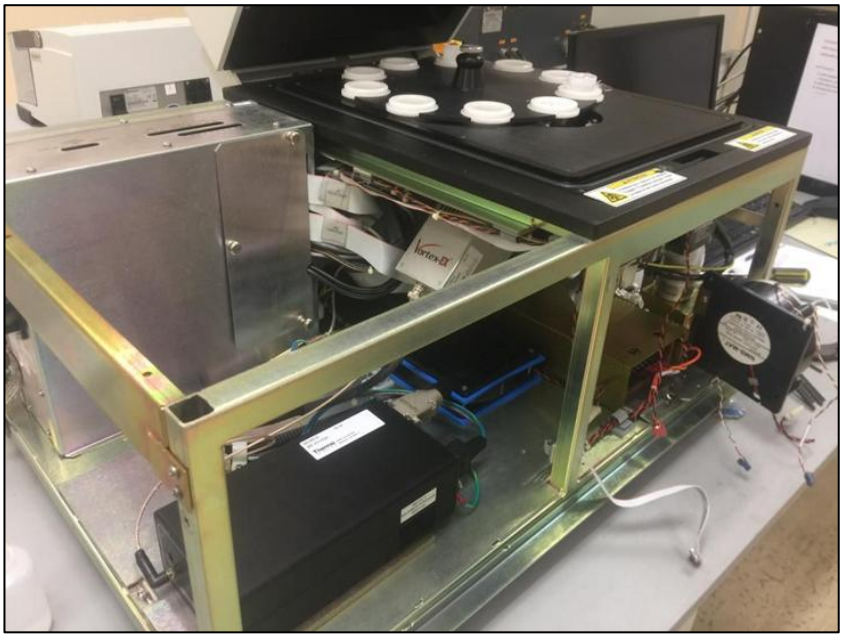

Figure 3.17 A Thermo ARL QUANT'X EDXRF Spectrometer with a Silicon Semiconductor Detector (SDD) by using Peltier Cooling and High Energy Resolution

Figure 3.18 A High Flux 50 W Rhodium Anode X-ray Tube was used in this Study

The usage of 20 kilovolts (kV) and 50 kilovolts (kV) was sufficient to excite an electron from the K-shell of silver and copper, and the target gold from the L-shell. Copper and palladium filters were used to remove dominant X-rays from the X-ray tube that may have overlapped with the fluorescence element of interest. A thick copper filter was selected because of its ability to absorb zinc and aluminium energy from X-ray emission lines to produce a higher-fidelity silver peak spectrum. The palladium medium filter adsorbs silver energy from X-ray emission lines to produce a higher fidelity gold and copper peak spectrum. The filters were analysed under vacuum to eliminate the ambient atmosphere between the sample and detector while optimizing light element sensitivity. Figure 3.19 shows various sizes of X-ray collimator beams such as 1.0 mm, 2.0 mm, 3.5 mm, and 8.8 mm, which have been used to study the optimization of the fluorescence signal count toward the surface area of the target samples. Table 3.4 shows the estimated effective surface area based on the size of the collimator beams

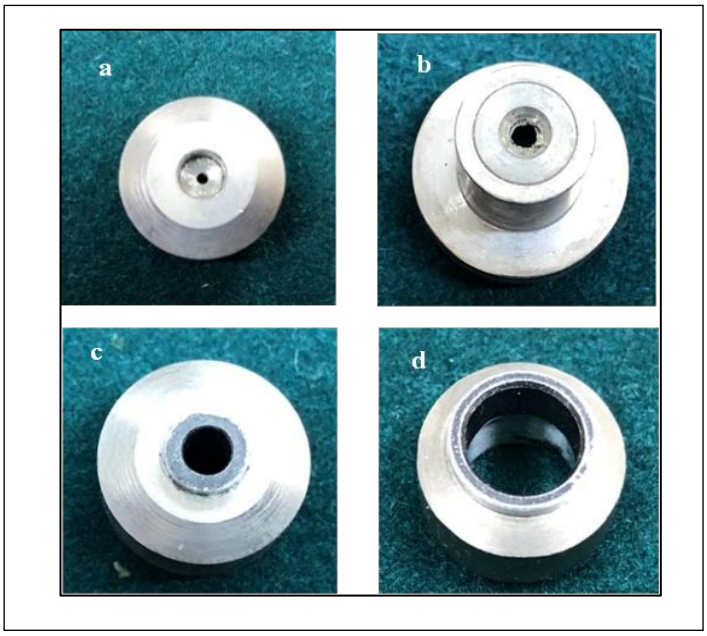

Figure 3.19 Collimator Beam with Different Circular Diameter Sizes at a) 1.0 mm, b) 2.0 mm, c) 3.5 mm, and d) 8.8 mm

Table 3.5
The Estimated Effective Surface Area Based on the Size of the Collimator Beams

Type	Diameter size of collimator beam, *d* (mm)	Effective diameter *(d*1.5)* mm	Effective spot area, (πr^2) mm^2
Collimator 1	1.00	2.06	3.33
Collimator 2	2.00	3.10	7.55
Collimator 3	3.50	5.60	24.63
Collimator 4	8.80	13.00	132.73

The 45-degree angle configuration of the X-ray tube plays a crucial role in optimizing the delivery of X-rays onto the sample surface. By positioning the X-ray tube at this angle, the generated X-rays are directed in a manner that maximizes interaction with the sample material. This setup is expected to minimize any potential interference from background radiation or extraneous sources, which can compromise measurement accuracy. As a result, the configuration leads to the collection of high-quality data, producing more precise and sensitive measurements of the sample's characteristics. The detailed arrangement of the X-ray tube and detector, depicted in Figure 3.20, illustrates the effectiveness of this setup, highlighting how the angle contributes to improved signal-to-noise ratios and overall measurement reliability.

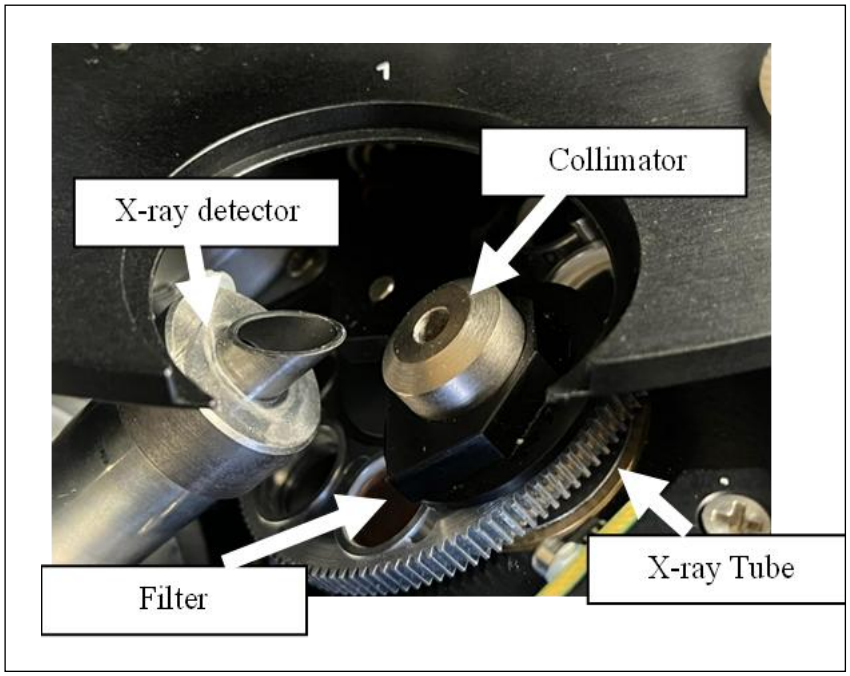

Figure 3.20 Setup of the X-ray Tube and Detector

3.4.3.2 Calibration Strategies of the EDXRF Method

In this study, the combination of fundamental parameters (FP) and empirical calibration materials was used to develop calibration of the EDXRF method measurement for gold alloy analysis. The application calibration materials as discussed in section 3.3.1. Table 3.6 displays a summary of the setup parameters of the EDXRF method.

Table 3.6
Set up Parameters of the EDXRF Method with the Combined Calibration Method

Filter	Condition	Selected Element(s)	Counting Rate (seconds)	Method
Pd Medium,	20 kV, Vacuum medium	**Au, Cu,** Zn, Pt, Ni, W, Fe, Cr, Ti, Co, Si, Hg	120	Combination of Fundamental Parameter (FP) and empirical calibration materials
Cu Thick	50 kV, Vacuum medium	**Ag**, Pd, Mo, Sn, Pb, Cd, Rh, In,	120	Combination of Fundamental Parameter (FP) and empirical calibration materials

The measurement of alloy purity was performed by calculating the areas of measured spectrum peaks of each element concerning each other, followed by

calculating the analysis result by “matrix-matching”. Matrix-matching compares the measurement of the object under study to a measurement of calibration materials with a known elemental composition as prepared in section 3.3.1. The data were then plotted to establish a calibration curve between the reference values with the experimental values in mass fraction (wt%). In this study, Equation 3.1 shows the calibration model for each element.

$$C_i = a_0 + c_i \left(a_i + a_{ii} c_i + \sum_j a_{ij}\, c_j \right) + c_j \left(a_j + a_{jj} c_j + \sum_{k \neq j} a_{jk}\, c_k \right) \qquad (3.1)$$

where C_i is the certified analyte concentration in the standard (*wt%*), c_i is the analyte concentration from the standardless FP module (*wt%*), and *cj* and c_k are the concentrations (%) of other elements in the standard calculated by the standardless FP method. The best model was chosen with the quadratic stepwise multiple regression algorithm, eliminating statistically insignificant parameters from groups a_0, a_i, a_{ii}, a_{ij}, a_{jj}, and a_{jk} before determining significant parameters.

3.4.3.3 Realignment of the EDXRF Method Measurement

Further, the method validation will be performed using the certified reference materials (CRMs) as discussed in section 3.3.2. This may cover a variety of gold alloy Au-Ag-Cu with a range of 75.00 *wt%* to 99.99 *wt%*. In this study, these CRMs were validated to determine the correction *k-factor* values k_{fac}. The corrective *k-factor* values were determined for each alloy mixture to realign the EDXRF method measurement. The values were applied to the computation of each analysed sample based on the similarity of the elements in the gold mixture. The correction factor is the quotient of the certified value of gold measured by gravimetric $m(Au, CRM^{grav})$ against, and the observation measured by EDXRF method, $m(Au, CRM_{obs}^{XRF})$. The validated ratio of gold value determined the corrective *k-factor* with the aid of the gravimetric method against the gold value measured with the EDXRF method, as shown in Equation 3.2.

$$k_{fac} = \frac{m(Au, CRM^{grav})}{m(Au, CRM_{obs}^{XRF})} \quad (3.2)$$

where,

$m(Au, CRM^{grav})$	The certified value of gold measured by the gravimetric in CRM was close to the sample material
$m(Au, CRM_{obs}^{XRF})$	XRF measurement of gold in the CRM that was close to the sample material

The corrective means of gold in each unknown sample, $\bar{y}_i$ was then determined by applying the corrected measured means by the EDXRF method measurement, y_i with *k-factor values,* k_{fac}, as shown in Equation 3.3, to realign the EDXRF method measurement of the gold element in each mixture of alloys of (Mazuki et al., 2023).

$$(\bar{y}_i) = (y_i).k_{fac} \quad (3.3)$$

3.4.3.4 Method Validation of the EDXRF Measurement

The method then was validated with a variety types of commercial samples as provided in section 3.3.3 to study the robustness of the development method. The relative error was calculated as the absolute error of the measurement divided by the actual measurement. The relative error implied the accuracy of the EDXRF measurement concerning fire assay values. The relative error ($rel\ \%$) was calculated with Equation 3.4

$$rel\ \% = \left(\left|\frac{x_i - x_o}{x_o}\right|\right).100 \quad (3.4)$$

where x_o is the measured value from the fire assay method, and x_{oi} refers to the measured value from EDXRF. Meanwhile, the relative standard deviation (*%rsd*) was calculated to evaluate the reproducibility of measurements. It was expressed as a percentage and accomplished by dividing the standard deviation by the EDXRF measurement, followed by a multiplication of 100. The corrective *k-factor* has been applied to various commercial gold mixtures before and after to study the effectiveness of the measurement.

To study the comparison of the two analysis methods, a student's t-test was performed to verify the null hypothesis in the absence of a significant difference in the results means of results for the methods, fire assay method and corrected EDXRF measurement were studied. The following parameters were calculated for the student's t-test: the mean value of measurements (x) for each sample, the standard deviation for repeated measurements (s), and the pooled standard deviation (Sc). Au1, Au5, Au11, and Au13 samples were selected to represent the diverse mix of gold alloys. One of the following hypotheses was investigated: H_0, there is no significant difference in mean values if *($p \geq 0.05$).;* H_1; there is a significant difference in mean values if *($p < 0.05$)*.

3.4.3.5 Uncertainty Calculation of the EDXRF Measurement

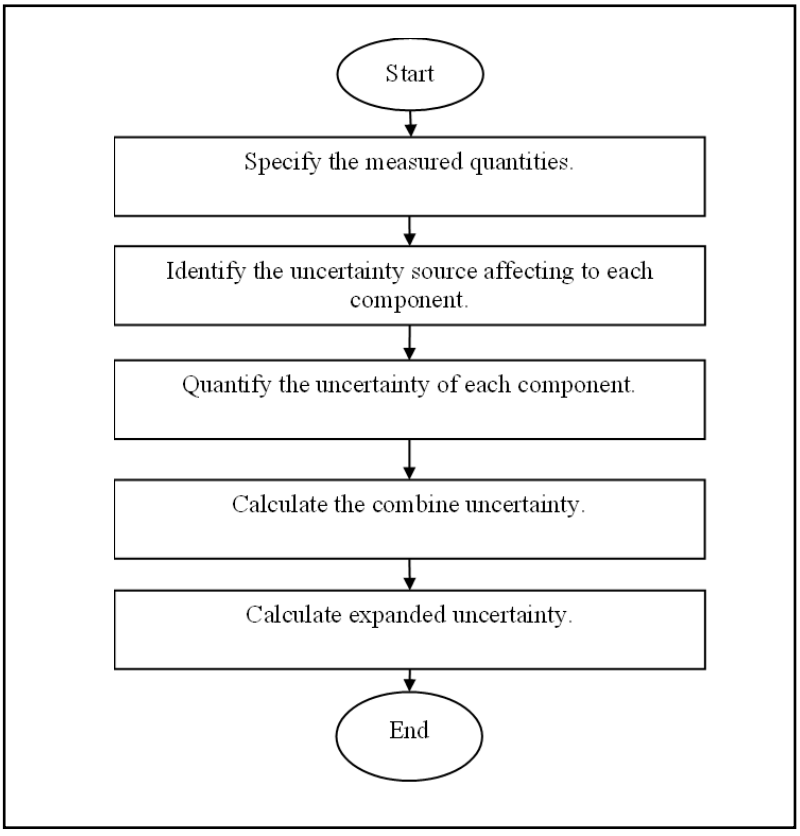

Figure 3.21 The Steps in Uncertainty Calculations

The expression of the results must include stated uncertainties, resulting from a careful inspection of an uncertainty budget comprising the main stages in calibration, validation, and the quantification model applied. The uncertainty estimation process

comprises the steps summarized in Figure 3.21. In this study, the calculation of the measurement uncertainty for gold analysis by EDXRF begins with the analysis of uncertainty sources according to the Ishikawa diagram, as shown in Figure 3.22. The source is a component of statistics methods, and in this study, it is related to the repeatability of standard deviations, intermediate precision uncertainty, the bias of CRM uncertainty, calibration curve uncertainty, and EDXRF digital resolution uncertainty (Krummenauer et al., 2021).

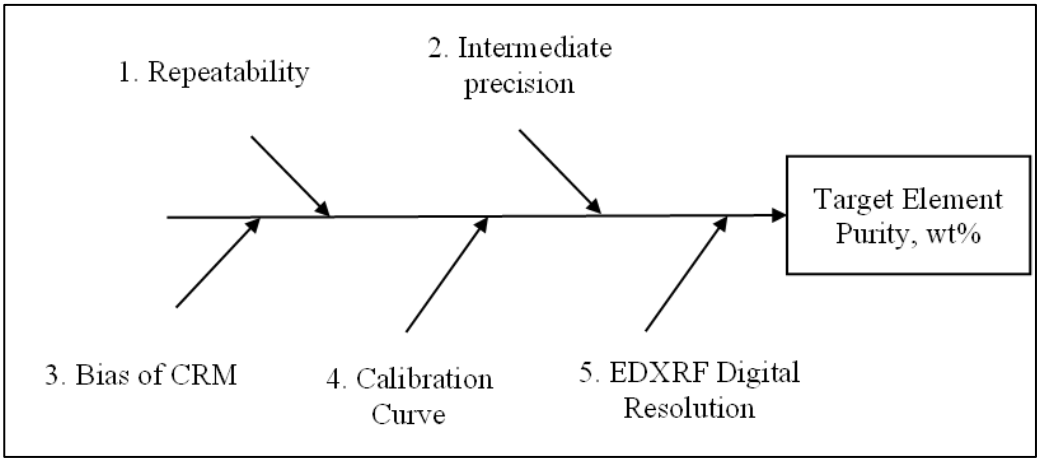

Figure 3.22 Ishikawa Diagram of Uncertainties for the EDXRF Method

3.4.3.6 Interlaboratory Comparison (ILC)

The new optimization of the EDXRF method has demonstrated the capability through interlaboratory comparison (ILC) with the Institute of Metrology Bosnia & Herzegovina (IMBIH), to validate the results with ISO/IEC 17043:2023, which is a requirement of conformity assessment proficiency testing schemes and may be used as a basis for specific technical requirements for fields of application. The requirements for proving testing capabilities at the international level for gold content in yellow gold alloys. The raw ILC test material is prepared in the form of wire by IMBIH with the following nominal composition of 750 ± 20 mg/g. The ILC results were processed using the *z-score* as a statistical tool to evaluate the NMIM success, following Equation 3.5 (Cordeiro et al., 2022):

$$z' = \frac{x_i - x_{pt}}{\sqrt{U_{x_{pt}}^2 + U_{x_i}^2}} \tag{3.5}$$

Where:

x_{pt}	The assigned value from IMBIH.
x_i	The NMIM result
ux_{pt}	The measurement uncertainty of the IMBIH
ux_i	The measurement uncertainty stated by the NMIM

The following interpretation is given to z' numbers:

$\|z'\| \leq 2$	"satisfactory result"
$2 \leq \|z'\| \leq 3$	"questionable result"
$\|z'\| > 3$	"unsatisfactory result"

3.4.3.7 Reliability of the EDXRF Method for Gold Purity Measurement

The reliability of the developed EDXRF method was established through systematic analysis of specific gold reference materials with certified mass fractions of ternary gold (Au), silver (Ag), and copper (Cu) matrices, providing a direct link to Standard International (SI) units. These homogenised certified reference materials (CRMs) were characterized using primary reference methods, such as fire assay (cupellation), through high-accuracy calibrated balances and validated chemical procedures. Multiple replicate measurements were then performed using the optimised EDXRF method to assess repeatability, while intermediate precision was evaluated across different days and instrument sessions. Measured values were compared against the certified values, and deviations were assessed within the framework of expanded uncertainty, ensuring that all significant sources of uncertainty along the traceability chain were accounted for. The consistent agreement of optimised EDXRF results with the SI-traceable reference values confirmed both the trueness and reproducibility of the method, demonstrating that the developed approach provides reliable, non-destructive, and SI-traceable measurements of gold alloy purity. Furthermore, the optimised EDXRF approach was used to assign the purity of secondary specific gold materials, which then served as reference materials to demonstrate the traceability chain for

commercial XRF instruments. A summary of the traceability chain for the EDXRF measurements is presented in Figure 3.23.

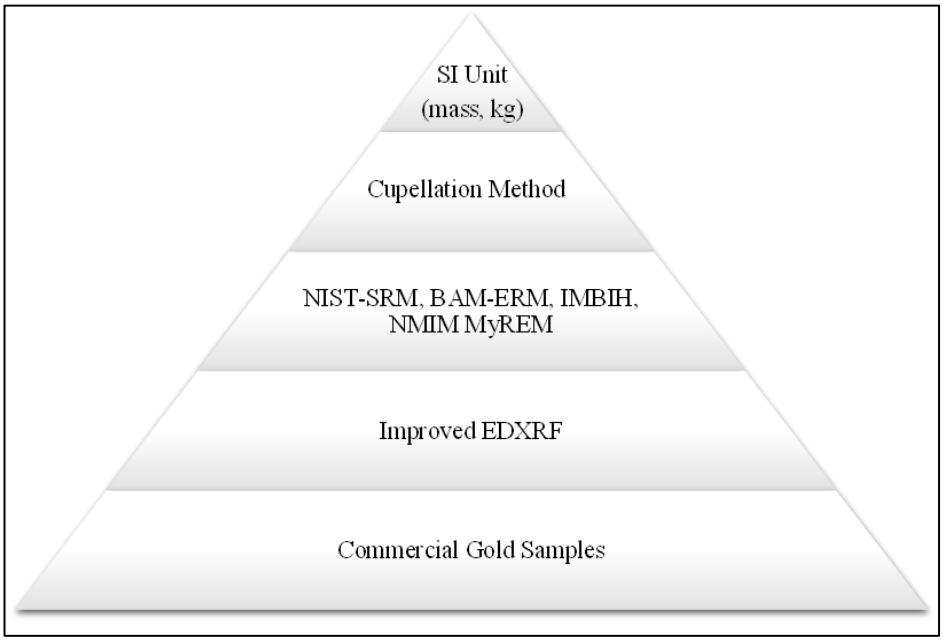

Figure 3.23 Traceability Chart of EDXRF Measurement

3.5 Summary of the Methodology

The experimental framework in this study has been considered to improve and validate the EDXRF method as a potential alternative to the destructive fire assay or cupellation method. The limitation of this study has been identified in terms of the scope of the study, source, and range of samples available in the market. The experiment has been divided into four phases: matrix effect correction, instrument optimization, method validation, and robustness study. These considerations focused on specific features of the implemented method and analytical practice for choosing the most suitable approach for the EDXRF method in gold purity measurement. The findings of the experiment have been discussed in Chapter 4.

CHAPTER 4
RESULTS & DISCUSSION

4.1 Introduction

This chapter discusses the detailed procedures for measuring the purity of gold alloy samples utilizing the EDXRF method. The measurement technique is significantly influenced by both the instrumentation setup tuning and the enhancement procedure undertaken. This approach established the optimum accuracy of the EDXRF method as a potential alternative to the cupellation method for determining gold purity. Furthermore, an international laboratory comparison (ILC) was conducted in collaboration with the Institute of Bosnia and Herzegovina (IMBIH). The main objective of this comparative study is to validate the effectiveness of the enhanced EDXRF procedure and the corresponding instrument tuning adjustment in measuring gold purity. This comparative evaluation offers an important perspective on the performance and reliability of the EDXRF method applications.

4.2 Environmental Monitoring Results

Environmental stability is crucial in ensuring the reliability of laboratory experiments, as deviations outside the defined range can lead to variability in the EDXRF experimental outcomes. To ensure that the laboratory environment met the required conditions for accurate and reliable experimental results, daily temperature and relative humidity monitoring were conducted monthly. The findings from the monitoring process, as illustrated in Figure 4.1, demonstrate that the average monthly temperature remained consistently within the acceptable range of 19°C to 25°C. This range aligns with the operational requirements of EDXRF instruments, which are sensitive to thermal fluctuations. Temperature variations can influence the stability of X-ray tube outputs, detector response, and overall system calibration. By maintaining a stable temperature, the laboratory ensured that the instrument operated within its optimal performance window, minimizing errors and enhancing the repeatability of measurements.

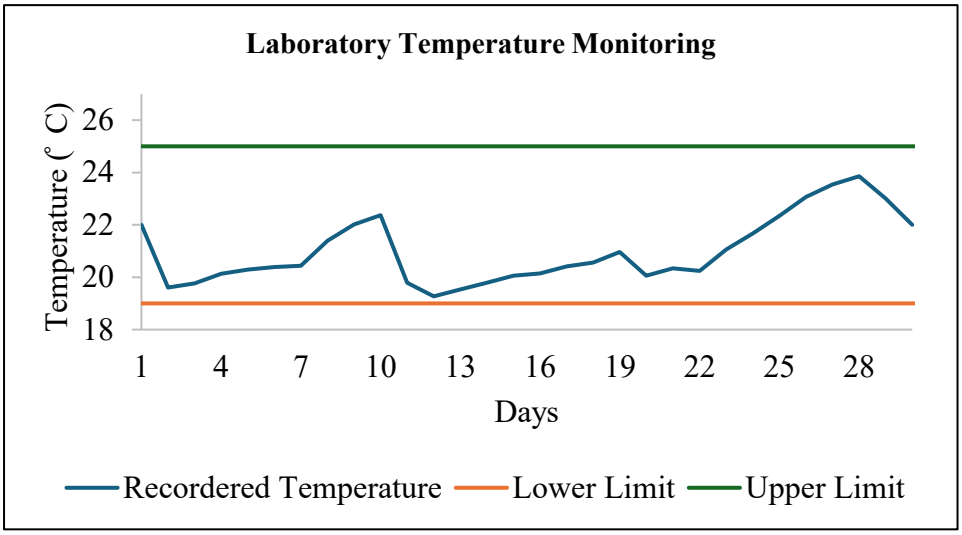

Figure 4.1 Ambient Laboratory Temperature Measurement over a Month

Figure 4.2 highlights that the relative humidity levels were recorded within the desired range of 50% to 80%. Humidity control is equally critical in EDXRF analyses, as excessive humidity can lead to condensation on the sample or instrument components, while low humidity levels can cause static buildup, both of which can distort measurement accuracy. Consistent relative humidity regulation ensures that the sample matrix remains unchanged and that the instrument operates without interference from environmental factors.

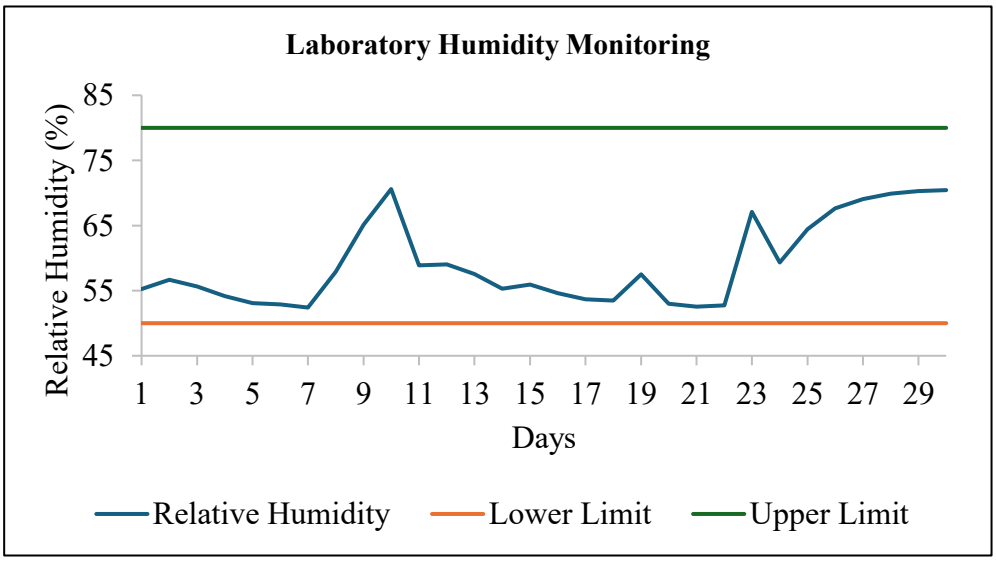

Figure 4.2 Ambient Laboratory Humidity Measurement over a Month

4.3 Energy Adjustment of EDXRF Results

Energy adjustment is the process by which the system adjusts the energy scale so that peaks appear at the correct energy in the spectra. In this study, the energy adjustment was performed using 99.9 *wt%* pure copper (Cu). The selection of copper is due to the characteristics of the X-ray emission line, which is useful in providing a clear reference point for calibration and adjustment of the energy scale. The characteristic X-rays emitted were detected by an EDXRF detector, producing a spectrum with peaks of Kα at 8.041 keV and Kβ at 8.907 keV as shown in Figure 4.3. The limit of energy adjustment error should be less than ± 0.0015 keV. Adjustments are made to the instrument software to ensure the energy scale is accurate across the entire range of interest and does not overlap.

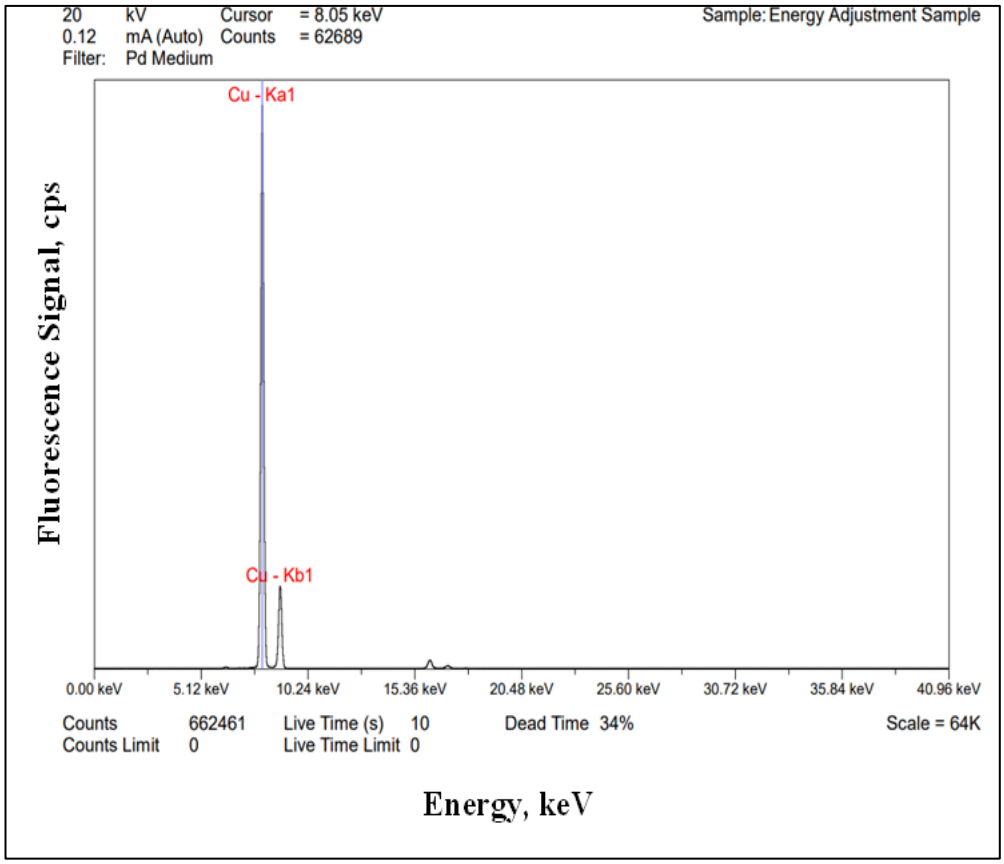

Figure 4.3 Energy Adjustment Copper Spectra

4.4 Optimisation of EDXRF Configurations

The spectrum acquired with an EDXRF spectrometer shows simultaneously the peaks of all the elements present in the gold-silver-copper alloy, as shown in Figure 4.4. The energy scale is determined and expressed in units of kiloelectron volt (keV). The copper peak appeared at a lower energy with 8.041 keV for Cu Kα, while Cu Kβ appeared at 8.907 keV. The gold peak demonstrated their L-shell at 9.711 keV for Au Lα and 11.439 keV for Au Lβ. Peak detected at higher energy values is connected to the Ag Kα peak at 22.104 keV and 24.987 keV for Ag Kβ. This selection was driven by the characteristics of the EDXRF tube used in experiments. The EDXRF tube, or generator, specifically excites the L-shell of gold due to the limitations imposed by its operational voltage and the maximum photon energy it can generate, which is capped at 50 kV. This limitation prevents it from effectively exciting the K-shell of gold, which requires a much higher energy threshold of 80.7 keV. In contrast, for the elements copper and silver, we chose to analyses the K-shell lines. The EDXRF tube's energy output is sufficient to adequately excite the gold, silver, and copper elements, allowing for effective analysis. The selection of the spectrum is based on the higher intensity and better signal-to-noise ratio, resulting in an accurate measurement.

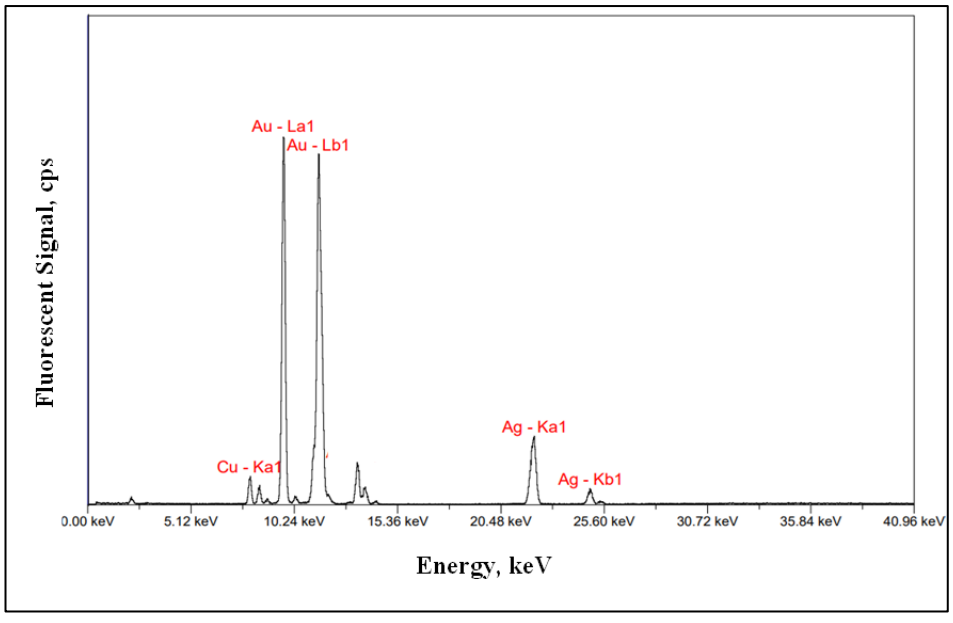

Figure 4.4 EDXRF Spectrum of Au–Ag–Cu Alloy.

4.4.1 Selection of Optimum Collimator Beam Sizes

Table 4.1 shows the fluorescence signal response of AuLα and AuLβ with the unit of count per second (cps) against the collimator beam size for a series of certified reference materials (CRMs). The data were then plotted in the graph to demonstrate the influence of collimator beam size on the fluorescence signal captured by EDXRF, as shown in Figure 4.5 and Figure 4.6. The changes in the gold (Au) element peak at 9.72 keV for AuLα and 11.44 keV were observed. From observation, as the collimator beam size increases, the fluorescence signal is discovered to increase in tandem. The increase in Au peaks' fluorescence signal was due to the height of the solid angle, which was subtended by the detector as the opening of the collimator increased. Thus, the detection of the Au EDXRF peak was achieved by increasing the diameter of the collimator beam, indicating the increase in the acceptance angle of the detector's face. AuLα is the L-alpha emission of gold, where the electron transitions occur between the L-shell and K-shell of an atom. This is a more common and energetic transition. AuLβ is the L-beta emission, where the electron transitions occur between higher energy levels (L-shell to M-shell). For most CRM materials, the AuLα signal is generally higher than the AuLβ signal at all collimator sizes. This suggests that the AuLα emission of gold is generally stronger and more detectable than the AuLβ emission.

Table 4.1

Fluorescence Signal Response of AuLα and AuLβ in Count Per Second (cps) with Different Collimator Beam Sizes for a Series of Certified Reference Materials (CRMs)

Collimator Size	CRM	AuLα (cps)	AuLβ (cps)
1.0 mm	SRM 685R	15220	12559
	MyRM 22K	6880	5880
	MyRM 5.102	7380	5880
	ERM 508	9600	7100
2.0 mm	SRM 685R	19500	18300
	MyRM 22K	14750	13750
	MyRM 5.102	12960	11760
	ERM 508	15000	13000
3.5 mm	SRM 685R	8880	8680
	MyRM 22K	21258	21008
	MyRM 5.102	19874	19594
	ERM 508	19029	18729
8.8 mm	SRM 685R	6483	6383
	MyRM 22K	25555	25455
	MyRM 5.102	22742	22622
	ERM 508	7368	5854

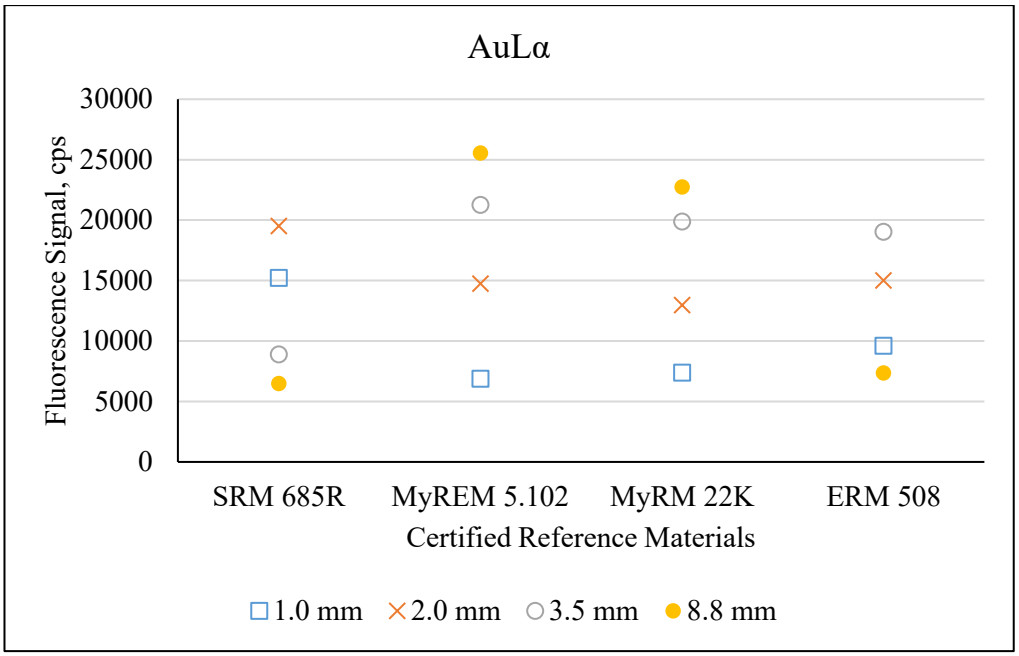

Figure 4.5 The Graph to Demonstrate the Influence of Collimator Beam Size on the Highest Fluorescence Signal of AuLα Captured by EDXRF

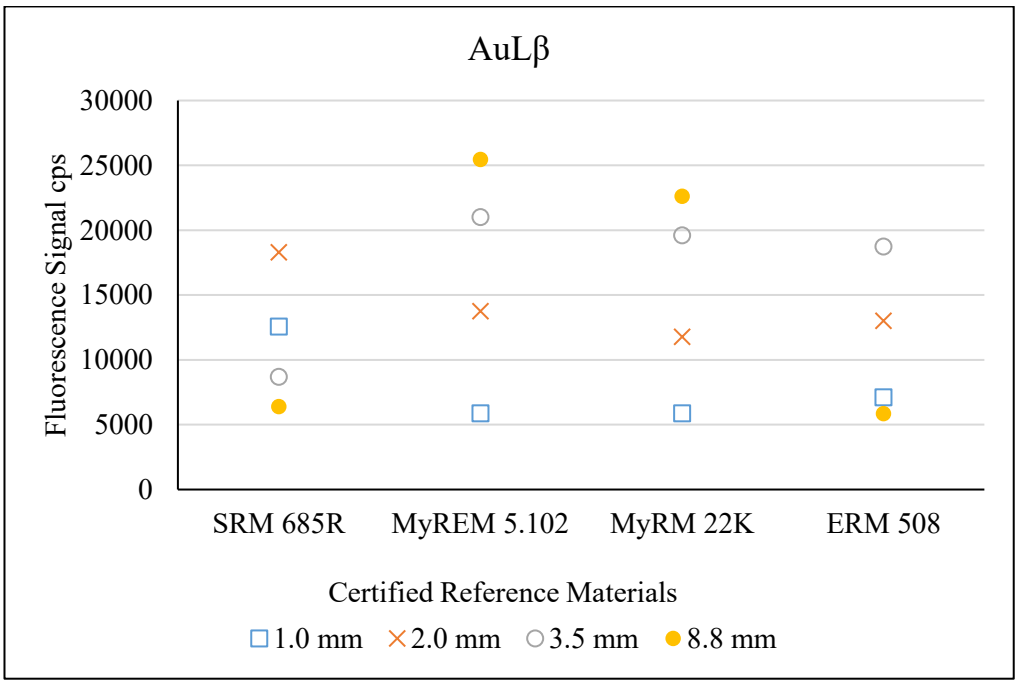

Figure 4.6 The Graph to Demonstrate the Influence of Collimator Beam Size on the Highest Fluorescence Signal of AuLβ Captured by EDXRF

The SRM 685R observed a low fluorescence signal when an 8.8 mm and a 3.5 mm collimator was used. Meanwhile, ERM 508 had low signals at an 8.8 mm collimator. This is due to the discrepancies between the measured area and the size of

the targeted sample led to the 'void', resulting in loss of fluorescence signal. However, smaller collimators are not without their flaws. With smaller collimators, the EDXRF detector could only capture a low fluorescence signal due to the narrower X-ray beam on the sample target. This minimal fluorescence signal led to poor spectral distribution. Furthermore, the presence of more dominant elements in the sample could have contributed to this low signal observation.

4.4.2 Selection of Optimum Spectral Peak

The measurement of the composition of an alloy, in mass fraction in percentage (wt %), is made by computing the areas of measured spectrum peaks of each element concerning each other and then calculating the analysis result using a "matrix-matching" method. Matrix-matching is based on comparing the measurement results of the object under study to a result obtained with a reference material with a known elemental composition. High-resolution detectors, such as Silicon Drift Detectors (SDDs), are preferable as they can better resolve closely spaced peaks. The differences in gold (Au) purity percentage against the certified values of CRMs are summarised in Table 4.2. These disparities came about due to the range of applied collimator beam sizes.

Table 4.2
The EDXRF Experimental Result of Gold Purity Compared to the Certified Values

CRM	Collimator Size	Certified value (wt%)	EDXRF Experimental Result (*wt%*)			
			AuLα	*d*	AuLβ	*d*
SRM 685R (Au)	1.0 mm	99.99	99.90	0.09	99.81	0.18
	2.0 mm		99.94	0.05	99.84	0.15
	3.5 mm		99.78	0.21	99.68	0.31
	8.8 mm		98.06	1.93	97.95	2.04
ERM 508 (Au-Ag)	1.0 mm	75.12	75.40	-0.28	75.52	-0.40
	2.0 mm		75.28	-0.16	75.39	-0.27
	3.5 mm		75.23	-0.11	75.33	-0.21
	8.8 mm		75.76	-0.53	75.76	-0.64
MyRM 22K (Ag-Cu)	1.0 mm	91.80	91.27	0.53	91.18	0.62
	2.0 mm		91.30	0.50	91.20	0.60
	3.5 mm		91.42	0.38	91.32	0.48
	8.8 mm		91.55	0.25	91.44	0.36
MyREM 5.102 (Au-Ag-Cu)	1.0 mm	91.80	91.59	0.55	91.50	0.64
	2.0 mm		91.62	0.52	91.52	0.62
	3.5 mm		91.78	0.36	91.68	0.46
	8.8 mm		91.90	0.24	91.79	0.35

d = differences

From the results, for AuLα results of SRM 685R certified reference materials, the collimator beam of sizes 8.8 mm, 3.5 mm, and 1.00 mm recorded differences of 1.93 *wt%,* 0.21 wt.%, and 0.09 *wt%,* respectively. The 2.00 mm collimator beam had the smallest difference at 0.05 wt%. The loss in fluorescence signal was caused by the application of a collimator beam that was larger than the target sample. This phenomenon compromised measurement accuracy. A similar trend can be observed for AuLβ results; however, there is a slightly higher difference as compared to AuLα, resulting in 2.04 *wt%*, 0.31 *wt%*, 0.15 wt%, and 0.18wt%, respectively, for 8.0 mm, 3.5 mm, 2.0 mm, and 1.0 mm. This might be due to the fluorescence signal capture being less strong than the AuLα signal. Minimizing the loss in fluorescence signal and improving measurement accuracy can be achieved by utilizing a smaller collimator beam. For ERM 508, the collimator beams of sizes 8.8 mm, 3.5 mm, 2.00 mm, and 1.0 mm recorded differences of -0.53 *wt%*, -0.11 *wt%,* -0.16 *wt%*, and -0.28 *wt%*, respectively. The negative differences might be due to a mixture of gold with silver. The enhancement effect increases the signal of gold, since the energy of silver is higher than that of gold. This has also affected the higher differences for results for AuLβ with -0.64 *wt%,* -0.21 *wt%,* -0.27 *wt%,* and -0.40 *wt%.* This might be due to less signal and interference with other elements. The sizes of the collimator beam matched the area of the target samples and, thus, contributed to better measurement accuracy. Even though the 1.0 mm and 3.5 mm collimator beams were not significantly different in terms of size, the recorded differences between the experimental value and the certified value were remarkable.

The low fluorescence signal caused the rest of the elements in the sample to assert their dominance over gold, which subsequently compromised the measurement accuracy. For MyRM 22K and MyRM 5.102, a similar pattern has been observed for both samples. Good accuracy was achieved when an 8.8 mm collimator beam was used instead of the smaller collimator size beam due to a high fluorescence signal. Overall, the collimator beam size, the results proved, factors in the accuracy of EDXRF analysis. The precious metal sample's size and shape can influence the measurement's accuracy as it affects the amount of outbound fluorescence signal captured by the detector as the beam diameter is changed. An appropriate selection of peak collimator beam size suitable to the area of the target sample is important to optimize EDXRF analysis.

4.4.3 Optimisation of Calibration Method

Table 4.3 shows that the EDXRF measurement is based on a set of calibration materials (CM), as discussed in Chapter 3. The precision is expressed as an expanded standard deviation at a 95% confidence interval, which represents the ten (10) repeatability of the measurements for gold was less than 0.17 *wt%*, while the other alloys (silver and copper) were less than 0.1 *wt%*. Introducing specific gold calibration materials to the FP method was expected to improve the data accuracy and precision.

To compare the performance of the two analytical methods (corrected and non-corrected EDXRF method) against the fire assay method, a t-test was performed on a range of samples from CM1 through CM7, as shown in Table 4.4. The main goal of this analysis was to assess how well these methods measure the primary gold content. The results showed that there was no statistically significant difference between the data obtained from the corrected EDXRF method and the fire assay results. This conclusion was supported by all the *p-values* exceeding the threshold of 0.05, suggesting that the corrected EDXRF method produces results that are close to the fire assay. In contrast, the findings from the non-corrected EDXRF method were significantly different. Across all samples tested, this method exhibited statistically significant differences when compared to the fire assay, with *p-values* recorded less than 0.05. This highlights the inadequacy of the non-corrected approach in accurately measuring gold compositions.

Table 4.3

The Purity Measurement is Based on a Series of Calibration Materials. The Precision Is Expressed as an Expanded Standard Deviation at a 95% Confidence Interval

Code of Calibration sample	Composition in mass fraction of percent (*wt%*)								
	Fire Assay	WDXRF		Corrected [a]			Non-Corrected [b]		
	Au	Ag	Cu	Au	Ag	Cu	Au	Ag	Cu
CM1	76.34 ± 0.05	23.66 ± 0.08	0.00 ± 0.00	76.30 ± 0.15	23.70 ± 0.09	0.00 ± 0.00	77.89 ± 0.32	21.74 ± 0.16	0.21 ± 0.15
CM2	75.85 ± 0.05	0.00 ± 0.00	24.15 ± 0.10	75.70 ± 0.15	0.00 ± 0.00	24.30 ± 0.10	74.20 ± 0.30	0.14 ± 0.15	21.82 ± 0.19
CM3	74.00 ± 0.05	15.00 ± 0.07	11.00 ± 0.07	74.15 ± 0.16	14.88 ± 0.08	10.97 ± 0.09	77.56 ± 0.41	12.56 ± 0.18	8.90 ± 0.18
CM4	91.89 ± 0.05	8.11 ± 0.0.5	0.00 ± 0.00	91.79 ± 0.15	8.21± 0.06	0.00 ± 0.00	94.45 ± 0.28	9.03 ± 0.15	0.23 ± 0.15
CM5	91.67 ± 0.05	4.72 ± 0.04	3.61 ± 0.04	91.60 ± 0.15	4.78 ± 0.05	3.65± 0.05	93.10 ± 0.27	3.28 ± 0.15	5.23 ± 0.17
CM6	92.02 ± 0.05	0.00 ± 0.00	7.98 ± 0.05	91.88 ± 0.17	0.00 ± 0.00	8.12 ± 0.06	90.89 ± 0.28	0.15 ± 0.05	6.15 ± 0.17
CM7	99.90 ± 0.04	0.00 ± 0.00	0.00 ± 0.00	99.90 ± 0.15	0.00 ± 0.00	0.00 ± 0.00	99.60 ± 0.20	0.10 ± 0.15	0.20 ± 0.15

[a] *The element composition was determined by combining fundamental parameters (FP) and an empirical standard calibration approach.*
[b] *The element composition was determined by fundamental parameters (FP) only.*

Table 4.4
T-test Comparison of Corrected and Non-corrected EDXRF Measurements Against Fire Assay

	Corrected EDXRF													
	CM1		CM2		CM3		CM4		CM5		CM6		CM7	
	FA (wt%)	*XRF (wt%)*	*FA (wt%)*	*XRF (wt%)*	*FA (wt%)*	*XRF (wt%)*	*FA (wt%)*	*XRF (wt%)*	*FA (wt%)*	*XRF (wt%)*	*FA (wt%)*	*XRF (wt%)*	*FA (wt%)*	*XRF (wt%)*
Mean	76.34	76.30	75.85	75.80	74.00	74.05	91.89	91.83	91.67	91.62	92.02	91.98	99.90	99.90
Variance	0.00	0.01	0.00	0.01	0.00	0.01	0.00	0.01	0.00	0.01	0.00	0.01	0.00	0.01
Observations	10	10	10	10	10	10	10	10	10	10	10	10	10	10
Pearson Correlation	0.00		0.00		-0.06		-0.07		0.33		0.32		-0.12	
Hypothesized Mean Difference	0		0		0		0		0		0		0	
df	9		9		9		9		9		9		9	
t Stat	1.329		2.080		-1.974		2.211		2.074		1.535		-0.040	
P(T<=t)	0.217		0.067		0.080		0.054		0.068		0.159		0.969	
t Critical	2.262		2.262		2.262		2.262		2.262		2.262		2.262	

	Non-Corrected EDXRF													
	CM1		CM2		CM3		CM4		CM5		CM6		CM7	
	FA (wt%)	*XRF (wt%)*	*FA (wt%)*	*XRF (wt%)*	*FA (wt%)*	*XRF (wt%)*	*FA (wt%)*	*XRF (wt%)*	*FA (wt%)*	*XRF (wt%)*	*FA (wt%)*	*XRF (wt%)*	*FA (wt%)*	*XRF (wt%)*
Mean	76.34	77.89	75.85	74.20	74.00	77.56	91.89	93.45	91.67	93.10	92.02	90.88	99.90	99.60
Variance	0.00	0.02	0.00	0.02	0.00	0.04	0.00	0.02	0.00	0.02	0.00	0.02	0.00	0.01
Observations	10	10	10	10	10	10	10	10	10	10	10	10	10	10
Pearson Correlation	-0.3		0.0		-0.3		-0.2		0.4		0.3		0.5	
Hypothesized Mean Difference	0		0		0		0		0		0		0	
df	9		9		9		9		9		9		9	
t Stat	-29.380		34.436		-52.543		-34.188		-36.024		27.004		10.210	
P(T<=t)	2.99E-10		7.25E-11		1.65E-12		7.73E-11		4.85E-11		6.34E-10		3.01E-06	
t Critical	2.262		2.262		2.262		2.262		2.262		2.262		2.262	

The data were then plotted to form a correlation graph between the fire assay and WDXRF as the reference, with the EDXRF experimental values in mass fraction (wt%), as shown in Figures 4.7 to 4.9. Figure 4.7 presents a comparative analysis of gold (Au) content determined using EDXRF and fire assay in the range of 75.00 wt% to 99.99 wt%. The results are shown under two conditions: corrected and non-corrected data. This graph highlights how correction protocols impact the accuracy and consistency of EDXRF measurements when compared to the fire assay method.

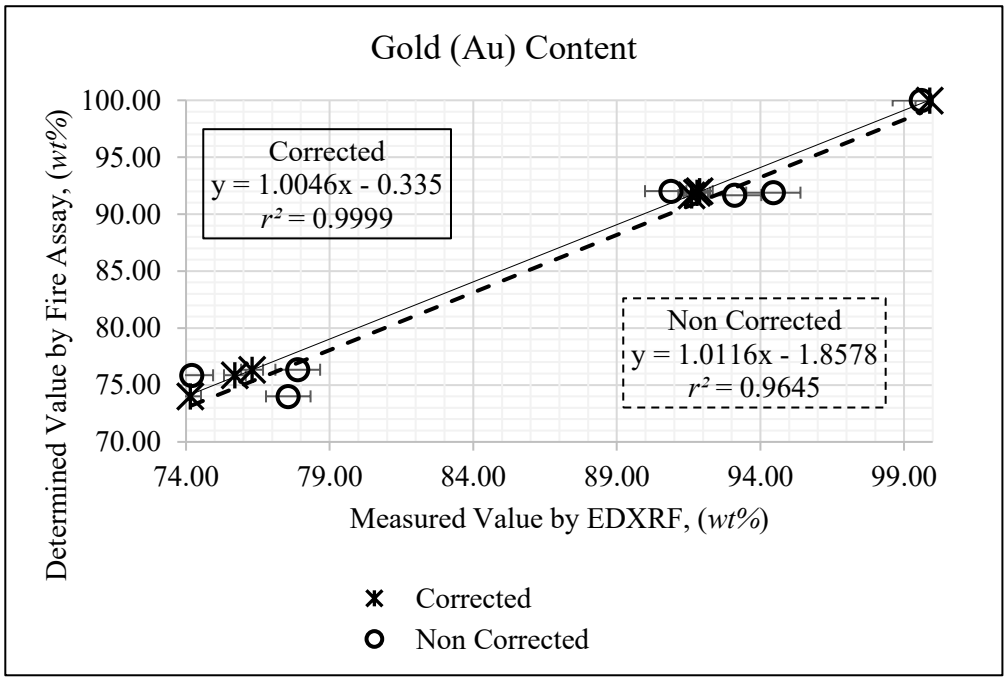

Figure 4.7 Correlation Graph Between Fire Assay Value and EDXRF Measurement (Matrix Corrected and Non-corrected) on Gold (Au) Content

The corrected data, represented by the solid line, follows the regression equation y = 1.0046x - 0.335 with a regression r^2 value of 0.9999. The slope, which is very close to 1, indicates a nearly perfect linear relationship between EDXRF-measured values and Fire Assay reference values. The intercept of -0.335 is minimal, suggesting negligible deviation across the measurement range. The exceptionally high r^2 value confirms the consistency and reliability of the corrected EDXRF results. This strong correlation validates the effectiveness of the correction protocols implemented to address potential systematic errors in the raw data. In contrast, the non-corrected data, represented by the dashed line, follows the regression equation y = 1.0116x - 1.8578 with an r^2 value of 0.9645. While the linear relationship remains strong, the slope

deviates more noticeably from 1, and the intercept is significantly larger. This indicates a systematic bias in the raw data. Such deviations suggest that no correction, EDXRF measurements may overestimate or underestimate gold content depending on the sample composition. The lower r^2 value reflects increased variability in the non-corrected data, making it less reliable for accurate elemental analysis.

The significant differences in r^2 values and regression equations between the corrected and non-corrected data underscore the importance of implementing correction protocols. These protocols are essential for mitigating factors such as matrix effects, instrumental biases, and calibration errors that can compromise the accuracy of EDXRF measurements. By applying these corrections, the alignment between EDXRF and Fire Assay results is greatly improved, allowing EDXRF to produce results that closely resemble those obtained through the Fire Assay technique. The corrected data establish EDXRF as a viable and efficient alternative to fire assay for routine gold content analysis. With its ability to deliver accurate results quickly and cost-effectively, EDXRF can be utilized in various industrial and research settings, particularly when corrections are applied. Non-corrected data, while still indicative of trends, lack the precision required for critical applications, which limits their utility in high-stakes decision-making or regulatory compliance.

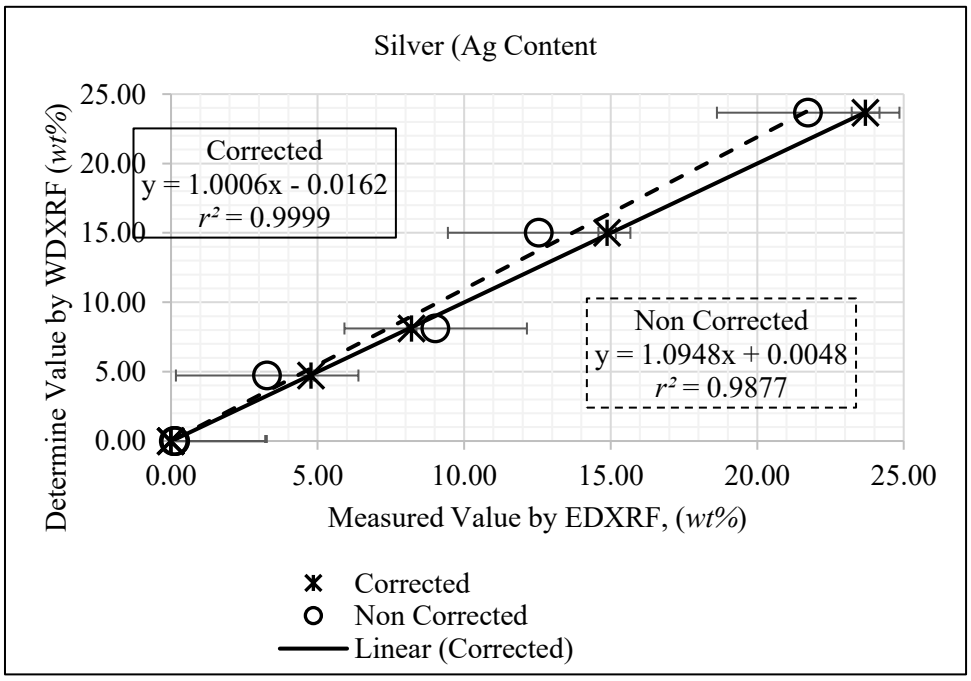

Figure 4.8 Correlation Graph Between WDXRF Value and EDXRF Measurement (Matrix Corrected and Non-Corrected) on Silver (Ag) Content

Figure 4.8 illustrates the correlation between silver (Ag) content determined by two methods: Energy Dispersive X-ray Fluorescent (EDXRF) and Wavelength Dispersive X-ray Fluorescent (WDXRF). This analysis compares the accuracy and reliability of EDXRF measurements against WDXRF results, which are considered the reference standard, under two conditions: corrected and non-corrected data. The corrected data are represented by a solid line with the equation y = 1.0006x - 0.0162 and a regression, r^2 value of 0.9999. The slope of the regression line, which is nearly equal to 1, indicates a near-perfect linear relationship between the measured values from EDXRF and the reference values from WDXRF. The intercept value of -0.0162 is negligible, suggesting that the corrected data closely aligns with the reference method across the entire range of measured silver content. The high r^2 value demonstrates the precision and reliability of the corrected EDXRF measurements, confirming their suitability for accurate silver content analysis. In contrast, the non-corrected data are represented by a dashed line with the equation y = 1.0948x + 0.0048 and r^2 value of 0.9877. Although the linear relationship remains strong, the slope deviates significantly from 1, indicating a systematic overestimation of silver content when corrections are not applied. Additionally, while the intercept value is small, it contributes to the observed discrepancies between the EDXRF and WDXRF measurements. The lower r^2 value compared to the corrected data indicates increased variability and reduced reliability in the non-corrected dataset.

This finding emphasizes the critical importance of data correction in EDXRF measurements to improve their accuracy and comparability with the WDXRF method. The correction process minimizes systematic errors, such as matrix effects, calibration discrepancies, and instrumental biases, ensuring that EDXRF results closely match the reference standard. The corrected data demonstrate greater consistency and precision, making EDXRF a more reliable tool for silver content analysis, particularly in applications where high accuracy is essential, such as quality control and material characterization. The comparison highlights the practicality of using corrected EDXRF data as a faster and cost-effective alternative to WDXRF without sacrificing accuracy. While non-corrected data may be suitable for preliminary assessments or less critical applications, they lack the precision required for detailed and regulatory analysis. Corrected EDXRF data thus provides a viable option for industries and researchers looking to streamline silver analysis while maintaining confidence in the results.

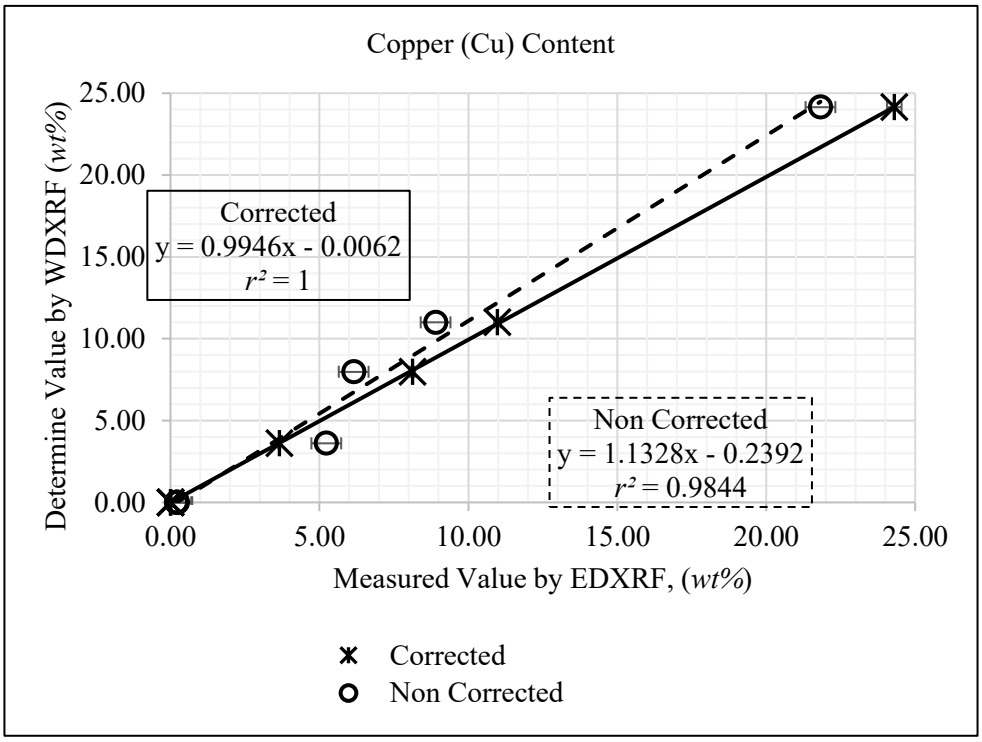

Figure 4.9 Correlation Graph Between WDXRF Value and EDXRF Measurement (Matrix Corrected and Non-Corrected) on Copper (Cu) Content

Figure 4.9 presents a comparative analysis of copper (Cu) content measured using Energy Dispersive X-ray Fluorescent (EDXRF) and Wavelength Dispersive X-ray Fluorescent (WDXRF), focusing on both corrected and non-corrected data. This analysis aims to evaluate the reliability and accuracy of EDXRF measurements compared to WDXRF, which serves as the reference method. The corrected data, represented by the solid line, follow the regression equation y = 0.9946x - 0.0062 with a coefficient of determination r^2 equal to 1. This indicates a perfect linear relationship between the EDXRF measurements and the WDXRF reference values. The slope of 0.9946 is almost equal to 1, confirming a high degree of accuracy in the corrected EDXRF results. The intercept, -0.0062, is negligible, indicating minimal deviation across the measurement range. These results highlight the effectiveness of the correction protocols in aligning EDXRF data with the reference standard, eliminating systematic biases, and ensuring high precision. In contrast, the non-corrected data, represented by the dashed line, follow the regression equation y = 1.1328x - 0.2392 with an r^2 value of 0.9844. While the relationship remains strongly linear, the slope

deviates significantly from 1, suggesting that non-corrected EDXRF measurements systematically overestimate copper content. Furthermore, the intercept value of -0.2392 indicates a bias in the measurements, contributing to the observed discrepancies between the non-corrected EDXRF and the WDXRF results. The lower r^2 value compared to the corrected data reflects increased variability, underscoring the limitations of non-corrected measurements for accurate elemental analysis.

The comparison of corrected and non-corrected EDXRF data against WDXRF underscores the necessity of implementing data correction protocols. Corrected EDXRF data exhibit exceptional accuracy and consistency, aligning closely with the reference method. This demonstrates the capability of EDXRF as a dependable analytical tool for copper content analysis, provided that robust correction protocols are integrated into the measurement workflow. These findings support the broader adoption of corrected EDXRF for precise elemental analysis in various industrial and research settings. Overall, the figures effectively demonstrate how data correction influences the accuracy of EDXRF measurements. The corrected data align closely with reference methods such as fire assay and WDXRF, validating the necessity of implementing correction protocols in analytical workflows. The findings support the broader adoption of EDXRF for elemental analysis, provided that appropriate correction techniques are applied to achieve consistent and reliable results.

4.4.4 Optimisation of the Corrective *k-factors*

Table 4.5 provides a comparison between certified values and EDXRF measurements for a series of alloy mixtures, demonstrating the impact of applying a corrective *k-factor* to improve the accuracy of EDXRF results. The *corrective k-factor* is calculated as the ratio of the certified value to the experimental EDXRF measurement, as expressed in Equation 3.2. This corrective *k-factor* is essential for realigning EDXRF measurements to match the certified reference values.

The corrective *k-factors* is critical in compensating for systematic biases inherent in the EDXRF measurement process. These biases may arise due to variations in detector sensitivity, calibration inconsistencies, or differences in the surrounding composition of alloy samples that can affect fluorescence signal intensities. By applying the corrective *k-factor*, the EDXRF measurements are adjusted to align closely with the certified values, as demonstrated by the improved accuracy across the samples.

Table 4.5
Corrective *k-factor* based on the Compositions of Gold Reference Materials.

Mixture	CRM Code	Certified Value, *wt%* $m(Au, X^{grav})$	XRF Measurement, *wt%* $m(Au, RM_{obs}^{XRF})$	Corrective Factor, $k = \frac{m(Au, X^{grav})}{m(Au, RM_{obs}^{XRF})}$
Au	NIST -SRM 685R	99.99 ± 0.05	99.95 ± 0.15	1.0004 ± 0.0005
Au-Ag	BAM ERM 508	75.12 ± 0.11	75.19 ± 0.18	0.9991 ± 0.0011
Au-Cu	MyRM 22K	91.80 ± 0.15	91.95 ±0.17	0.9985 ± 0.0014
Au-Ag-Cu	MyRM 5.102	92.14 ± 0.16	92.26 ±0.18	0.9987 ± 0.0016

The corrective *k-factor* is applied to the raw EDXRF measurements to correct the deviations observed in the experimental results. For each sample analysed, the corrective *k-factor* is determined based on the specific composition of the alloy mixture. The findings highlight how the corrected EDXRF values exhibit better agreement with the certified values, particularly for complex mixtures containing gold (Au), silver (Ag), and copper (Cu). In a gold alloy mixture with a high percentage of silver, the corrective *k-factor* adjusts the EDXRF measurement to account for the fluorescence signal contributions of both gold and silver, ensuring a more accurate representation of the true composition. However, in the case of pure gold, the corrective *k-factor* accounts for overestimations in the experimental ratio, which could result from calibration challenges inherent to pure elements. These findings emphasize the importance of incorporating correction protocols into EDXRF workflows to enhance their accuracy and reliability for elemental analysis.

Table 4.6

Comparison of EDXRF Measurements with and without the Corrective *k-factor,* k_{fac}, Against the Fire Assay Method Results

Mix	Sample Code	Composition of gold in mass fraction of percent (wt%)						
		Fire Assay (*wt%*) A	XRF result without k_{fac} (*wt%*) B	*%rsd*	*rel%* (A-B)/A*100	XRF result with k_{fac} (*wt%*) C	*%rsd*	*rel%* (A-C)/A*100
				k_{fac}1.0004 ± 0.0005				
Au	AU1	99.92 ± 0.05	99.86 ± 0.16	0.16	0.06	99.90 ± 0.11	0.11	0.02
	AU2	99.99 ± 0.05	99.94 ± 0.15	0.15	0.05	99.98 ± 0.10	0.10	0.01
	AU3	99.99 ± 0.05	99.93 ± 0.15	0.15	0.06	99.97 ± 0.10	0.10	0.02
	AU4	99.99 ± 0.05	99.93 ± 0.16	0.16	0.06	99.97 ± 0.11	0.11	0.02
				k_{fac}0.9991 ± 0.0011				
Au-Ag	AU5	83.50 ± 0.05	83.63 ± 0.18	0.22	-0.13	83.52 ± 0.13	0.16	-0.02
	AU6	91.70 ± 0.05	91.86 ± 0.16	0.17	-0.16	91.74 ± 0.11	0.12	-0.04
	AU7	87.50 ± 0.05	87.70 ± 0.17	0.19	-0.2	87.57 ± 0.12	0.14	-0.07
	AU8	75.10 ± 0.05	75.25 ± 0.17	0.23	-0.15	75.15 ± 0.12	0.16	-0.05
				k_{fac}0.9985 ± 0.0014				
Au-Cu	AU9	91.88 ± 0.05	92.02 ± 0.16	0.17	-0.14	91.94 ± 0.11	0.12	-0.06
	AU10	91.90 ± 0.05	92.03 ± 0.15	0.16	-0.13	91.95 ± 0.10	0.11	-0.05
	AU11	76.12 ± 0.05	76.27 ± 0.16	0.21	-0.15	76.15 ± 0.11	0.14	-0.03
	AU12	83.58 ± 0.05	83.70 ± 0.18	0.22	-0.12	83.62 ± 0.13	0.16	-0.04
				k_{fac}0.9987 ± 0.0016				
Au-Ag-Cu	AU13	91.89 ± 0.05	92.03 ± 0.19	0.21	-0.14	91.95 ± 0.14	0.15	-0.06
	AU14	76.34 ± 0.05	76.50 ± 0.18	0.24	-0.16	76.42 ± 0.13	0.17	-0.08
	AU15	75.10 ± 0.05	75.24 ± 0.19	0.25	-0.14	75.17± 0.14	0.19	-0.07
	AU16	74.55 ± 0.05	74.70 ± 0.20	0.27	-0.15	74.63 ± 0.15	0.20	-0.08

Table 4.6 displays the comparison between fire assay and EDXRF measurements with two decimal places. In addition, the table lists the values of various elements in the gold mixture with and without the corrective *k-factor*. The relative error was calculated as the absolute error of the measurement divided by the actual measurement. The relative error implied EDXRF's accuracy concerning fire assay values. The relative error (*rel%*) was calculated with the formula, $rel\% = (|x_1 - x_0|)/x_0) * 100$, where x_0 is the measured value from the fire assay method, and x_1 refers to the measured value from EDXRF. The relative error of the method approached was consistently improved and aligned with fire assay values for less than 0.1 *rel%* compared to corrective *k-factor* application for all measured metals.

The relative standard deviation (*%rsd*) was calculated to evaluate the reproducibility of measurements. It was expressed as a percentage and accomplished by dividing the standard deviation by EDXRF measurement, followed by a multiplication of 100. The results indicated that the measurements improved with less than 0.11 *%rsd* for pure Au, 0.16 *%rsd* for Au-Ag and Au-Ag-Cu mixtures, and less than 0.20 *%rsd* for mixtures of Au-Ag-Cu for measurement with *k*-factor correction, instead of 0.16*%rsd*, 0.23 *%rsd*, 0.22 *%rsd* and 0.27 *%rsd* for measurement without correction, respectively. This might be due to the improved closeness result and reduced bias as compared to the fire assay. The corrective *k-factor* has been applied to various commercial gold mixtures.

For comparison of the two analysis methods, Student's t-test was performed to verify the null hypothesis on the absence of significant difference in results means value for both methods, fire assay and EDXRF measurement were studied. The following parameters were calculated for the student's t-test: the mean value of measurements (x) for each sample, the variance (s), observation of repeated measurements (n), and the pooled variance (Sc). Au1, Au5, Au11, and Au13 samples were selected to represent the diverse mix of gold alloys.

Table 4.7

Paired t-test Comparison of Non-corrective and Corrective *k-factors* of EDXRF Measurement and Fire Assay Results

Measurement non-corrective *k-factor*								
Description	Au1		Au5		Au11		Au13	
	Fire Assay (wt%)	*EDXRF (wt%)*	*Fire Assay (wt%)*	*EDXRF (wt%)*	*Fire Assay (wt%)*	*EDXRF (wt%)*	*Fire Assay (wt%)*	*EDXRF (wt%)*
Mean (x)	99.92	99.85	83.50	83.63	76.12	76.27	91.89	92.03
Variance (s)	0.0005	0.0076	0.0006	0.0075	0.0007	0.0063	0.0006	0.0092
Observations (n)	10	10	10	10	10	10	10	10
Pooled Variance (Sc)	-0.083		0.425		-0.235		0.117	
Hypothesized Mean Difference (H)	0		0		0		0	
df	9		9		9		9	
t_{Stat} (95%)	2.4057		-5.2782		-5.2851		-4.7388	
P($T<=t$) (95%)	0.0395		0.0005		0.0005		0.0011	
$t_{Critical}$ (95%)	2.2622		2.2622		2.2622		2.2622	
Measurement with corrective *k-factor*								
Description	Au1		Au5		Au11		Au13	
	Fire Assay (wt%)	*EDXRF (wt%)*	*Fire Assay (wt%)*	*EDXRF (wt%)*	*Fire Assay (wt%)*	*EDXRF (wt%)*	*Fire Assay (wt%)*	*EDXRF (wt%)*
Mean (x)	99.92	99.90	83.50	83.52	76.13	76.15	91.89	91.95
Variance (s)	0.0005	0.0029	0.0006	0.0040	0.0007	0.0028	0.0006	0.0052
Observations (n)	10	10	10	10	10	10	10	10
Pooled Variance (Sc)	0.154		0.002		-0.356		-0.707	
Hypothesized Mean Difference (H)	0		0		0		0	
df	9		9		9		9	
t_{Stat} (95%)	0.8589		-0.828		-1.315		-2.0757	
P($T<=t$) (95%)	0.4127		0.4391		0.2209		0.0677	
$t_{Critical}$ (95%)	2.2622		2.2622		2.2622		2.2622	

Table 4.7 shows the student's t-test outcomes to verify the null hypothesis on the equivalence between mean values of results for two analyses of EDXRF as compared to fire assay method. One of the following hypotheses was investigated: H_0; there is no significant difference in mean values if *p-value is greater than 0.05;* H_1; there is a significant difference in mean values if *p-value is less than 0.05*. From the table, it has been shown that the *p-value* of the corrected EDXRF demonstrated results was greater than 0.05, as indicating there is no significant difference between fire assays. Meanwhile, the data showed that the *p-value* of non-corrected EDXRF values was less than 0.05, indicating there is a significant difference between the methods. The null hypothesis on the equivalence between mean values of results from fire assay and corrected EDXRF was confirmed. By obtaining from the table data for the student's t distribution for 9 degrees of freedom (*df*) and 95 % confidence level, it was discovered that corrected EDXRF gave an acceptable precision while verifying the null hypothesis on the equivalence between mean values of results and the fire assay.

4.5 Interlaboratory Comparison (ILC)

The NMIM laboratory has successfully participated in an interlaboratory comparison initiative with the Institute of Metrology of Bosnia and Herzegovina (IMBIH). This collaboration aimed to evaluate and establish the technical competence of the NMIM laboratory's analytical methods. To achieve this, IMBIH organized the Bilateral Proficiency Testing Scheme, designated as IMBIH.LH-B01.PT/20, specifically focused on the analysis of gold alloys. This testing followed the international standard ISO/IEC 17043, which outlines the general requirements for proficiency testing in conformity assessment. As part of the proficiency testing process, IMBIH prepared and distributed an unknown sample of gold alloy to the participating laboratories. The purity of this gold sample was determined using the traditional fire assay method, recognized for its accuracy and reliability in measuring metal content. The raw PT test material was prepared in the form of a wire with the gold assigned value of the sample, with a measurement uncertainty of 734.45 ± 0.23 mg. The PT sample was prepared by cutting the wire into equal pieces of approximately 1.0 gram, which were identified and labelled with MA-279/Au.

In contrast, the NMIM laboratory employed an enhanced EDXRF method to analyse the same sample. The first step is performed the qualitative analysis is to identify the possible elements in the PT sample. A spectrum in Figure 4.10 illustrates the spectrum for the MA-279/Au sample, highlighting the fluorescence signal intensities (cps) as a function of energy (keV). The spectrum shows distinctive peaks associated with specific elements in the sample, providing insights into its compositional analysis. The most prominent peaks are found around 9.711 keV and 11.439 keV, indicating the presence of elements that emit X-ray fluorescence in this energy range, primarily representing gold (AuLα and AuLβ). Additional peaks are noted at approximately 8.041 keV and 22.104 keV, implying contributions from other alloys such as Copper (CuKα) and Silver (AgKα), respectively. The general background intensity and smaller peaks may reflect the effects of the matrix or the presence of non-metallic components within the sample.

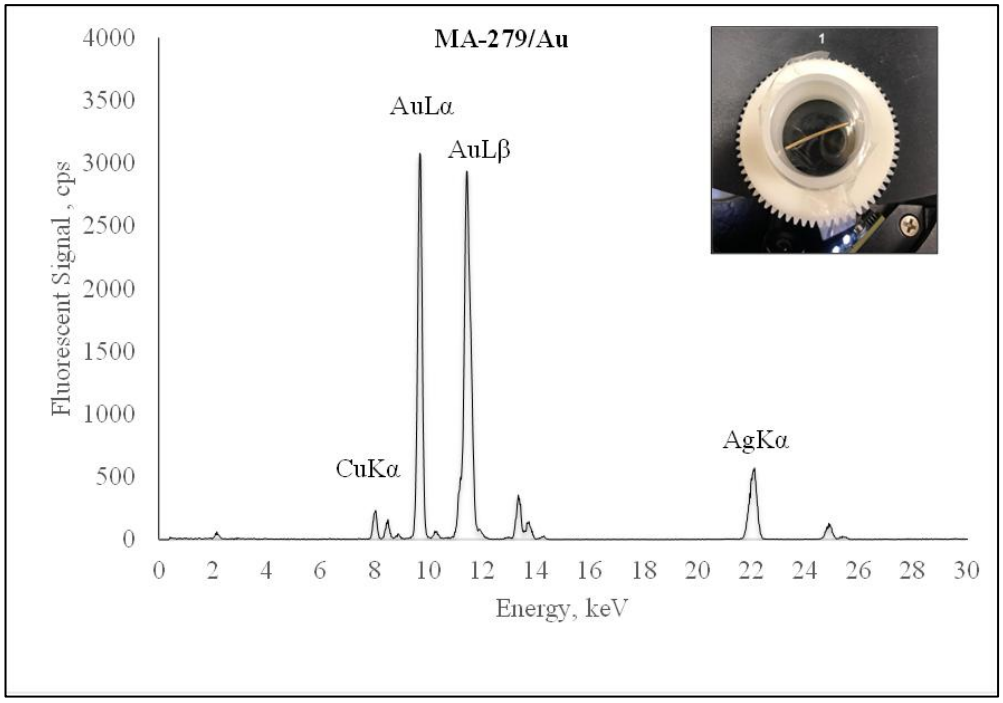

Figure 4.10 Pre-screening to Identify Possible Elements in the ILC Samples

Figure 4.11 shows a spot target area of the sample analysed. The image sequence displays the positioning and alignment of the MA-279 sample within the experimental setup, likely for X-ray fluorescence analysis. This visual documentation is crucial for ensuring accurate placement of the sample, optimal signal detection, and

reproducibility of results. The red circles in the image may indicate the focused areas where the instrument performed spot analysis at a 1.0 mm collimator size. Each spot corresponds to different locations or phases of the analysis.

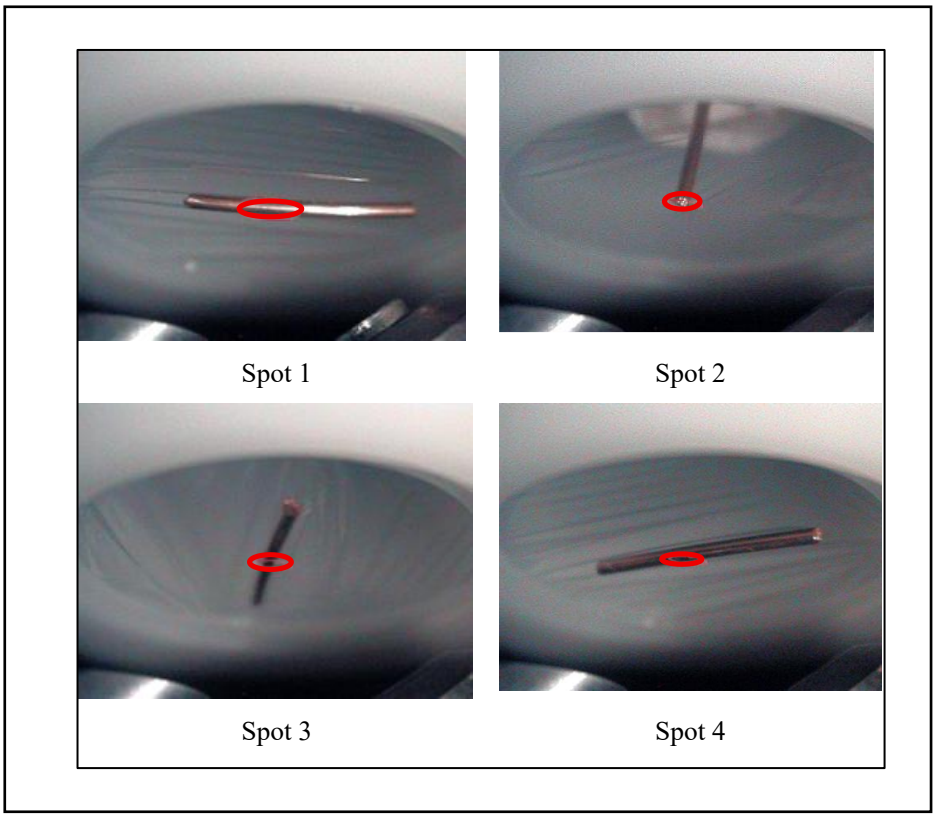

Figure 4.11 Different Spot Areas Using a 1.0 mm Collimator Size

Table 4.8 presents the results of gold (Au) concentration measurements in the MA-279/Au sample obtained by the NMIM (National Metrology Institute Malaysia). Measurements were conducted at four distinct spots on the sample, and their mean concentration, as well as the associated measurement uncertainty, were calculated. The values across the four spots are highly consistent, with minimal variation (± 0.95 mg/g).

Table 4.8
NMIM Reporting Results of gold (Au) Concentration Measurements in the MA-279/Au Sample

PT Samples	NMIM Results, mg/g					
	Spot 1	Spot 2	Spot 3	Spot 4	Mean, x	Measurement Uncertainty u
MA-279/Au	734.50	734.52	734.83	734.13	734.50	0.95

This indicates high accuracy in the measurement process and suggests that gold is uniformly distributed within the sample. This homogeneity is critical for applications requiring consistent material properties. The small measurement underscores the reliability and accuracy of the improvised EDXRF method by NMIM. The uncertainty accounts for potential errors in measurement equipment, sample handling, or environmental conditions. this result validates the presence of gold as a dominant component in the sample.

Table 4.9
Gold Concentration Analysis Results for the MA-279/Au Sample by Two Laboratories

Lab	Method Analysis	Mean, x	Measurement Uncertainty u
IMBIH	Fire Assay	734.45	0.23
NMIM	EDXRF	734.50	0.95

Table 4.9 presents gold concentration analysis results for the MA-279/Au sample obtained through two independent laboratory methods: Fire Assay (IMBIH) and Energy-Dispersive X-ray Fluorescent (EDXRF, performed by NMIM). These methods provide complementary approaches to quantifying gold content, with differences in mean values and associated uncertainties. The mean concentrations reported by both methods are highly consistent, differing by only 0.05 mg/g, suggesting excellent agreement between the two methods. The slight difference in mean values is within the range of measurement uncertainty, suggesting that the results are statistically indistinguishable. The slightly higher uncertainty observed in EDXRF measurements with 0.95 mg/g is expected from its non-destructive nature, which renders the method more susceptible to matrix effects, sample form, instrument stability, and limitations in calibration accuracy. In contrast, fire assay provides significantly lower uncertainty, with 0.23 mg/g, which is due to the complete isolation of gold during the analytical procedure. However, the reduction of the random error (precision) during the calibration method has greatly improved the uncertainty of the measurement.

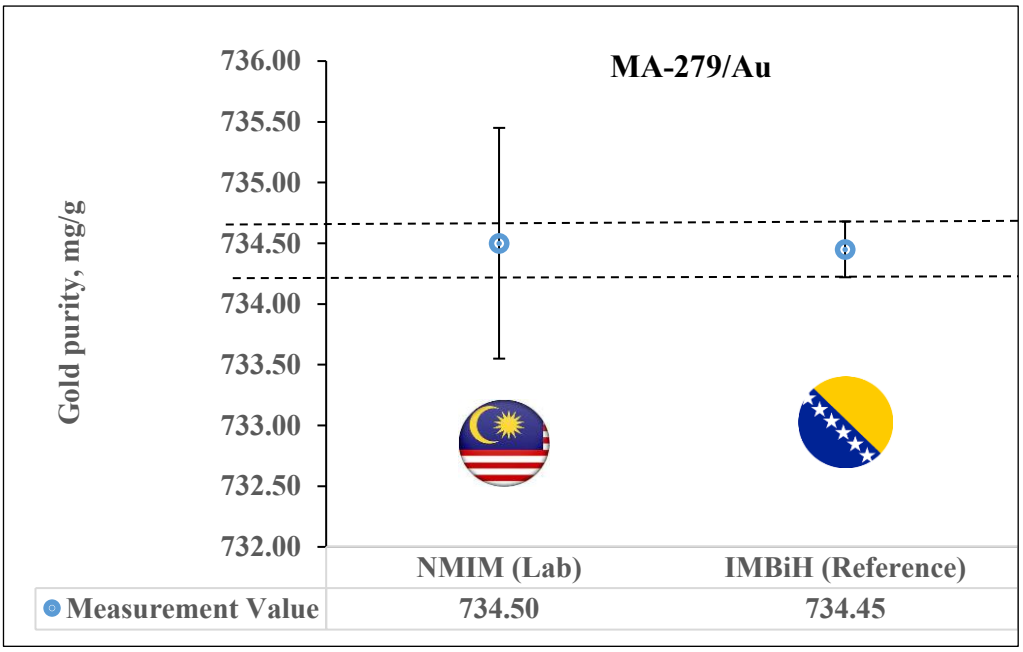

Figure 4.12 Comparison of Optimised EDXRF Method with Fire Assay through Proficiency Testing (PT)

The comparison results, illustrated in Figure 4.12, provide clear evidence of the traceability of the EDXRF method to the fire assay results. This finding validates the accuracy of the gold purity measurements obtained using the EDXRF technique. Consequently, this successful proficiency testing not only highlights the technical capabilities of the NMIM laboratory but also underscores the robustness of the EDXRF method in analysing gold alloys within a regulated framework.

Table 4.10
Results of Proficiency Testing (PT) for the MA-279/Au Sample, Comparing the Measured Value by NMIM EDXRF of Gold Purity with an Assigned Value by the Reference Lab, IMBIH

PT sample	Measured Value (%)				Lab - Ref	*z' score*
	Ref	u_{REF}	*Lab*	u_{LAB}		
MA 279/Au	734.45	0.230	734.500	0.950	0.050	0.05

Table 4.10 summarizes the results of proficiency testing (PT) for the MA-279/Au sample, comparing the measured value by NMIM EDXRF of gold purity with an assigned value by the reference lab, IMBIH. The table also includes the z'-score, which evaluates the laboratory's performance relative to the reference. The measured value reported by the laboratory (lab) is 734.50 with an associated uncertainty (u_{lab}) of 0.95 mg/g. The reference value (ref) is 734.45 mg/g with a reference uncertainty (u_{ref}) of 0.23 mg/g. A z'-score of 0.05 is well within the acceptable range ($|z'| \leq 2$ indicating that the laboratory's result is consistent with the reference value and falls within acceptable performance limits. In conclusion, the proficiency testing results for the MA-279/Au sample demonstrate a high degree of accuracy and reliability in the laboratory's measurements. The close alignment between the measured value and the reference value confirms the laboratory's strong performance and adherence to quality standards. These findings support the validity of the reported gold concentration and highlight the robustness of the analytical methods employed.

4.6 Traceability of EDXRF Method for Gold Purity Measurement

4.6.1 Development of Gold Certified Reference Materials

Gold Certified Reference Materials, known as MyREM Au with code 103, have been carefully produced as secondary standards for the EDXRF method. This MyREM for gold matrices was developed to fulfill the strong demand for CRMs of Malaysian precious metal standardization, since only a few are available internationally. These reference materials cater to a range of yellow gold applications in quality control processes within Malaysian markets. These materials were independently designed from calibration materials (CM) used previously in the development method to ensure the validity and bias of the procedure are under control. The materials are lightweight and portable; specifically designed for establishing calibration or quality control of portable EDXRF equipment. As shown in Figure 4.13, a gold certified reference material is shaped into a round form with a diameter of 12 mm and is securely embedded in a sturdy plastic disc with a diameter of 25 mm. The homogeneity of MyREM Au was assessed using purity assays conducted by EDXRF on ten random sample spots. The results indicated that the materials are sufficiently homogeneous, as

the variation in analysis results between the samples was not significantly different at a 95% confidence level when compared to repeat analyses of the same samples.

Figure 4.13 Gold Certified Reference Materials Known as MyREM Au in the Form of a Round Slice with a 12 mm Diameter Embedded in Plastic Discs with a 30 mm Diameter

4.6.2 Measurement Uncertainty Sources for MYREM Au by EDXRF

The calculation of the measurement uncertainty for MyREM Au by EDXRF begins with the analysis of uncertainty sources according to the previous discussion of the Ishikawa diagram, chapter 3.4.3.5. The sources of uncertainty may be Type A or Type B. The Type A source is a component of statistical methods, and in this study, is related to the repeatability of standard deviations, intermediate precision uncertainty, bias of CRM uncertainty, and calibration curve uncertainty. The sources of uncertainty, Type B, however, are components evaluated by methods other than the series of observations. In the case of the EDXRF method, the following were considered as Type B components: EDXRF digital resolution uncertainty (Edition, 2012).

4.6.2.1 Standard Uncertainty from Repeatability

The statistical results of the MyREM samples Au after correction with *k-factor values* are presented in Table 4.11. The corrective means of gold, $\bar{y}$ was determined by corrective measured means, y_i with *k-factor values,* k_{fac}, as discussed previously by Equation 3.3. The standard deviations of samples $s(x_i)$ and standard deviations of the

means $s(\bar{x}_i)$ were calculated using Equation 4.1, where n is the number of measurements (Krummenauer et al., 2021).

$$s(\bar{x}_i) = \frac{s(x_i)}{\sqrt{n}} \tag{4.1}$$

The repeatability standard deviation is a source of uncertainty Type A determined by n repeated and independent observations (in this study n = 10), where the standard uncertainty Type A is $u(x_i) = s(\bar{x}_i) = u(s_{\bar{x}})$ and the degrees of freedom are $v_i = n - 1$, for elements in each sample (Ramsey & Ellison, 2015).

Table 4.11
Statistical Parameters for Gold Element in MyREM Au Samples (Code MyREM 103) with Corrective *k-factors, k_{fac}*

Samples Code	MyRM_Au 103		
No.	Au (*wt%*)	Ag (*wt%*)	Cu (*wt%*)
1	75.320	12.382	12.252
2	75.381	12.402	12.315
3	75.383	12.251	12.210
4	75.392	12.272	12.301
5	75.366	12.420	12.286
6	75.392	12.219	12.300
7	75.409	12.252	12.290
8	75.461	12.480	12.202
9	75.351	12.211	12.172
10	75.400	12.362	12.174
$\bar{y}$	75.386	12.325	12.250
$s(x_i)$	0.037	0.095	0.056
n	10	10	10
$\boldsymbol{s(\bar{x}_i)}$	**0.12 *wt%***	**0.30 *wt%***	**0.18 *wt%***

4.6.2.2 Standard Uncertainty from Intermediate Precision

Standard uncertainty from intermediate precision $u(s_i)$ is determined based on the variation observed in results under different conditions. In this study, EDXRF measurements were performed on tens (10) replicates monthly for 5 months at varying temperatures and humidity to study the stability of the gold element in the MyREM Au 103 samples. Table 4.12 shows the stability study of the gold elements in the MyREM Au 103 samples for 5 months, which is a measure of the consistency and reliability of

a method over time in the same method setup. The goal is to evaluate the robustness of a method and ensure that it produces reliable results even under varying circumstances. The $u(s_i)$ was calculated using Equation 4.2.

$$(s_i) = \sqrt{\frac{1}{n}\sum_{i=1}^{n}(x_i - \bar{x})^2} \tag{4.2}$$

where:

$u(s_i)$	the uncertainty from intermediate precision (pooled).
x_i	the value of each repeated measurement.
$\bar{x}$	the mean of all the measurements.
n	the total number of measurements taken under different conditions (times)

Table 4.12
The Stability Study of the Gold Elements in the MyREM Au 103 Samples for 5 Months.

Samples Code	MyRM_Au 103				
No.	Month 1 (19℃, 60 %RH) (*wt%*)	Month 2 (21℃,70 %RH) (*wt%*)	Month 3 (21℃, 73 %RH) (*wt%*)	Month 4 (23℃, 57 %RH) (*wt%*)	Month 5 (25℃, 77 %RH) 5 (*wt%*)
1	75.320	75.321	75.388	75.339	75.332
2	75.381	75.391	75.382	75.373	75.352
3	75.383	75.378	75.329	75.323	75.385
4	75.392	75.312	75.372	75.372	75.359
5	75.366	75.362	75.355	75.401	75.367
6	75.392	75.390	75.361	75.410	75.402
7	75.409	75.371	75.389	75.408	75.441
8	75.461	75.401	75.444	75.442	75.400
9	75.351	75.400	75.361	75.357	75.382
10	75.400	75.395	75.400	75.392	75.406
Mean of all measurements ($\bar{x}$)	75.380				
Pooled of stdev	0.033				
Number of measurements (n)	50				
Uncertainty from intermediate precision (pooled). $\boldsymbol{u(s_i)}$	**0.05 wt%**				

4.6.2.3 Standard Uncertainty from Bias of CRM

The standard uncertainty relating to the bias of CRM value, $u(CRM_{bias})$, is calculated based on the bias of repeatability measurement of CRM and data from the ERM 508 certificate shown in Table 4.13. This expanded uncertainty value, U_{cert} must be divided by its coverage factor, *k* to obtain the standard uncertainty u_{cert}. Equation 4.3 shows a standard uncertainty u_{CRMrep} due to the measurement repeatability is the standard deviation of the mean of the repeat readings.

$$u_{CRMrep} = \sqrt{\frac{\sum_{i=1}^{i=n}(\bar{x} - x_i)^2}{n-1}} \tag{4.3}$$

where

u_{CRMrep}	standard uncertainty for repeatability of EDXRF measurement of CRM
$\bar{x}$	the mean value of the data set
x_i	the ith values of data set
n	the number of values in the data set

Since the assessment of the uncertainty due to systematic bias resulting from the quantification model, matrix effects, the presence of instrumental blank signal or due to other sources can be estimated from the standard deviation of the bias of the results (q_i) of replicate analysis, Equation 4.4 demonstrated bias is defined as the difference between the obtained result and the certified value.

$$q_i = x_i - x_{cert} \tag{4.4}$$

The average bias is further used to correct the results and the uncertainty due to bias $u(CRM_{bias})$, can be quantified using Equation 4.5.

$$u(CRM_{bias}) = \sqrt{(u_{CRM_{rep}})^2 + \left(u_{q_i}\right)^2 + (u_{cert})^2} \tag{4.5}$$

where,

$u(CRM_{bias})$	combine the standard uncertainty from the CRM bias
$u_{CRM_{rep}}$	uncertainty of repeatability of CRM
u_{q_i}	uncertainty from bias
u_{cert}	uncertainty from the CRM certificate

Table 4.13
The Standard Uncertainty Relating to the Bias of CRM Value is Calculated Based on the Bias of the Repeatability Measurement of CRM and Data from the ERM 508 Certificate

Uncertainty from the bias of CRM (Au element)			
BAM ERM 508			
No	Certificate, wt% x_{cert}	Measured, wt% x_i	Bias, wt% $q_i = x_i - x_{cert}$
1	75.120	75.132	0.032
2	75.120	75.159	0.059
3	75.120	75.174	0.074
4	75.120	75.175	0.075
5	75.120	75.082	0.018
6	75.120	75.132	0.032
7	75.120	75.159	0.059
8	75.120	75.174	0.074
9	75.120	75.175	0.075
10	75.120	75.082	0.018
Mean	75.120	75.144	0.052
		$u_{CRM_{rep}} = 0.039$	$u_{q_i} = 0.017$

The certificate of analysis of BAM ERM 508 shows a value of expanded uncertainty U_{cert} value of 0.110 wt% with a coverage factor of *k= 2.5*, corresponding to a level of confidence of about 95%. To convert into the standard uncertainty u_{cert}, the value must be divided by 2.5.

$$u_{cert} = \frac{0.110}{2.5} = 0.044 \text{ wt\%}$$

Hence, all the uncertainties that contribute to the bias have to combine to determine $u(CRM_{bias})$ value.

$$u(CRM_{bias}) = \sqrt{(0.039)^2 + (0.017)^2 + (0.044)^2} = 0.061 \text{ wt\%}$$

4.6.2.4 Standard Uncertainty from Calibration Curve

The standard uncertainty for the calibration curve, $u(curve)$, considers the correlation between the intercept of the y-axis (c) and the slope (m) of the linear equation (y = mx + c), and is estimated using Equation 4.6. The data for the calibration materials is based on a correlation graph between fire assay EDXRF measurements (corrected) and gold (Au) content, as shown previously in Figure 4.7.

Table 4.14 determines the estimation of standard uncertainty for the calibration curve based on a plotted calibration curve between fire assay EDXRF measurements (corrected) and gold (Au) content.

$$u(curve) = \frac{rsd}{m}\sqrt{\frac{1}{N}+\frac{1}{n}\frac{(y_0-\bar{y})^2}{m^2\left(\sum_{i=1}^{n}x_i{}^2-\frac{\left(\sum_{i=1}^{n}x_i\right)^2}{n}\right)}} \quad (4.6)$$

where *rsd* is the residual standard deviation and shown in Equation 4.7

$$ursd = \sqrt{\frac{\sum_{i=1}^{n}(y_o-\hat{y}_i)^2}{n-2}} \quad (4.7)$$

Table 4.14
Estimating Standard Uncertainty for the Calibration Curve Based on a Plotted Calibration Curve Between Fire Assay EDXRF Measurement (Corrected) on Gold (Au) Content

Symbol	Description	Values
rsd	residual standard deviation	0.109
m	the slope	1.005
c	the intercept of the y-axis (c)	-0.335
y_0	the observed response for the unknown samples	75.386
$\hat{y}_i$	the predicted response for each calibration sample	85.903
N	the number of measurements of the response of the unknown (y_o)	3
n	the number of points in the calibration line	21
$u(curve)$	the standard deviation of the prediction concentration	**0.67** ***wt%***

4.6.2.5 Standard Uncertainty from EDXRF Digital Resolution

The Arl Quant EDXRF equipment resolution from the manufacturer was 0.001 wt%. The standard uncertainty of the digital resolution, $u(res)$, was calculated using Equation 4.8. The $u(res)$ is a rectangular distribution, and it is assumed that the degrees of freedom tend towards infinity for this distribution.

$$u(res) = \frac{resolution}{\sqrt{12}} = \frac{0.001}{\sqrt{12}} = 0.000289\ wt\% \quad (4.8)$$

4.6.2.6 Combine standard uncertainty calculation

After transforming all the uncertainties (Type A & Type B) into standard uncertainties $u(\bar{x}_i)$, it may be combined using Equation 4.9, which renders the combined uncertainty $u_c(y)$. Since all the sensitivity coefficients c_i for the $u(x_i)$, in this study are equal to 1 (because the contributions are given in wt%), Equation 4.9 can be simplified into Equation 4.10. The calculated values for $u_c(y)$ for each element, per sample is shown in Table 4.15.

$$u_c(y) = \sqrt{\sum_{i=1}^{n} [c_i]^2 \, u^2(x_i)} \tag{4.9}$$

$$u_c(y) = \sqrt{u(s_{\bar{x}})^2 + \, u(s_i)^2 + u(CRMbias)^2 \, + u(curve)^2 \, + \, u(res)^2} \tag{4.10}$$

$$u_c(y) = \sqrt{(0.012)^2 + \, (0.005)^2 + (0.061)^2 \, + (0.067)^2 \, + \, (0.000289)^2}$$

$$u_c(y) = 0.092 \; wt\%$$

The uncertainty contributions for the gold (Au) element in the MyREM Au 103 sample. The sources of uncertainty can have different relative weights in the composition of the combined standard uncertainty value. The observation shows that the calibration curve and bias from CRM measurement sources are the major contributors. The sources from EDXRF digital resolution might be negligible. It may be concluded that the calibration method and corrective factor for EDXRF are essential improvements to improve accuracy in minimizing error and ensuring robustness and reliability of analytical results. It is important to be able to quickly and easily identify the main contributors to the final uncertainty value and whether it needs to be optimized to reduce the expanded uncertainty or not. Its presentation is vital in studies that calculate measurement uncertainty.

Table 4.15

Calculation of Standard Uncertainty $u_c(y)$ of Au Element in MyREM Au 103

Input Quantity X_i	Type	Estimate x_i (wt%)	Probability distribution	Divider	Standard uncertainty $u(x_i)$ (%m/m)	Sensitivity coefficient c_i	Contribution to uncertainty $c_i(y) = u(x_i).c_i$	Degree of freedom v_i
Repeatability	A	$s = \bar{x}_i$ 0.037	normal	$\sqrt{n}$	$u(s_{\bar{x}})$ 0.012	1	$u_1(y) = 0.012$	$v_1 = n - 1$ $v_1 = 9$
Intermediate precision	A	$u(s_i)$ 0.033	normal	$\sqrt{n}$	$u(s_I)$ 0.005	1	$u_2(y) = 0.005$	$v_2 = n - 1$ $v_2 = 49$
Bias of CRM	A	$u(CRM)$ 0.110	normal	*k = 2.5*	$u(CRM_{bias})$ 0.061	1	$u_3(y) = 0.061$	$v_3 = n - 1$ $v_3 = 9$
Calibration curve	A	---	normal	---	$u(curve)$ 0.067	1	$u_4(y) = 0.067$	$v_4 = n - 2$ $v_4 = 19$
Digital Resolution	B	0.001	rectangular	$\sqrt{12}$	0.000289	1	$u_5(y) = 0.000289$	$v_5 = \infty$

4.6.2.7 Expanded Uncertainty Calculations

Firstly, the effective degrees of freedom v_{eff} are calculated using the Welch-Satterthwaite formula, Equation 4.11, rounding the integer values downwards. Later, the coverage factor k_p is calculated using Equation 4.12 where t_p is obtained from the bilateral *t*-distribution (Student's distribution) (Ramsey & Ellison, 2015).

$$v_{eff} = \frac{u_c^4(y)}{\sum_i^N \frac{u_i^4(y)}{v_i}} com\ v_{eff} \leq \sum_{i-1}^{N} v_i \tag{4.11}$$

$$k_p = t_p\left(v_{eff}\right) \tag{4.12}$$

Finally, the uncertainty of the measurement or expanded uncertainty (U_p) is obtained by multiplying the combined standard uncertainty $u_c(y)$ by the coverage factor ($k_p = 2$) for a 95% confidence interval according to Equation 4.13 (Edition, 2012).

$$U_p = k_p \,.\, u_c(y) \quad (4.13)$$
$$U_p = 2.(0.092) = \ 0.183\ wt\%$$

Therefore, to express the final measurement with the corresponding measurement uncertainty in the analysis of gold element in MyREM Au 103 samples, the value is already rounded to three significant digits for the uncertainty.

$$Gold\ (Au)\ purity\ in\ MyREM\ Au\ 103: \ = mean\ \pm U_p$$
$$Gold\ (Au) purity\ in\ MyREM\ Au\ 103: \ = 75.386\ wt\% \ \pm 0.183\ wt\%$$

A certificate of analysis has been issued for each set of MyREM Au, detailing the results, expanded uncertainty, method used, traceability, batch number, and expiry date for this CRM production (Figure 4.14). To ensure accuracy and reliability, these certified reference materials are traceable to the National Metrology Institute (NMI), which establishes their credibility. It is an essential tool for laboratories and organizations that aim to maintain high standards of quality assurance in precious metal testing and analysis.

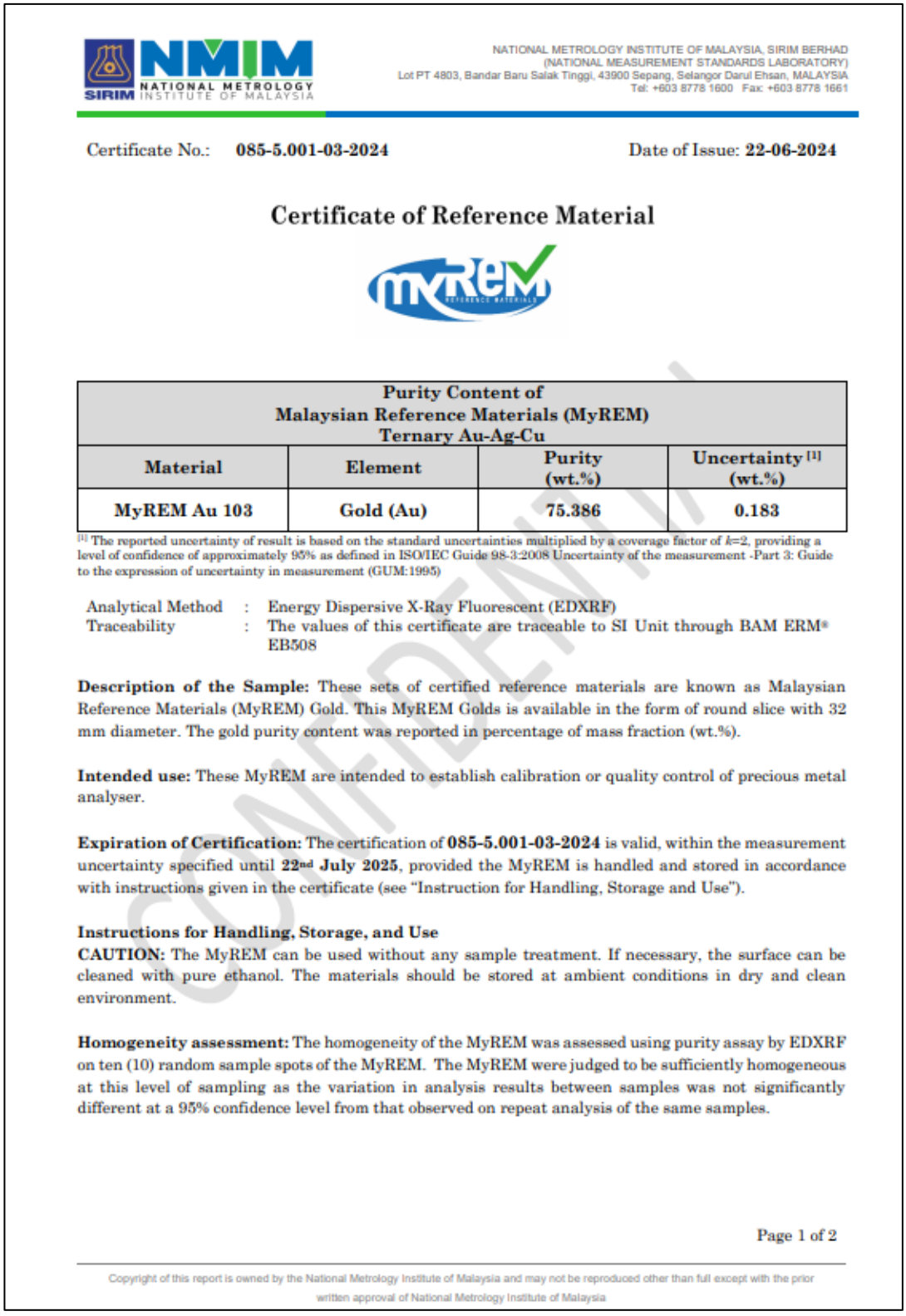

NATIONAL METROLOGY INSTITUTE OF MALAYSIA, SIRIM BERHAD
(NATIONAL MEASUREMENT STANDARDS LABORATORY)
Lot PT 4803, Bandar Baru Salak Tinggi, 43900 Sepang, Selangor Darul Ehsan, MALAYSIA
Tel: +603 8778 1600 Fax: +603 8778 1661

Certificate No.: **085-5.001-03-2024** Date of Issue: **22-06-2024**

Certificate of Reference Material

Purity Content of Malaysian Reference Materials (MyREM) Ternary Au-Ag-Cu			
Material	**Element**	**Purity (wt.%)**	**Uncertainty [1] (wt.%)**
MyREM Au 103	**Gold (Au)**	**75.386**	**0.183**

[1] The reported uncertainty of result is based on the standard uncertainties multiplied by a coverage factor of k=2, providing a level of confidence of approximately 95% as defined in ISO/IEC Guide 98-3:2008 Uncertainty of the measurement -Part 3: Guide to the expression of uncertainty in measurement (GUM:1995)

Analytical Method : Energy Dispersive X-Ray Fluorescent (EDXRF)
Traceability : The values of this certificate are traceable to SI Unit through BAM ERM® EB508

Description of the Sample: These sets of certified reference materials are known as Malaysian Reference Materials (MyREM) Gold. This MyREM Golds is available in the form of round slice with 32 mm diameter. The gold purity content was reported in percentage of mass fraction (wt.%).

Intended use: These MyREM are intended to establish calibration or quality control of precious metal analyser.

Expiration of Certification: The certification of **085-5.001-03-2024** is valid, within the measurement uncertainty specified until **22nd July 2025**, provided the MyREM is handled and stored in accordance with instructions given in the certificate (see "Instruction for Handling, Storage and Use").

Instructions for Handling, Storage, and Use
CAUTION: The MyREM can be used without any sample treatment. If necessary, the surface can be cleaned with pure ethanol. The materials should be stored at ambient conditions in dry and clean environment.

Homogeneity assessment: The homogeneity of the MyREM was assessed using purity assay by EDXRF on ten (10) random sample spots of the MyREM. The MyREM were judged to be sufficiently homogeneous at this level of sampling as the variation in analysis results between samples was not significantly different at a 95% confidence level from that observed on repeat analysis of the same samples.

Page 1 of 2

Figure 4.14 Main Information in MyREM Au 103 Certificate

Optimisation of tuning configuration and calibration setup of the EDXRF method eliminates variability and contributes to the reliability of the analytical results.

The application of the optimised EDXRF method, as discussed previously, provides a non-destructive, accurate, and efficient means of determining the elemental composition of gold alloys. Regular calibration and validation of the instrument using certified reference materials is critical to eliminating errors and maintaining accuracy. The inclusion of MyREM Gold underscores its indispensable role in instrument calibration, method validation, and quality control through the optimization of theoretical algorithms and correction factors for portable EDXRF practical applications, disseminated measurement uncertainty, and enabling accurate gold purity assessments in the gold industry.

In conclusion, by ensuring the accuracy, traceability, and application versatility of the non-destructive EDXRF method, the workflow may contribute to increased confidence among consumers and stakeholders, enhanced regulatory compliance, and prevention of fraudulent practices in gold markets, also strengthening scientific methodologies for future advancements in elemental analysis.

CHAPTER 5
CONCLUSIONS

5.1 Conclusions

This study effectively achieved its objectives, resulting in significant advancements in gold alloy analysis using the Energy-Dispersive X-ray Fluorescent (EDXRF) method.

First, the study successfully fabricated a homogeneous ternary calibration material (Au-Ag-Cu) with gold content ranging from 75.00 wt% to 99.99 wt%. This material serves as a critical reference for accurate gold analysis, ensuring measurement precision in EDXRF applications. Elemental purity tests confirmed uniform distribution of alloying components, with fire assay validation showing minimal variation (± 0.05 wt%), demonstrating high repeatability.

Second, the EDXRF method was optimized through precise parameter adjustments, including calibration methodology, which includes spectral peak selection (prioritizing AuLα for its stronger intensity and signal-to-noise ratio), collimator beam sizing (1.0 mm to 8.8 mm, tailored to sample area), and instrument realignment using corrective *k-factors*. The integration of empirical calibration with standardless Fundamental Parameters (FP) achieved exceptional accuracy, evidenced by a near-perfect regression (r^2 = 0.9999) for all metals. The t-test confirmed significant improvement post-optimization, validating the method's enhanced precision.

Third, the optimized EDXRF method was rigorously evaluated against the fire assay (the gold standard for purity analysis). Results showed strong agreement, with: Relative error < 0.1% across all matrices, Relative standard deviation (*rsd*) of < 0.11% (pure Au), 0.16% (binary alloys), and 0.20% (ternary alloys), and student's t-test ($p \geq 0.05$) confirming no statistically significant difference between optimised EDXRF and fire assay means, and successful interlaboratory comparisons (ILC) further demonstrated the method's reliability, positioning EDXRF as a viable alternative to destructive techniques.

Finally, the study successfully established metrological traceability for EDXRF measurements using MyREM gold reference materials (covering ternary mixtures), aligning with international standards (ISO 23345). This ensures credibility for critical

applications in precious metal trading and refining. By fulfilling its objectives, this study developed a reliable, accurate, and traceable EDXRF-based method for gold purity analysis. The advancements enhance EDXRF's utility in both industrial and scientific settings, offering a non-destructive, efficient, and compliant alternative to traditional assays.

Overall, this study demonstrates that EDXRF, when supported by purpose-built ternary calibration materials and a hybrid calibration strategy, can achieve analytical performance comparable to the fire assay method for gold purity determination. The most significant finding is that the integration of empirical calibration with the Fundamental Parameters (FP) approach effectively mitigates matrix effects and spectral interferences across binary and ternary gold alloys, enabling sub-0.1% relative error and excellent repeatability. The successful establishment of metrological traceability using MyREM certified reference materials further elevates EDXRF from a screening tool to a traceable quantitative technique compliant with international standards. Collectively, these findings confirm that optimized EDXRF is a reliable, non-destructive, and metrologically sound alternative for high-accuracy gold purity analysis, with direct applicability in hallmarking, precious metal trading, and industrial quality control.

CHAPTER 6
RECOMMENDATIONS

6.1 Recommendations

Although the study increased the accuracy of the EDXRF method for purity measurements of a gold alloy, there are certainly a couple of aspects that require future studies and implementation in practice. The following recommendations could help improve and broaden the applicability of this method:

i. Improve Calibration Models: This study only covered the application of the EDXRF method for ternary Au-Ag-Cu mixture in the range 75.00 wt% % to 99.99 wt%. This range may cover the range of common and popular Malaysian yellow golds. However, there has been a significant improvement in the calibration models, and it is still in need of optimization, especially for alloys beyond ternary gold-silver-copper with complicated compositions. Future research could work towards generating multi-elemental calibration standards, as advanced modelling tools could provide predictions regarding the effect of alloying elements on the fluorescence signal. Certain alloys, particularly those enriched with base metals, are difficult to effectively separate during analysis, so further investigation into more advanced model correction matrices is required to better facilitate these complex interferences. This might be considered to study the element beyond gold-silver-copper mixtures.

ii. Standardization of sample preparation: Measurement reproducibility was found to be influenced by sample geometry and surface roughness; thus, we suggest future studies should work towards standardization of sample preparation protocols. Such as, but not limited to, homogeneous sample thickness and an even surface. Designing custom sample holders or fixtures that minimize these effects would also aid in achieving greater consistency between different samples and testing locations.

iii. Integration of Other Techniques: The integration of EDXRF with other analytical methods, such as atomic absorption spectroscopy (AAS) or inductively coupled optical emission spectrometry (ICP-OES), should be explored to improve the reliability of purity measurements. The combination of

these methods can offer complementary information, which can be particularly useful for identifying very low concentrations of impurities that may not be measured by EDXRF alone.

iv. Field testing and Industry adoption: This study has limitations in laboratory conditions from 19℃ to 25℃ with 55 to 80 % of humidity conditions. Future work will entail analysing the optimized EDXRF technique at the industry level, concerning its outdoor application in gold mining and gold refining operations in different environmental conditions.

In summary, while this study significantly advances the EDXRF method for gold alloy purity measurement, continued research and development are necessary to address remaining challenges, further optimize the technique, and expand its industrial application. The proposed recommendations will help pave the way for more accurate, efficient, and accessible purity testing solutions in the precious metals industry

REFERENCES

Ab Majid, H., & Abdullah, A. (2019). Gold as an Alternative Asset Investment in Malaysia. *In Book: Islamic Fund & Wealth Management. A Way Forward*.

Abdullah, J., Samsudin, A., Omar, N. L., & Mananb, H. A. (2015). Non-destructive assaying gold jewellery using dual-energy micro-computed tomography. *Jurnal Teknologi*, *73*(3), 25–28.

Anggraini, D., Khumaeni, A., Hartadi, B. S., Sugito, H., & Wardaya, A. Y. (2020). Authentication of gold jewelry based on elemental composition using laser-induced breakdown spectroscopy. *Journal of Physics: Conference Series*, *1524*(1).

Artyukh, T., Hryhorenko, I., Ternova, A., Yaheliuk, S., & Cernavca, M. (2018). Influence of the alloy composition on determining the millesimal fineness of gold by X-ray fluorescent and assay analysis. *Eastern-European Journal of Enterprise Technologies*, *5*(12–95), 6–18.

ASTM E1335-08. (2017). Standard Test Methods for Determination of Gold in Bullion by Fire Assay Cupellation. *ASTM International*, *08*(Reapproved), 1–7.

Azizah Othman, N. H. & S. A. (2013). Perkembangan Ar-Rahnu di Terengganu : Kajian Kes Terhadap Ar-Rahnu Majlis Agama Islam dan Adat Melayu Terengganu (MAIDAM). *Persidangan Kebangsaan Ekonomi Malaysia Ke VIII (PERKEM VIII)*, *2*, 951–959.

Battaini, P., Bemporad, E., & De Felicis, D. (2014). The fire assay reloaded. *Gold Bulletin*, *47*(1–2), 9–20.

Belouafa, S., Habti, F., Benhar, S., Belafkih, B., Tayane, S., Hamdouch, S., Bennamara, A., & Abourriche, A. (2017). Statistical tools and approaches to validate analytical methods: Methodology and practical examples. *International Journal of Metrology and Quality Engineering*, *8*.

Bonizzoni, L., Maloni, A., & Milazzo, M. (2006). Evaluation of effects of irregular shape on quantitative XRF analysis of metal objects. X-Ray Spectrometry, 35(6), 390-399. *X-Ray Spectrometry*, *35*(6), 390–399.

Bonizzoni, L. (2015). ED-XRF analysis for Cultural Heritage: Is quantitative evaluation always essential? *Journal of Physics: Conference Series*, *630*(1).

Buccolieri, A., Castellano, A., Iacobellis, V. N., Paladini, F., & Buccolieri, G. (2021). ED-XRF analysis of the mediaeval copper-based door in Monte Sant'Angelo (Southern Italy). *Archaeological and Anthropological Sciences*, *13*(6).

Caporali, S., Bellandi, S., Innocenti, M., Lopilato, O., Romualdi, L., & Pezzatini, G. (2010). Determination of gold in alloys via potentiometric titration; An alternative to the fire assay. *Gold Bulletin*, *43*(2), 122–130.

Černohorský, T., Pouzar, M., & Jakubec, K. (2006). ED XRF analysis of precious metallic alloys with the use of combined FP method. *Talanta*, *69*(3), 538–541.

Chandra Sekhar, K., Gupta, K. K., Bhattacharya, S., & Chakravarthy, S. (2004). The determination of gold in ore samples by Inductively Coupled Plasma Optical Emission Spectrometry (ICP-OES). *Atomic Spectroscopy*, *25*(4), 165–169.

Conrey, R. M., Goodman-Elgar, M., Bettencourt, N., Seyfarth, A., Van Hoose, A., & Wolff, J. A. (2014). Calibration of a portable X-ray fluorescence spectrometer in the analysis of archaeological samples using influence coefficients. *Geochemistry: Exploration, Environment, Analysis*, *14*(3), 291–301.

Cordeiro, F., Emons, H., & Robouch, P. (2022). Is the z score sufficient to assess participants' performance in proficiency testing? The hidden corrective action. *Accreditation and Quality Assurance*, *27*(3), 145–153.

Corti, C. (2004). Blue , Black and Purple ! The Special Colours of Gold and Other Precious Metals. *In The Santa Fe Symposium on Jewelry Manufacturing Technology*, 121–133.

Cretu, C., & Van Der Lingen, E. (1999). Coloured gold alloys. *Gold Bulletin*, *32*(4), 115–126.

De Bièvre, P., Dybkaer, R., Fajgelj, A., & Hibbert, D. B. (2011). Metrological traceability of measurement results in chemistry: Concepts and implementation (IUPAC Technical report). *Pure and Applied Chemistry*, *83*(10), 1873–1935.

De Bièvre, P., & Taylor, P. D. P. (1997). Traceability to the SI of amount-of-substance measurements: From ignoring to realizing, a chemist's view. *Metrologia*, *34*(1), 67–75.

Edition, T. (2012). *Quantifying Uncertainty in Analytical Measurement*.

Ellison, S. L. R., & Willians, A. (Ed. (2019). *Eurachem/CITAC Guide: Metrological Traceability in Chemical Measurement*. www.eurachem.org.

Frahm, E. (2013). Validity of "off-the-shelf" handheld portable XRF for sourcing Near Eastern obsidian chip debris. *Journal of Archaeological Science*, *40*(2), 1080–1092.

Gallhofer, D., & Lottermoser, B. G. (2018). The influence of spectral interferences on critical element determination with portable X-ray fluorescence (pXRF). *Minerals*,

8(8), 320.

Ghosh, M., Swain, K. K., Chavan, T. A., Wagh, D. N., & Verma, R. (2015). Determination of gold and silver in dross using EDXRF technique. *X-Ray Spectrometry*, *44*(1), 13–15.

González, M. F., Saadatkhah, N., & Patience, G. S. (2024). Experimental methods in chemical engineering: X-ray fluorescence—XRF. *Canadian Journal of Chemical Engineering*, *102*(6), 2004–2018.

ISO 15093. (2020). Platinum and Palladium Jewellery Alloys - Difference Method Using Inductively Coupled Plasma Optical Emission Spectroscopy (ICP-OES).

ISO 15096. (2020). Jewellery - Determination of Silver In 999 0/00 Silver Jewellery Alloys - Difference Method Using Inductively Coupled Plasma Optical Emission Spectroscopy (ICP-OES).

ISO 17025. (2017). International Standard ISO / IEC competence of testing and calibration. *International Organization for Standardization*, *2017*, 1–38.

ISO 23345. (2021). Jewellery and precious metals — Non destructive precious metal fineness confirmation by ED-XRF.

Jalas, P., Ruottinen, J., & Hemminki, S. (2002). XRF Analysis of jewelry using fully standardless fundamental parameter approach. *Gold Technology*, *35*(May), 28–34.

Jotanović, A., Memić, M., Suljagić, Š., & Huremović, J. (2012). Comparison of x-ray fluorescent analysis and cupellation method for determination of gold in gold jewellery alloy. *Bulletin of the Chemists and Technologists of Bosnia and Herzegovina*, *38*, 13–18.

Jurado-López, A., Luque De Castro, M. D., & Pérez-Morales, R. (2006). Application of energy-dispersive x-ray fluorescence to jewellery samples determining gold and silver. *Gold Bulletin*, *39*(1), 16–21.

Klotz, U. E., Tiberto, D., & Held, F. (2017). Optimization of 18-karat yellow gold alloys for the additive manufacturing of jewelry and watch parts. *Gold Bulletin*, *50*(2), 111–121.

KPDN. (2021). *Keratan Akhbar dan Media Online*. 1–3.

Kraut, J. C., & Stern, W. B. (2000). The density of gold-silver-copper alloys and its calculation from the chemical composition. *Gold Bulletin*, *33*(2), 52–55.

Krummenauer, A., Dias, P. R., & Veit, H. M. (2021). Estimation of measurement uncertainty in the EDXRF spectrometry of stainless steel. *Journal of Physics: Conference Series*, *1826*(1).

Kumar, R., Rani, A., Singh, R. M., & Soni, R. (2018). EDXRF analysis of carat/under carat gold (Au) samples. *AIP Conference Proceedings*, *2006*.

Majcen, N., Majer, M., Svegl, I. G., & De Bievre, P. (2002). Traceability of results of measurements of gold in precious metal alloys by XRF. *Acta Chimica Slovenica*, *49*(1), 187-194.8.

Manchanda, D. (2011). The Role of inductively coupled plasma-optical emission spectrometry in determining the fineness of precious metals. *Platinum Metals Review*, *55*(4), 281–283.

Markowicz, A. (2011). *An overview of quantification methods in energy-dispersive X-ray fluorescence analysis*. *76*(2), 321–329.

Markowicz, A., Wegrzynek, D., Chinea-Cano, E., Bamford, S. a, Torres, D. H., & Alvarez, R. P. (2007). Quality management and method Validation in EDXRF analysis. *X-Ray Spectrometry*, *36*(1), 27–34.

Marucco, A. (2004). Low-energy ED-XRF spectrometry application in gold assaying. *Nuclear Instruments and Methods in Physics Research, Section B: Beam Interactions with Materials and Atoms*, *213*, 486–490.

Mazuki, A. A. M., Mahat, M. M., Abdullah, S., Ramli, R., & Nor, F. M. (2023). Improving the accuracy of EDXRF results in gold alloy analysis by matrix effect correction. *Spectrochimica Acta - Part B Atomic Spectroscopy*, *201*.

Mazuki, A. A. M., Mahat, M. M., Ramli, R., & Abdullah, S. (2021). Variation in the Collimator Beam Size of Energy-Dispersive X-Ray Fluorescence Spectroscopy for Improved Measurement of Gold Purity. *Journal of Applied Spectroscopy*, *88*(3), 552–556.

Mishra, P., Pandey, C., Singh, U., Keshri, A., & Sabaretnam, M. (2019). Selection of appropriate statistical methods for data analysis. *Annals of Cardiac Anaesthesia*, *22*(3), 297–301.

Mishra, P., Singh, U., & Pandey, C. M. (2019). *Application of Student ' s t - test , Analysis of Variance , and Covariance*. 407–411.

Mohamed, N., Mohammed, F., Yen, I. C., & Maharaj, R. (2016). A preliminary quality survey of gold jewellery sold in Trinidad and Tobago. *International Journal of Applied Chemistry*, *12*(4), 549–556.

Mozgai, V., Bajnóczi, B., May, Z., & Mráv, Z. (2021). Non-destructive handheld XRF study of archaeological composite silver objects—the case study of the late Roman Seuso Treasure. *Archaeological and Anthropological Sciences*, *13*(5).

Navas, M. J., Asuero, A. G., & Jimenez, A. M. (2016). A review of energy dispersive X-ray fluorescence (EDXRF) as an analytical tool in numismatic studies. *Applied Spectroscopy*, *70*(1), 207–221.

Nor, F. M., & Ismail, A. K. (2019). Fake Gold : Gold Purity Measurement Using Non Destructive Method. *8*(1.1), 165–172.

Nor, F. M., Tamuri, A. R., Ismail, A. K., & Mazuki, A. A. M. (2020). Verification of the hydrostatic weighing system with existing gold purity instruments. *IOP Conference Series: Materials Science and Engineering*, *824*(1).

Nordin, N., Embong, R., Ismail, S. K., Kamaruddin, K., Mohamed, Z., & Nawi, M. A. A. (2015). Understanding of gold investment among muslim professionals in Terengganu, Malaysia. *Mediterranean Journal of Social Sciences*, *6*(3), 110–115.

Ortega-Feliu, I., Gómez-Tubío, B., Ontalba Salamanca, M. Á., Respaldiza, M. Á., de la Bandera, M. L., & Ovejero Zappino, G. (2007). Gold and electrum jewellery in the strategic area of Gadir in Phoenician period. *Nuclear Instruments and Methods in Physics Research, Section B: Beam Interactions with Materials and Atoms*, *260*(1),

Preview, T. S. (2021). Jewellery and precious metals-Determination of gold-Cupellation method (fire assay), *ISO*, *2021*.

Ramsey, M., & Ellison, S. (2015). *EURACHEM / CITAC Guide Measurement uncertainty arising from sampling A guide to methods and approaches UK RSC Analytical Methods Committee First Edition 2007*. *November*.

Ridolfi, S. (2012). Portable X-ray Fluorescence Spectrometry for the analyses of Cultural Heritage. *IOP Conference Series: Materials Science and Engineering*, *37*(1), 012001.

Rousseau, R. M. (2006). Corrections for matrix effects in X-ray fluorescence analysis-A tutorial. *Spectrochimica Acta - Part B Atomic Spectroscopy*, *61*(7), 759–777.

Rousseau, R. M. (2009). The Quest for a Fundamental Algorithm in X-Ray Fluorescence Analysis and Calibration. *The Open Spectroscopy Journal*, *3*(1), 31–42.

Sargent, M. (2020). The provision and use of traceability statements for reference materials. *Accreditation and Quality Assurance*, *25*(5–6), 367–372.

Shackley, M. S. (2011). X-Ray Fluorescence Spectrometry (XRF) in Geoarchaeology. In *X-Ray Fluorescence Spectrometry (XRF) in Geoarchaeology*.

Silveira, P., & Falcade, T. (2022). Applications of energy dispersive X-ray fluorescence technique in metallic cultural heritage studies. In *Journal of Cultural Heritage*

(Vol. 57, pp. 243–255). Elsevier Masson s.r.l.

Sitko, R., & Zawisz, B. (2012). Quantification in X-Ray Fluorescence Spectrometry. *X-Ray Spectroscopy*, 137–162.

Sitko, R., Zawisza, B., & Malicka, E. (2009). Energy-dispersive X-ray fluorescence spectrometer for analysis of conventional and micro-samples: Preliminary assessment. *Spectrochimica Acta - Part B Atomic Spectroscopy*, *64*(5), 436–441.

Stankiewicz, W., Bolibrzuch, B., & Marczak, M. (1998). Gold and gold alloy reference materials for XRF analysis. *Gold Bulletin*, *31*(4), 119–125.

Thompson, M. (1997). Comparability and traceability in analytical measurements and reference materials. *Analyst*, *122*(11), 1201–1205.

Trade Description Act 2011. (2016). Trade Description Act 2011. *Trade Description Act 2011*, *July*, 1–57.

Trapmann, S., Botha, A., Linsinger, T. P. J., Mac Curtain, S., & Emons, H. (2017). The new International Standard ISO 17034: general requirements for the competence of reference material producers. *Accreditation and Quality Assurance*, *22*(6), 381–387.

Trojek, T., & Trojková, D. (2023). Uncertainty of Quantitative X-ray Fluorescence Micro-Analysis of Metallic Artifacts Caused by Their Curved Shapes. *Materials*, *16*(3).

VIM. (2021). International Vocabulary of Metrology Fourth edition. *Joint Committee for Guides in Metrology*, *January*, 1–55.

Wolff, N. L. R. W. H. (2006). Handbook of Practical X-Ray Fluorescence Analysis. In *Handbook of Practical X-Ray Fluorescence Analysis*. Yaacob, S. E. (2012). The reality of gold dinar application in Malaysia. *Advances in Natural and Applied Sciences*, *6*(3), 341–347.

Zhavoronkova, G., Zhavoronkov, V., Melenevskaya, D., & Panasiuk, I. (2021). Current trends in the world market of precious metals. *Innovations*, *133*(4), 129–133.

Zhitenko, L. P. (2013). State of the art and problems in determining high gold contents in alloys and articles (Review). *Inorganic Materials*, *49*(14), 1294–1302.

Zhou, J., Shi, J., Zhang, B., & Li, S. (2021). Determination of the Content of Impurity Elements in Aluminum Alloy by XRF Analysis. *Open Access Library Journal*, *08*(09), 1–6.

APPENDICES

APPENDIX 1

Preliminary study on the accuracy of commercial EDXRF using certified reference materials. The overlapping spectra and insufficient matrix effect correction between the peaks of LαAu and LβAu with a peak of KαCu resulted in inaccurate measurements. The certified value of the gold content of BAM ERM 508 was 75.12 wt%.

Test Report

Name	ERM 508	Time	60	Date	24/9/2020
Materials		**Content(%)**		**Weight (gm)**	
Copper		0.785			
Silver		19.755			
Gold		79.46			
Carat	19.073K				
Spectrum	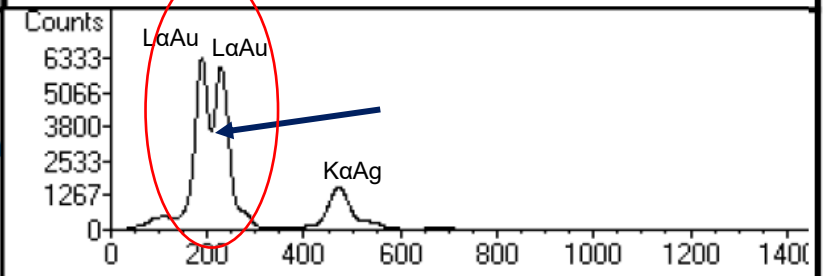				
Picture	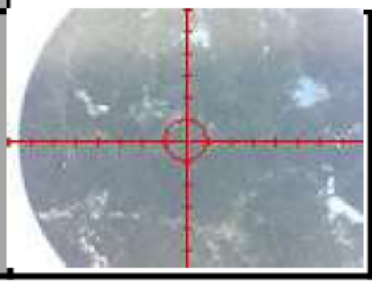				

APPENDIX 2

Newspaper clipping related to gold counterfeiting in the Malaysian industry.

OPERASI KETULENAN EMAS

42 kes logam 'cokia' dikesan

Oleh Zatul Iffah Zolkiply
zatuliffah@hmetro.com.my

Kuala Terengganu

Kementerian Perdagangan Dalam Negeri dan Hal Ehwal Pengguna (KPDNHEP) mengesan 42 kes penipuan ketulenan logam berharga di seluruh negara sejak Januari 2019 hingga Oktober tahun ini.

Pengarah Penguat Kuasa KPDNHEP Azman Adam berkata, ia membabitkan kes penipuan pembelian emas secara dalam talian, emas kurang berkualiti dan berat tidak sama seperti dicatatkan dalam resit jualan membabitkan keseluruhan rampasan RM53,463.

"Daripada jumlah aduan, sembilan kes dikesan membabitkan rampasan RM3,950. Azman

FOTO: GHAZALI KORI

PEGAWAI Agensi Nuklear Malaysia menguji ketulenan emas menggunakan mesin penganalisis logam berharga di sebuah kedai emas di Kuala Terengganu, semalam.

Beliau berkata, daripada jumlah itu, RM7,700 kompaun dikeluarkan dan denda RM20,000 dikenakan kepada syarikat atau individu terbabit.

Katanya, pihaknya menerima 11 aduan berkaitan isu ketulenan logam berharga dalam tempoh 10 bulan pertama tahun ini.

"Daripada jumlah aduan itu, sembilan kes dikesan membabitkan rampasan RM3,950.

"Kami pandang serius isu ketulenan logam berharga bagi melindungi hak pengguna dan mana-mana pihak didapati bersalah boleh dikenakan tindakan mengikut Peraturan-Peraturan Perihal Dagangan (Artikel-Artikel Yang Dibuat Daripada Logam Berharga 1994) di bawah Akta Perihal Dagangan 2011.

"Mana-mana syarikat atau individu gagal mematuhi mana-mana peruntukan di bawah akta berkenaan boleh dikenakan denda tidak melebihi RM25,000 bagi pertubuhan perbadanan dan denda tidak melebihi RM10,000 atau penjara tidak melebihi satu tahun atau kedua-duanya, jika sabit kesalahan," katanya selepas melakukan pemantauan ketulenan logam berharga di beberapa premis di sekitar daerah ini, semalam.

Pemilik kedai emas dikesan memanipulasi alat timbang untuk kaut untung

Tauke tipu pelanggan depan mata

Oleh NOR IDAYU BOSRO

PUTRAJAYA – Penipuan membabitkan alat timbang bertujuan untuk memperdaya pengguna bukan hanya dilakukan oleh peniaga-peniaga di kedai runcit, malah modus operandi itu turut digunakan oleh tauke kedai emas.

Lebih membimbangkan, perbuatan dan taktik licik pengusaha barang kemas yang menggunakan alat timbang tidak ditentusahkan ini dilakukan di depan pelanggan mereka sendiri.

Mendedahkan perkara itu, Pengarah Bahagian Penguat Kuasa Kementerian Perdagangan Dalam Negeri dan Hal Ehwal Pengguna (KPDNHEP), Azman Adam berkata, kesalahan itu terbongkar apabila kebanyakan kes yang diambil tindakan setakat ini adalah melibatkan urusan jual beli di premis perniagaan dan bukannya melalui kaedah transaksi secara dalam talian.

Katanya, selain menipu pelanggan menggunakan alat timbang yang tidak ditentusahkan, tauke-tauke ini turut melakukan kesalahan dagangan palsu berhubung standard ketulenan emas.

"Antara punca yang menyebabkan pengguna tertipu ialah mereka mudah terpedaya dengan tawaran harga yang lebih murah berbanding nilai pasaran semasa.

"Bila ada tawaran sedemikian, pengguna akan terburu-buru membeli dan tidak membuat penilaian sewajarnya termasuklah mendapatkan maklumat lengkap berkaitan produk yang ditawarkan," katanya kepada *Kosmo!* baru-baru ini.

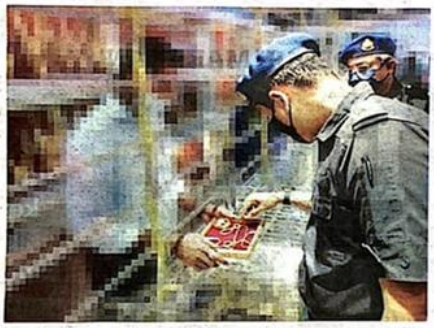

PENGUAT KUASA KPDNHEP melakukan pemeriksaan berkaitan standard ketulenan emas di sebuah premis di Lembah Klang baru-baru ini.

Tambahnya, KPDNHEP telah melatih anggotanya untuk mengenali ketulenan emas bagi memastikan penguatkuasaan dan pemantauan dapat dilaksanakan dengan lancar.

Menurut Azman, pihaknya juga telah memiliki dua unit alat menguji ketulenan logam berharga iaitu radas sinaran sinar-X dan alat XRF (X-Ray Flouresence).

"Alat XRF mampu membuat bacaan kandungan dan komposisi untuk lebih 100 jenis unsur logam seperti emas, perak, gangsa dan lain-lain nya. Alat ini menggunakan kaedah pengujian tanpa musnah.

AZMAN

"Bagaimanapun, ia hanya untuk prapengujian dan untuk ujian tepat masih perlu dilakukan di Jabatan Mineral dan Geosains Malaysia," katanya.

Ujar Azman, sejak Januari 2019 hingga Mei lalu, pihaknya telah membuka sebanyak 59 kertas siasatan selain mengeluarkan kompaun bernilai RM7,200 kepada syarikat-syarikat yang terlibat.

Menurut beliau, sebanyak 20 kertas siasatan dibuka pada 2019 dan 27 lagi kertas siasatan pada tahun lalu, iaitu peningkatan sebanyak tujuh kes.

"Sehingga Mei lalu, terdapat 12 kertas siasatan dibuka ke atas premis-premis menjual emas yang melibatkan kesalahan di bawah Akta Perihal Dagangan 2011 dan Akta Timbang dan Sukat 1972," katanya.

Sehubungan itu, Azman mengingatkan pengguna supaya lebih peka dan berhati-hati dengan tawaran harga murah emas selain sentiasa membuat penyelidikan dan melihat testimoni pelanggan sebelum membuat pembelian.

Katanya, pelanggan yang membeli secara dalam talian pula digalakkan menggunakan kaedah *cash-on-delivery* atau COD dan memastikan peniaga mengeluarkan resit pembelian yang mengandungi maklumat lengkap.

"Maklumat peniaga mestilah meliputi nama dan alamat pembekal, tarikh pembelian, nama dan jenis artikel, standard ketulenan artikel, harga logam berharga bagi setiap satu gram, berat artikel, harga artikel, kos pembuatan (jika ada) serta tandatangan jurujual," jelasnya.

STANDARD ketulenan emas yang diuji KPDNHEP adalah menggunakan alatan khas dikenali X-Ray Flouresence.

APPENDIX 3

Energy Adjustment Report

Energy Adjustment Report

Thermo Fisher Scientific Inc., Madison, Wisconsin, USA

Acquisition Manager 7.2 (Build 134) **Adjustment performed: 01/10/2021 12:14:34**

Conditions

Voltage (kV):	18
Filter:	Pd Medium

Energy of line (keV): 8.041

	Value
Initial gain DAC setting:	32514
Final gain DAC setting:	32514
Time Constant (µs)	2
Error (eV):	0.8
Uncertainty (eV):	1.38
FWHM (eV):	162.0
Zero Width (eV):	76.3
Peak Count Rate (cps/mA):	228817.61
Livetime (seconds):	10.28
Current (mA):	0.2

APPENDIX 4

L-shell x-ray emission of Au

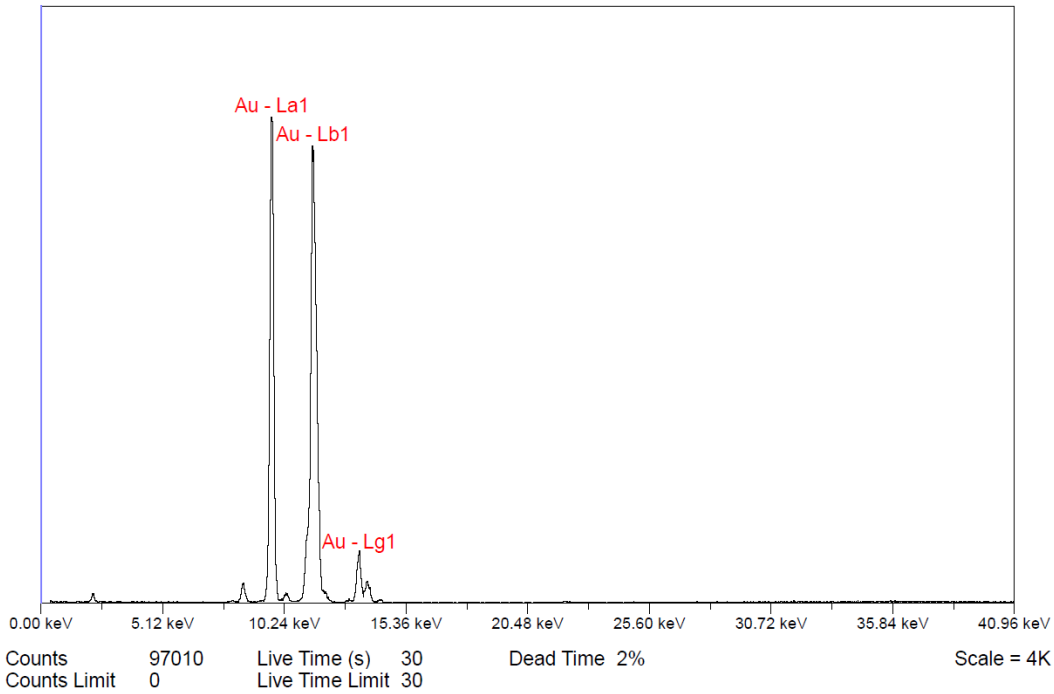

APPENDIX 5

L-shell x-ray emission of Ag

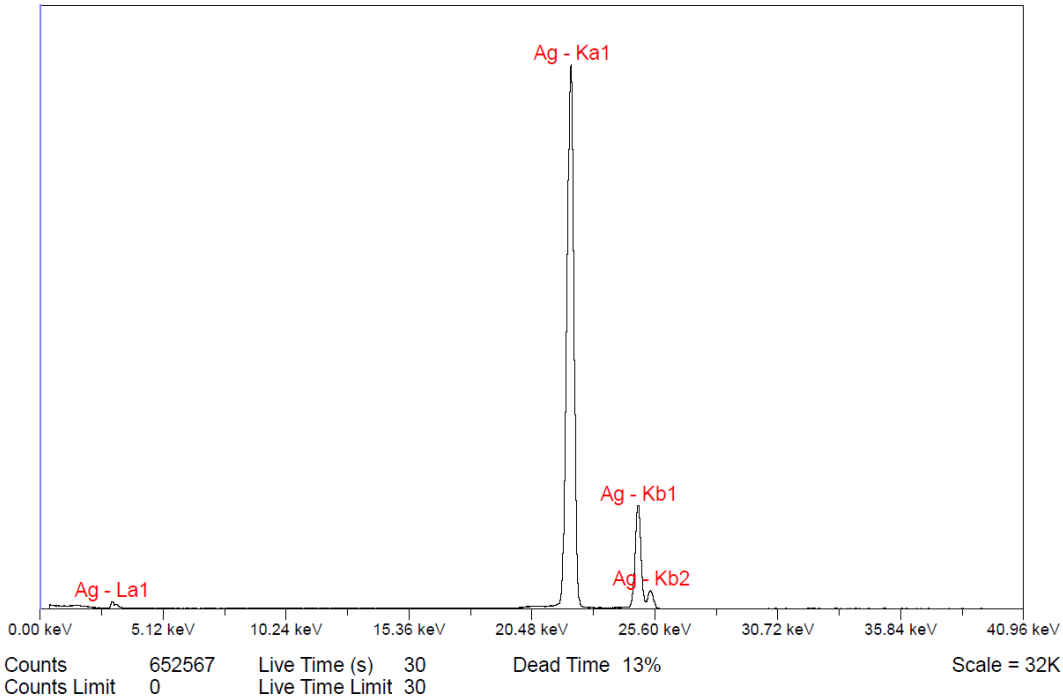

APPENDIX 6

X-ray emission of L-shell Au and K-shell of Cu

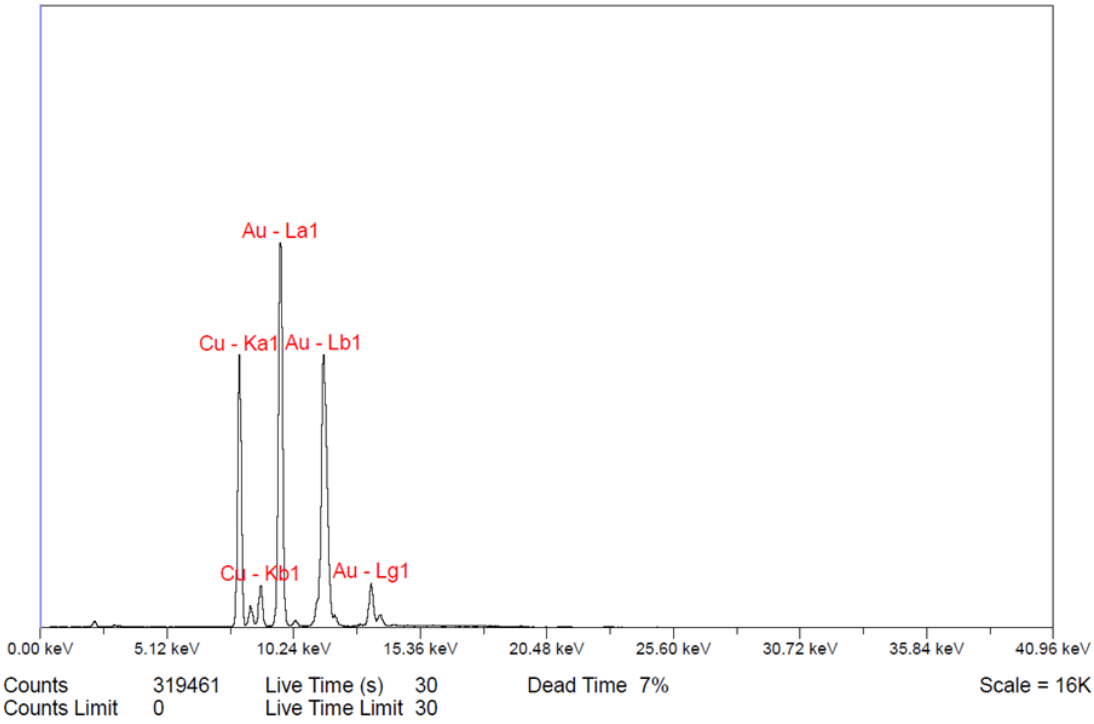

APPENDIX 7

X-ray emission of L-shell Au and K-shell of Ag

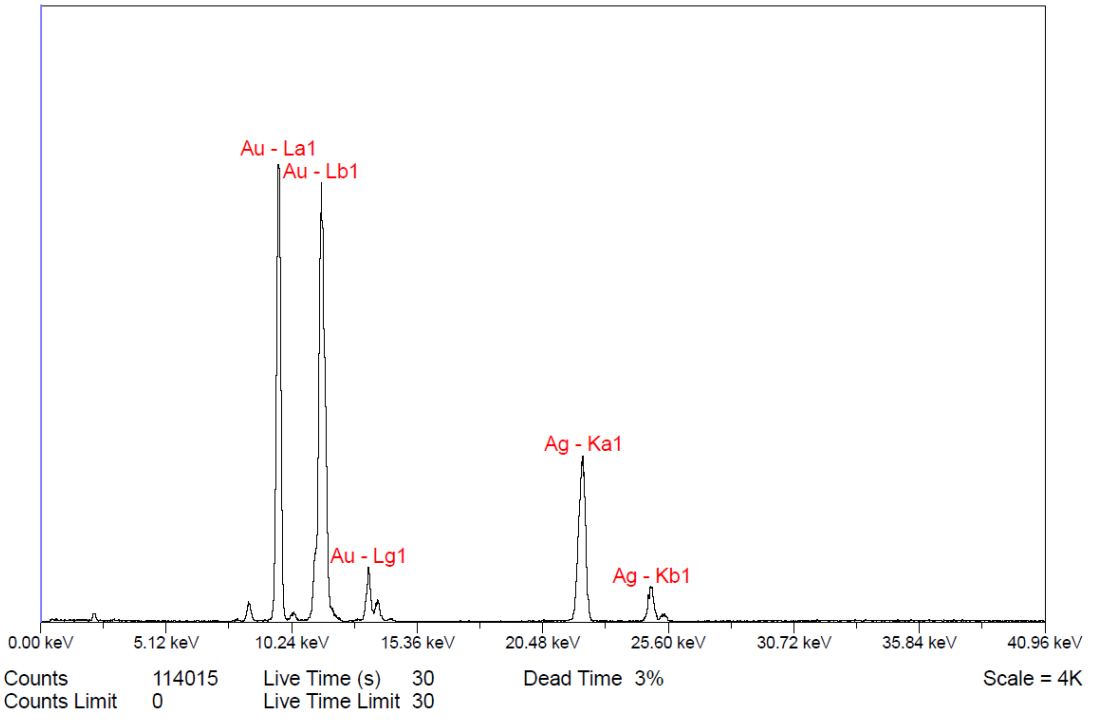

APPENDIX 8

X-ray emission of L-shell Au and K-shell of Cu and Ag

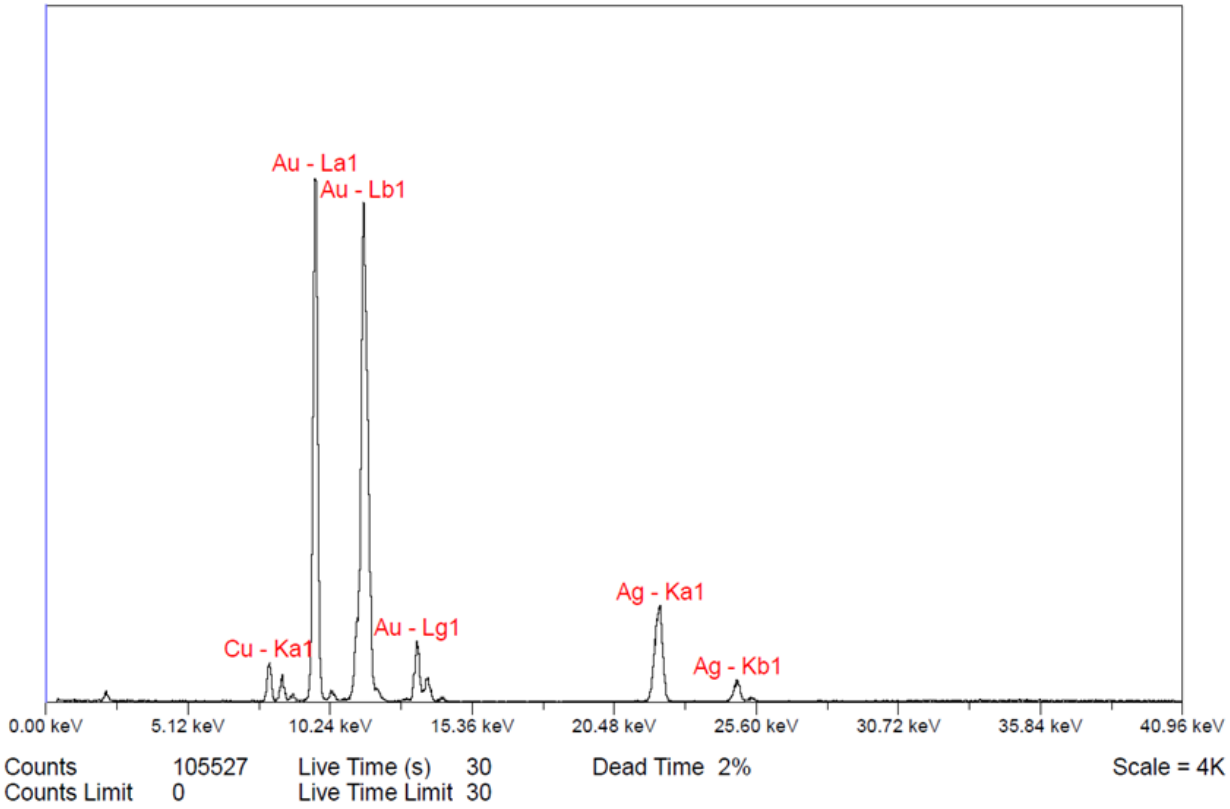

APPENDIX 9

Certificate of Analysis NIST SRM 685 R

U. S. Department of Commerce
Malcolm Baldrige
Secretary

National Bureau of Standards
Ernest Ambler, Director

Certificate of Analysis

Standard Reference Material 685

High–Purity Gold

This standard is provided as a reference source of gold of high purity. It is issued in two forms, wire and rod.[1] The wire form is intended for applications such as spark–source mass spectrometry where the low level of impurities in the standard should make it useful for evaluating instrument and system blanks. The rod form is intended for use in other methods of characterization and in other scientific applications.

INFORMATION ON THE COMPOSITION

	SRM No. 685–W		SRM No. 685–R	
Element	Best Indicated Value	Range of Values Reported[2]	Best Indicated Value	Methods of Analysis[3]
	(Concentration in Parts per Million by Weight)			
Copper	0.1	(<0.1 – 0.26)	0.1	a, b, c, d
Indium	0.00_7	(0.002 – 0.014)	0.00_7	a, d
Iron	0.3	(0.16 – 0.50)	0.2	b, c, d
Oxygen	[2][4]	(1.5 – 3.0)	[<2]	e
Silver	[0.1]	(0.05 – 0.11)	[0.1]	d

1. SRM No. 685–W is in the form of wire 1.4 mm (0.055 inch) in diameter and 10.2 cm (4 inches) long.
   SRM No. 685–R is in the form of rod 5.9 mm (0.23 inch) in diameter and 2.5 cm (1 inch) long.
2. The range of values reported is the extreme variation of the individual results from the methods of analysis used. The "best indicated value" is based on consideration of the estimated systematic bias of each of the methods employed.
3. Methods of Analysis:
   a. Neutron Activation Analysis (W. D. Kinard, D. A. Becker, P. D. LaFleur)
   b. Polarography (E. J. Maienthal)
   c. Spectrophotometry (T. A. Rush, D. H. Christopher, R. W. Burke)
   d. Spark–Source Mass Spectrometry – Isotopic Dilution (P. J. Paulsen, D. E. Kelleher, R. Alvarez)
   e. Vacuum Fusion (J. T. Sterling)
4. Values in brackets are possibly subject to greater error since only one method of analysis was employed.

The overall direction and coordination of the technical measurements leading to certification were performed under the chairmanship of B. F. Scribner.

The technical and support aspects involved in the preparation, certification and issuance of these Standard Reference Materials were coordinated through the Office of Standard Reference Materials by R. E. Michaelis.

Washington, D.C. 20234
October 1, 1981
(Revision of Certificate
dated 9/26/68)

George A. Uriano, Chief
Office of Standard Reference Materials

(over)

APPENDIX 10

Certificate of Analysis BAM ERM 508

BAM
in cooperation with the WG 'Precious Me
of the Committee of Chemists of GDMB

CHOICE *Analytical*
www.choiceanalytical.com.au
Tel: +61 2 9980 6240 Fax: +61 2 9980 6344

ERM
European Reference Materials

CERTIFICATE OF ANALYSIS

ERM®-EB508

Alloying Elements in Yellow Gold		
	Certified value [1]	Uncertainty [2]
Element	Mass fraction in %	
Au	75.12	± 0.11
Ag	24.90	± 0.05

[1] Unweighted mean value of the means of accepted sets of data, each set being obtained by at least 6 laboratories and/or with different methods of measurement. The values are traceable to the SI (Système International d'Unités) by the use of pure substances of known stoichiometry for calibration.

[2] Estimated expanded uncertainty *U* with a coverage factor of $k = 2.5$, corresponding to a level of confidence of about 95 %, as defined in the ISO/IEC Guide 98-3:2008 Uncertainty of measurement -- Part 3: Guide to the expression of uncertainty in measurement (GUM:1995).

This certificate is valid until 05/2064; this validity may be extended as further evidence of stability becomes available.

Accepted as an ERM®, 08.05.2014

BAM Department 1
Analytical Chemistry;
Reference Materials

[redacted]

Prof. Dr. U. Panne
(Head of Department)

BAM Division 1.6
Inorganic Reference Materials

[redacted]

Dr. S. Recknagel
(Head of Division)

APPENDIX 11

Certificate of Analysis of Cupellation (Fire Assay) Results

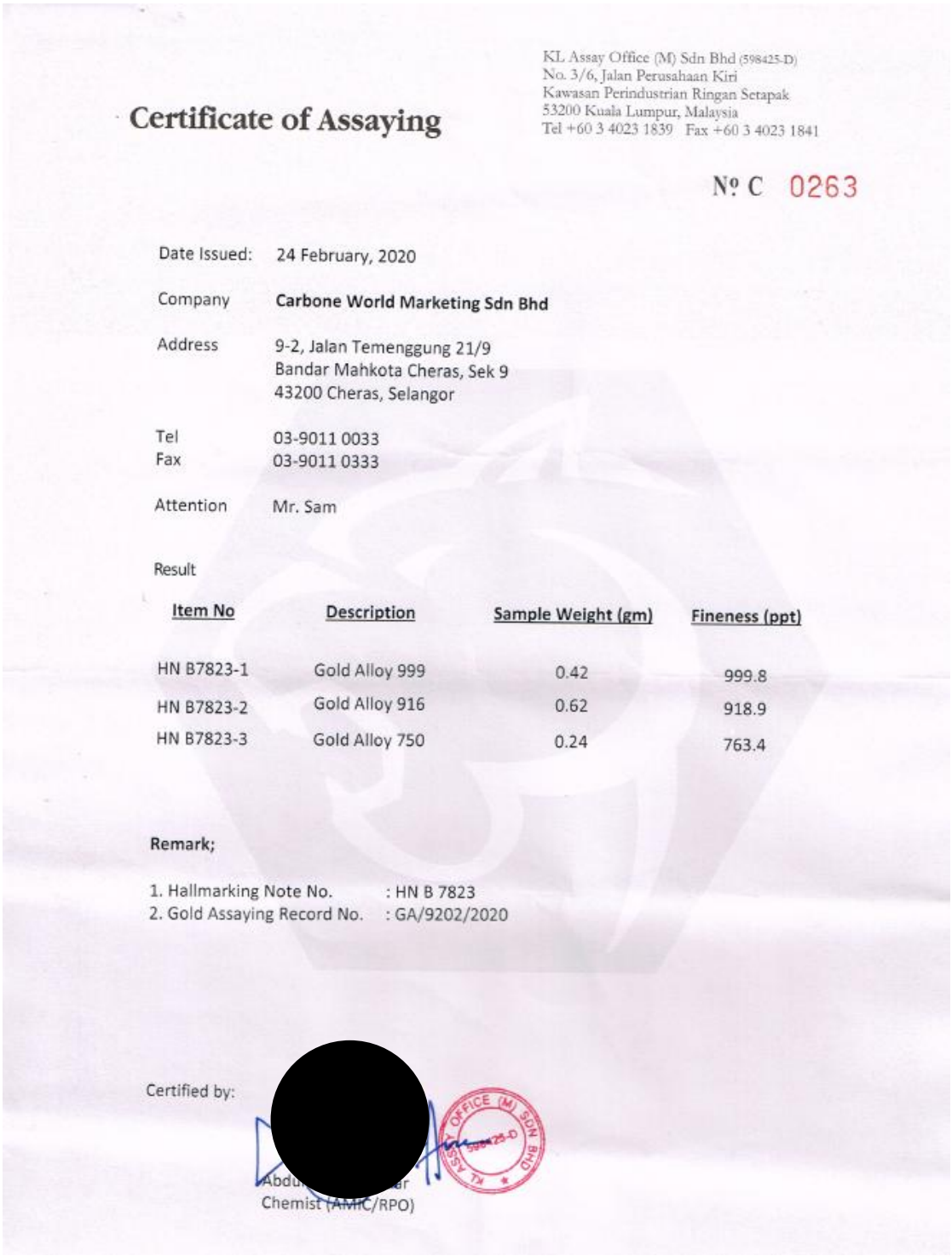

KL Assay Office (M) Sdn Bhd (598425-D)
No. 3/6, Jalan Perusahaan Kiri
Kawasan Perindustrian Ringan Setapak
53200 Kuala Lumpur, Malaysia
Tel +60 3 4023 1839 Fax +60 3 4023 1841

Certificate of Assaying

Nº C 0263

Date Issued: 24 February, 2020

Company **Carbone World Marketing Sdn Bhd**

Address 9-2, Jalan Temenggung 21/9
Bandar Mahkota Cheras, Sek 9
43200 Cheras, Selangor

Tel 03-9011 0033
Fax 03-9011 0333

Attention Mr. Sam

Result

Item No	Description	Sample Weight (gm)	Fineness (ppt)
HN B7823-1	Gold Alloy 999	0.42	999.8
HN B7823-2	Gold Alloy 916	0.62	918.9
HN B7823-3	Gold Alloy 750	0.24	763.4

Remark;

1. Hallmarking Note No. : HN B 7823
2. Gold Assaying Record No. : GA/9202/2020

Certified by:

[redacted]

Chemist (AMIC/RPO)

APPENDIX 12

WDXRF Calibration Curve

MVR Report — **D-SIRIM-Au, Measurement of Gold sample - 3mm mask**

Instrument: ARL Perform'X — DEMO Perform'X - MY

MVR Save State for channel Ag Ka 1,2 - Curve segment n°: 1

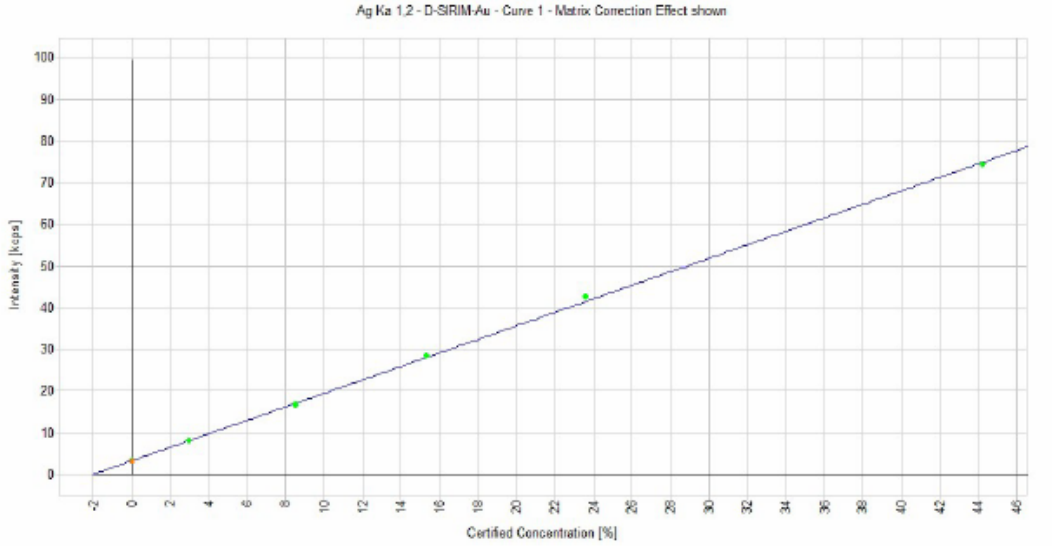

Base Curve Parameters

Element/Line	Intensity Low	Intensity High	A0	A1	A2	A3	Correction	Theo. Alphas	Poly. Deg.	Corr. Deg
Ag Ka 1,2	2.6210688	99.6332718	-1.48E+0	4.49E-1	0.00000	0.00000	MC	No	1	1

Regression Statistics

Element/Line	SEE [%]	R2	Samples	Interfering Elements	BEC	Q [cps/%]	LOD (8.00 s)
Ag Ka 1,2	0.296735	0.999575	12	1	-	-	-

Matrix Correction - MC

Interfering Element	Alpha 1	Beta	Fixed
Au Lb 1	0.0134730		

MVR Samples for Channel Ag Ka 1,2 - Curve segment n°: 1

Sample Name	Weight	Intensity	Given Conc.	Calcul. Conc.	Absolute Diff.	Relative Diff.[%]
AU01_1	0.00	3.3200	0.00000	0.03690	0.036896	>999
AU01_2	0.00	3.3198	0.00000	0.03663	0.036631	>999
AU01_3	0.00	3.3441	0.00000	0.06224	0.062240	>999
CAL230	100.00	3.2945	0.00000	0.00425	0.004247	>999
CAL274	100.00	3.2763	0.00000	-0.00391	-0.003909	>999

Date&Time: 7/16/2020-- 4:56:15PM — Software Name: OXSAS — Version No: 2.6.3.3984 — Page 1 of 13

APPENDIX 13

Preparation of gold calibration material

1.Prepared mixture of samples

2. The combination of samples was weighed to give a total of approximately 5 grams

3. The sample was then placed in a ceramic crucible and melted the samples at 1050℃ in furnace

4. Gold Button

5. Water quenched to cold the samples

6. Rolled the sample to give 0.25-0.30 mm thickness

7. The sample was cut into disc shape

8. Sample then polished at surface area

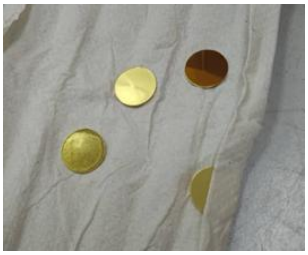

9. Final calibration materials at 12 mm diameter

APPENDIX 14

Sixteen (16) pieces of gold alloy with similar characteristics to the gold matrix-specific materials


AU1


AU5


AU9

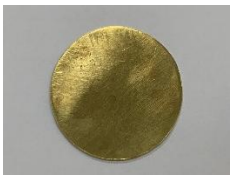
AU13

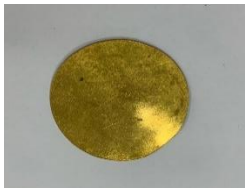
AU2


AU6


AU 10


AU14

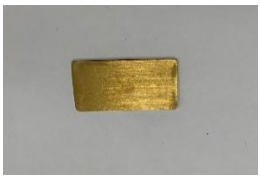
AU3

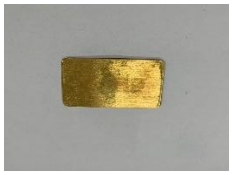
AU7

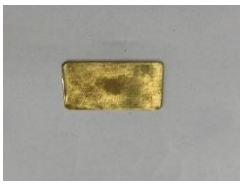
AU11

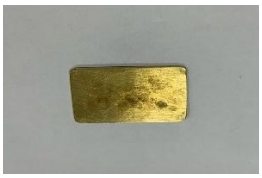
AU15

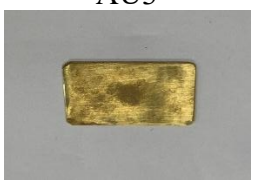
AU4

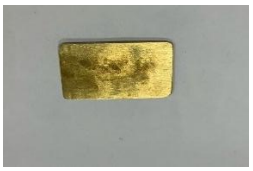
AU8

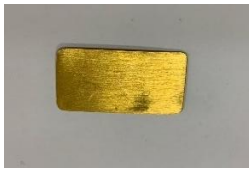
AU12

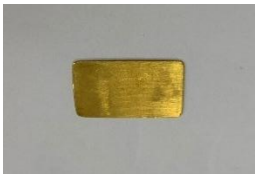
AU16

APPENDIX 15

The *'blind'* ILC test sample is prepared in the form of a wire prepared by IMBIH.

APPENDIX 16

Calibration Certificate of Temperature Humidity Data Logger

NMIM
NATIONAL METROLOGY INSTITUTE OF MALAYSIA

Instrument : Temperature Humidity Data Logger
Model Code : U14-001
Serial No. : 10857270

Page : 2 of 2
Certificate No. : NMIM-0052-T-201
Issue Date : 25 Jan 2021

Results :

Humidity : 40 %rh to 70 %rh
Temperature : 15 °C to 35 °C
Digital Resolution : Relative Humidity : 1 %rh
Temperature : 0.1 °C

Relative Humidity

Measured Value of 10857270 (%rh)	Temperature during calibration (°C)	Correction of 10857270 (%rh)	Expanded Uncertainty of 10857270 (%rh)
44	23	-4	3
53	23	-3	3
71	23	-1	3

Temperature

Measured Value of 10857270 (°C)	Relative Humidity during calibration (%rh)	Correction of 10857270 (°C)	Expanded Uncertainty of 10857270 (°C)
15.0	54.0	0.0	0.2
25.1	54.0	0.0	0.2
35.1	54.0	-0.1	0.2

Note 1 : Actual Value = Measured Value of Equipment + Correction
Note 2 : %rh is used as shorthand for % relative humidity

Uncertainty :

The standard uncertainty of the standards represents a combination of the uncertainties arising from calibration and estimated stability of the reference standards.

The standard uncertainty of measurement is calculated by combining the uncertainty of the standards, calibration chamber and the instrument for the period of the test. Drift of the instrument is not included in the uncertainty calculation.

Measurement Standard Used :

Description	Maker/Model No.	Serial No.	Traceability
1. Humidity Generator	ESPEC CORP PSL-2J	15014743	NPL-UK
2. Temperature and Humidity Transmitter	VAISALA HMT333	D2620045	NPL-UK
3. High Precision Thermometer	CTR 5000	K0352A-1-4	NMIM SIRIM

END OF RESULTS

APPENDIX 17

Satisfactory results of EDXRF Measurement in interlaboratory comparison (ILC) report by Institute Metrology of Bosnia and Herzegovina (IMBIH)

4. EVALUATION OF RESULTS

- **Data records**

The responsibility of laboratory participant was to deliver the results as defined in the previously delivered document "Statistical protocol and operating instructions". Coordinator of PT cycle has reviewed the submitted results. All submitted data was in accordance with the stated document.

Results of participants are presented in the table below, al data in mg/g:

LAB	*PT sample*	*x'*	*x''*	*x'''*	*x''''*	x_i	u_{xi} *(k=1)*	U_{xi} *(k=2)*
NIM	MA-279/Au	734.50	734.52	734.83	734.13	734.50	0.95	1.90

Table 3: Participant results

$x^{1,2,3,4,5}$ *is the participant individual results*
x_i *is mean value of the participant individual results*
u_{xi} *is the combined standard uncertainty of participant results*
U_{xi} *is the expanded standard uncertainty of participant results*

- **Evaluation of performance**

Evaluation of successfulness and statistical parameters including participant's values of z' scores as well as E_n number are presented in Table 4 below; all data in mg/g.

LAB	x_i	u_{xi}	U_{xi}	z'	E_n
NIM	734.50	0.95	1.90	0.09	0.03

p	1	*Number of participants*
x_{pt}	734.45	*Assigned value*
$u_{x_{pt}}$	0.23	*Standard uncertainty of the assigned value*
$U_{x_{pt}}$	0.50	*Expanded uncertainty of the assigned value*
σ_{pt}	0.5	*Standard deviation for proficiency assessment*

Table 4: Successfulness data and related statistical parameters

x_i *is mean value of the participant's individual results*
u_{xi} *is standard uncertainty of participant's results*
U_{xi} *is expanded uncertainty of participant's results*
z' *is evaluation score*
ζ *is evaluation score*

APPENDIX 18

Journal of Applied Spectroscopy

Variation In the Collimator Beam Size of Energy-Dispersive X-Ray Fluorescence Spectroscopy for Improved Measurement of Gold Purity

DOI 10.1007/s10812-021-01208-1
Journal of Applied Spectroscopy, Vol. 88, No. 3, July, 2021 (Russian Original Vol. 88, No. 3, May–June, 2021)

VARIATION IN THE COLLIMATOR BEAM SIZE OF ENERGY-DISPERSIVE X-RAY FLUORESCENCE SPECTROSCOPY FOR IMPROVED MEASUREMENT OF GOLD PURITY

A. A. M. Mazuki,[a,b,*] M. M. Mahat,[a*] R. Ramli,[a] and S. Abdullah[a]

UDC 543.427

The demand to improve the efficiency of precious metal trade has been increasing of late. Due to its non-destructive nature, energy-dispersive X-ray fluorescence has the potential to supplant the fire assay procedure. Improved accuracy in the measurement of gold purity can be achieved by optimizing the X-ray fluorescent signal by selecting a suitable collimator beam size. Four homogenous materials with different alloy matrix of gold-certified reference were investigated. The effects of collimator beam sizes on the accuracy of gold purity evaluation were observed. The findings can be treated as the foundation to improve the accuracy of gold purity measurement with X-ray fluorescence.

Keywords: *gold, X-ray fluorescence, collimator beam.*

Introduction. The purity of gold (Au) and other precious metals can be evaluated with several chemical and spectroscopic methods [1–4]. However, the most common method to measure gold content is the traditional fire assay. The assay chemically separates gold content through cupellation from the whole material. The second step requires the application of a high-accuracy weighing scale to determine the percentage of gold content. The fire assay conforms to the ISO 11426 standard, which guarantees accuracy and repeatability [4–6]. For instance, Jotanovic et al. reported a deviation of less than 0.03% after performing a fire assay (cupellation) method on 14-carat jewellery [4]. Due to its unparalleled accuracy, Artyukh et al. stated that the fire assay method is popular among the member countries of the International Convention [5]. Battaini et al. echoed the same statement, adding that the fire assay method is still practised among goldsmiths [6].

However, despite its widespread use, the fire assay method entails a few inherent disadvantages, such as its destructive nature [4, 5], reliance on chemicals [6], and time-consuming process [7]. Several spectrometry techniques have been developed to fulfill the needs of quality assurance of alloys and assaying of final products. These novel techniques include inductively coupled plasma (ICP) [8, 9], atomic absorption spectrometry (AAS) [9], laser-induced breakdown spectrometry–partial least squares (LIBS–PLS) [10], and X-ray fluorescence spectroscopy [11, 12].

Among the techniques stated above, energy-dispersive X-ray fluorescence spectroscopy (EDXRF) has gained immense popularity in recent years. It is a superior alternative to the standard fire assay method due to its nondestructive method, rapid test results, and easier sample preparation [13–15]. Nevertheless, the size and shape of the precious metal sample are factors for EDXRF's accuracy. The dimension of the sample can influence the accuracy of the measurement through the detected outbound fluorescent signal (X-ray out) as the beam diameter changes [16, 17]. The effectiveness of the collimator beam to narrow the X-ray beam on the target sample is shown in Fig. 1. Selecting a suitable collimator beam size that is relevant to the area of the target sample can optimize the X-ray fluorescent signal that contributes to measurement accuracy.

The collimator, some researchers have claimed, should be selected based on the sample's dimension and the objective of generating excitation of elements of interest [18]. The selection of the best collimator is crucial for the nondestructive analysis of nonhomogeneous samples, including jewelry [14, 19–21]. It is important to note that the outbound fluoresced

*To whom correspondence should be addressed.

[a]Universiti Teknologi MARA, Faculty of Applied Science, 40450 Shah Alam, Selangor, Malaysia; email: mmuzamir@uitm.edu.my, adlan@sirim.my; [b]National Metrology Institute of Malaysia, SIRIM Berhad 43900 Sepang, Malaysia. Published in Zhurnal Prikladnoi Spektroskopii, Vol. 88, No. 3, pp. 432–436, May–June, 2021. Original article submitted April 23, 2020.

APPENDIX 19

Spectrochimica Acta Part B: Atomic Spectroscopy

Improving the accuracy of EDXRF results in gold alloy analysis by matrix effect correction

Spectrochimica Acta Part B: Atomic Spectroscopy 201 (2023) 106629

Contents lists available at ScienceDirect

Spectrochimica Acta Part B: Atomic Spectroscopy

journal homepage: www.elsevier.com/locate/sab

Improving the accuracy of EDXRF results in gold alloy analysis by matrix effect correction

A.A.M. Mazuki [a,b,*], M.M. Mahat [a,*], S. Abdullah [a], R. Ramli [a], F.M. Nor [b]

[a] Faculty of Applied Sciences, Universiti Teknologi MARA, 40450 Shah Alam, Selangor, Malaysia
[b] National Metrology Institute of Malaysia, SIRIM Berhad, 43900 Sepang, Malaysia

ARTICLE INFO

Keywords:
Gold alloy
Matrix effect
Energy dispersive X-ray fluorescent

ABSTRACT

Energy-Dispersive X-Ray Fluorescence (EDXRF) is a faster non-destructive analysis and demands less sample preparation than the fire assay technique. This research sought to minimise the matrix effect (inter-element) by studying the role of matrix-specific materials and thus improving the accuracy of EDXRF in gold alloy analysis. The combination of empirical calibration with standardless Fundamental Parameter (FP) was expected to fine-tune the analysis of precious metals, such as gold (Au), silver (Ag), and copper (Cu). The acquired R^2 of 0.9999 for all metals signalled an alignment between the certified value and EDXRF measurement. The technique was validated with CRMs to determine corrective *K-factors* to realign systematic measurement errors due to alloy mixture. The relative error (*rel*%) for all measurements was <0.1 *rel*%. The relative standard deviation (%*rsd*) was reduced to <0.11%*rsd* for pure Au, 0.16%*rsd* for Au-Ag and Au-Cu mixture, and <0.20%*rsd* for Au-Ag-Cu mixture with *K-factor* correction. A similarity to the fire assay might reduce bias. The null hypothesis of equal mean values of fire assay and XRF data was confirmed by the student's *t*-test. This outcome showed that the XRF provided acceptable precision and verified the null hypothesis on the equivalence between mean results.

1. Introduction

The non-destructive and rapid EDXRF is a feasible alternative to the destructive fire assay procedure. However, EDXRF has its drawbacks. Existing calibrations fall short of harnessing the full potential of commercial EDXRF due to the manufacturer's no-tampering policy [1–4]. The default calibration from the manufacturer is not suitable for assessing complex precious metals [1,5]. Gold alloys and their variants in jewellery have disruptive properties in an EDXRF analysis, especially the interelement effect (matrix) [6–8]. Outcomes from EDXRF analysis are often employed as supporting data. On the other hand, the fire assay has been favoured for decades as a standard reference with an accuracy of up to 0.05 wt% [5,9–12].

EDXRF calibration curves must reflect elements of interest, such as gold (Au) in pieces of jewellery [13–15]. The remaining alloying elements are the matrix. However, the matrix effect can disrupt analysis. If the sample's matrix elemental composition contradicts the matrix-specific material, the result can be disputed [16–18]. Based on empirical calibration curves, EDXRF can only provide outstanding results if the calibration material is similar to the sample. An extensive set of calibration standards is required to calculate matrix effects correction coefficients. Its accuracy depends on size and surface quality similarities between samples and calibration material [19,20]. Fundamental parameter (FP) modelling can also produce reliable results. Instead of solely focusing on gold, this model factors all elements' results in the matrix. According to the FP modelling, EDXRF minimally relies on sample size and surface preparation quality. The FP calculation modelling offers greater statistical accuracy for irregular samples, such as gold rings or archaeological artefacts, than the empirical calibration curve [21,22].

Nevertheless, its accuracy can complicate FP applications in precious metals analysis. A previous study exhibited a total absolute error of 0.5 wt% to 1.5 wt% in the gold assay of gold-silver-copper (Au-Ag-Cu) alloy with the fundamental parameters (FP) in the absence of a calibration material. When compatible calibration materials and software were applied, the absolute error of gold assay in jewellery alloy improved to <0.27 wt% [5].

This study combined standardless FP with empirical calibration using matrix-specific materials. For the first step, relevant element concentrations were computed with the standardless FP approach. These estimated concentration values were independent of sample size and surface quality, and the values replaced the intensities of

* Corresponding authors at: Faculty of Applied Sciences, Universiti Teknologi MARA, 40450 Shah Alam, ~~Selangor~~, Malaysia.
E-mail addresses: adlan@sirim.my (A.A.M. Mazuki), mmuzamir@uitm.edu.my (M.M. Mahat).

https://doi.org/10.1016/j.sab.2023.106629
Received 31 August 2022; Received in revised form 23 January 2023; Accepted 23 January 2023
Available online 25 January 2023

APPENDIX 20

IOP Conference Series: Materials Science and Engineering

Verification of the hydrostatic weighing system with existing gold purity instruments

IOP Conf. Series: Materials Science and Engineering **824** (2020) 012007 doi:10.1088/1757-899X/824/1/012007

Verification of the hydrostatic weighing system with existing gold purity instruments

Fazrul Mohd Nor[1,2]*, Abd Rahman Tamuri[2], Abd Khamim Ismail[2], A.A.M.Mazuki[1]
[1]National Metrology Institute of Malaysia, 43900 Sepang, Selangor, Malaysia
[2]Department of Physics, Faculty of Science, Universiti Teknologi Malaysia, 81310 Skudai, Johor, Malaysia

E-mail: *mfazrul@sirim.my

Abstract. Determination of gold bar purity remains one of the most challenging tasks in gold industry. Currently, the existing instruments have a limitation to determine the purity, which in turn have produced inaccurate gold purity measurement. For example, X-ray fluorescence (XRF) technique has a limitation to penetrate the gold bar and XRF was only used to determine the surface purity. Therefore, an improved non-destructive method and precise technique has been developed to determine the gold purity. Gold density measurement can verify the purity of the gold and in this study, the density of gold bar was calculated using a custom made hydrostatic weighing system (HWS). Several measurements of density were carried out for gold bar and tungsten bar. Using HWS, the density of gold bar and tungsten bar were 19.268 g/ml and 19.206 g/ml respectively. The expanded uncertainty was also evaluated and the value was 0.006 g/ml. The new developed HWS method was also verified with existing density measurement instruments where the same density results has been obtained but the existing instruments have produced bigger uncertainty of 0.2 g/ml. Thus, this study demonstrates that the developed HWS is appropriate to be used to measure the density of gold bar accurately. Furthermore, the new developed system of HWS have shown better measurement with smaller uncertainty and hence the improvement in gold bar purity measurement.

1. Introduction

Gold, silver, platinum and palladium are types of the precious metal and among these metal, gold remains the world's most precious commodities [1, 2]. For several centuries, it continues to be a secure investment for most of people. A gold with high purity is the most expensive metal therefore, its purity must be analysed through highly accurate and precise method [3]. The inspection and verification of the gold content in gold trading is also significant due to gold price is based on gold purity [4]. Pawn broking industry also need to measure the gold purity due to the requirement to pay the same value of gold to borrower by the pawn broker [5].

Presently, there are two main methods to determine the gold purity: Destructive method and Non-destructive method. Fire assay and Inductively Coupled Plasma Optical Emission Spectrometry (ICP-OES) are the techniques in destructive method [6-11]. However, these techniques are inappropriate because the pawnbroker cannot cutting or drilling the gold items that want to be leased as stated in Pawnbroker Act 1972. For non-destructive methods, the equipment such as X-ray Fluorescence (XRF), needle, chemical solution, tri-electronic and touchstone can be used to determine the gold purity without destruct the sample [12-14].

APPENDIX 21

MyIPO registered of copyright MyREM Trademark

Perbadanan Harta Intelek Malaysia
Intellectual Property Corporation of Malaysia
Unit 1-7, Ground Floor, Menara UOA Bangsar, No. 5, Jalan Bangsar Utama 1,
59000 Kuala Lumpur. Tel: +603-2299 8400 Fax: +603-2299 8989
Website: http://www.myipo.gov.my

TRADEMARK DETAILS

Disclaimer: The information available is not intended to be comprehensive information, Perbadanan Harta Intelek Malaysia (MyIPO) shall not be liable to any consequences of errors or omissions.

Application number : TM2021031839
Application Date : 15 Nov 2021
Legal Status : Registered
Date of Legal Status : 08 Sep 2022
Nature of Mark : Word & Figurative
Type of Registration : Trademark
Transliteration :
Translation :
Disclaimer/Condition :

Date Gazetted: : 30 Jun 2022
Date Registered : 15 Nov 2021
Date of Cert. Issued : 08 Sep 2022
Expiry date : 15 Nov 2031

Applicant:
SIRIM BERHAD
Default Address: NO. 1, PERSIARAN DATO' MENTERI, SECTION 2, Shah Alam, Selangor 40000, Malaysia

Correspondence Address:
A. Rahman Bin Zuhri
Default Address: SIRIM Berhad 1, Persiaran Dato' Menteri, Seksyen 2 Shah Alam, Selangor 40000, Malaysia

Denomination: myReM REFERENCE MATERIALS
Mark:

Mark Description:
Color Condition:
Classes and list of Goods and Services: Class 14
Precious metals and their alloys.

Date Printed : 05 May 2023
Printed By : System Customer
Note: This document is computer generated and no signature is required.

Page 1 of 1

APPENDIX 22

Certificate of Gold Award in MTE 2023 on Gold Certified Reference Materials for Portable XRF Analyser Verification

APPENDIX 23

Certificate of 2nd Runner up in Anuegrah Inovasi Selangor (AINS) 2023 on Kit Standard Verifikasi Peralatan Pemantauan Kuetulenan Emas (MyREM Au)

Sijil Pengiktirafan

NATIONAL METROLOGY INSTITUTE OF MALAYSIA
(NMIM), SIRIM BERHAD

Produk Inovasi

KIT STANDARD VERIFIKASI PERALATAN
PEMANTAUAN KETULENAN EMAS (MyREM Au)

di atas kemenangan

NAIB JOHAN II
KATEGORI SWASTA
ANUGERAH INOVASI NEGERI SELANGOR (AINS) TAHUN 2023

pada

18 HINGGA 21 SEPTEMBER 2023

secara

DALAM TALIAN (ONLINE)

dengan pencapaian

YAB. DATO' SERI AMIRUDIN BIN SHARI
DATO' MENTERI BESAR SELANGOR

APPENDIX 24

Certificate of Attendance (Competency) in Training Course on Precious Metal Testing at IMBIH, Sarajevo

INSTITUT ZA MJERITELJSTVO BOSNE I HERCEGOVINE

IMBIH

INSTITUTE OF METROLOGY OF BOSNIA AND HERZEGOVINA

Certificate No. 04.3-46-9-1052-4

CERTIFICATE OF ATTENDANCE

ADLAN AKRAM BIN MOHAMAD MAZUKI

has successfully participated at

"Training course on Precious Metals Testing"

held at

Institute of Metrology of Bosnia and Herzegovina

Sarajevo, 05-09 December 2022

This workshop covered the following subjects:

- QMS according to ISO/IEC 17025; ISO/IEC 17043 and ISO 17034 implemented at Institute of metrology of Bosnia and Herzegovina
- Metrological traceability; Validation/Verification of methods; Control Charts; Data Analysis & Measurement Uncertainty
- Gold Assay Method using X-Ray Fluorescent Spectroscopy for Precious Metal Hallmarking on precious metals
- CMC for gold analysis using gravimetry method according ISO 11426 / IMBIH example

Alda Jotanovic
Head of Depertment / IMBIH

Katarina Hafner-Vuk
Head of Laboratory / IMBIH

Gala Kosarac
Chemical Analyst-Specialist / IMBIH

DIRECTOR
Dr sc. Zijad Džemić, Dipl.-Ing.

09th December 2022

APPENDIX 25

Newspaper clipping on EDXRF research for gold purity measurement by NMIM

AHLI Metrologi, Fazrulhisyam Mohd Noor (kiri) bersama Adlan Akram (tengah) melihat Noor Razinah Rahmat melakukan pengujian.

ADLAN Akram menunjukkan antara mesin yang digunakan di NMIM.

YaPEIM kesan 500 cubaan tipu emas

Kuala Lumpur: Sebanyak 500 kes cubaan menipu emas fizikal semasa transaksi gadaian direkodkan Yayasan Pembangunan Ekonomi Islam Malaysia (YaPEIM) termasuk membabitkan emas logam tungsten.

Data itu dikumpulkan YaPEIM sejak tahun 2001 dan ia masih dikesan berlaku sehingga kini.

Ahli Lembaga Pemegang Amanah YaPEIM, Dr Zaharuddin Abdul Rahman berkata, penipuan membabitkan gadaian Ar-Rahnu YaPEIM itu adalah 0.01 peratus daripada 5 juta bilangan transaksi pelanggan.

Menurutnya, bilangan kes dicatatkan agak kecil berbanding nilai dan transaksi gadaian namun secara umumnya tidak membabitkan sebarang kerugian kerana urus niaga dihentikan sebaik sahaja ketulenan emas diragui.

Katanya, bagi mengelakkan penipuan berlaku, Ar-Rahnu YaPEIM konsisten mengusahakan perniagaan YaPIEM Gold sejak 2012 dengan menggunakan peralatan pengujian ketulenan dan ketumpatan emas serba moden dan berteknologi tinggi.

"YaPEIM mengorak langkah menggunakan mesin pengujian emas tepati standard teknologi mulai tahun 2010 di semua cawangan Ar-Rahnu yang membabitkan kos mahal bagi mengelak pelanggan tertipu dan memastikan kualiti emas disimpan terjamin.

"Selain magnet dan densimeter, alat pengujian emas berteknologi jerman seperti *X-Ray Fluorescence* (XRF) dan *Eddy Current* turut digunakan bagi fasa komersial dalam urusniaga YaPEIM Gold.

"Semua alatan ini diuji dan disahkan mengikut standard piawaian Sirim setiap setahun sekali dalam aspek ketepatan sebelum ia dibenarkan beroperasi," katanya.

Beliau turut mengakui, penggunaan alatan mesin pengujian berkenaan banyak membantu YaPEIM mengesan penipuan emas, sekali gus meminimumkan risiko kes kerugian.

"Alatan ini saling melengkapi kerana setiap mesin pengujian mempunyai kelebihan dan kekurangan yang tersendiri dalam aspek bacaan ketepatan dan ketumpatan emas.

"Setiap kakitangan Ar-Rahnu YaPEIM juga wajib melengkapkan prosedur operasi standard (SOP) saring emas menggunakan teknologi XRF yang turut memaparkan maklumat kandungan emas.

"Kaedah ini nyata lebih telus serta selamat bagi mengelak sebarang kes penipuan," katanya.

Standard Pengukuran Kebangsaan di bawah Akta Sistem Pengukuran Kebangsaan 2007 (Akta 675).

Menurutnya, NMIM mula memberi Sijil MyRM sejak Mac 2017 bagi alat tentukuran densimeter, tentukuran XRF, pengukuran ketumpatan emas dan pengukuran ketulenan emas sekaligus mampu mengesan penipuan ini.

Difahamkan kes penipuan emas klon ini turut gagal dibendung di negara jiran Thailand dan Vietnam apabila *Gem and Jewellery Institute of Thailand* (GIT) turut mengeluarkan amaran terhadap lambakan emas palsu ini.

Kegagalan mengesan besi tungsten ini menyebabkan ramai mangsa menyimpan emas rugi besar.

Sindiket biasanya mencampurkan emas klon ini bersama jongkong emas tulen, sekali gus menyukarkan kegiatan itu dikesan.

Malah krisis pemalsuan emas ini turut berlaku di Eropah apabila bank terkemuka di Switzerland turut mengesan jongkong emas bernilai 50 juta paun (RM267 juta) berada di dalam peti simpanan bank itu Ogos tahun lalu.

APPENDIX 26

Appointed as a technical committee on the SIRIM Industrial Standard of gold purity testing for Pawnbroking

SIRIM ACADEMY SDN BHD (formerly known as SIRIM STS SDN BHD)
Company No. 199701032750 (448249-A)
Building 3, SIRIM Complex 1, Persiaran Dato' Menteri Section 2,
P.O. Box 7035 40700 Shah Alam, Selangor Darul Ehsan, MALAYSIA
Tel: +603-5544 6000/6211 Email: sirimacademy@sirim.my
https://www.sirimacademy.my

Rujukan: SDCS 408/10-126
Tarikh: 7 Jun 2024

Ts. Adlan Akram Bin Mohamad Mazuki
Senior Metrologist
National Metrology Institute of Malaysia (NMIM)
Lot PT 4803, Bandar Baru Salak Tinggi
43900 Sepang
Selangor Darul Ehsan.

Tuan,

PERLANTIKAN SEBAGAI AHLI DI DALAM JAWATANKUASA PROJEK PENILAIAN EMAS DAN PERAK

Kami dengan segala hormatnya merujuk kepada perkara di atas.

2. Jawatankuasa Projek Penilaian Emas dan Perak yang ditubuhkan oleh SIRIM Academy ini bertanggungjawab untuk membangunkan *SIRIM Industry Standard* yang menggariskan keperluan-keperluan berkaitan kaedah penilaian emas dan perak sebagai barang gadaian yang dibenarkan oleh undang-undang. Ia bertujuan untuk memastikan penilaian emas dan perak dijalankan dengan tepat dan efisyen di premis pajak gadai.

3. Dengan ini, kami memaklumkan secara rasmi keanggotaan Tuan dalam Jawatankuasa tersebut sebagai ahli jawatankuasa. Pihak kami percaya bahawa dengan kepakaran yang ada pada Tuan akan dapat membimbing jawatankuasa dan membantu melicinkan lagi perjalanan aktiviti jawatankuasa bagi menghasilkan standard industri yang praktikal dan memenuhi keperluan negara.

4. Pihak kami akan berhubung secara terus dengan Tuan berkenaan sebarang aktiviti jawatankuasa tersebut. Untuk sebarang pertanyaan, Tuan boleh menghubungi saya, Puan Nor Azian di talian 03-5544 6089 atau emel norazian@sirim.my. Kerjasama daripada pihak Tuan kami dahului dengan ucapan terima kasih.

Yang benar;

(NOR AZIAN DURIAT)
SIRIM Academy Sdn Bhd

SIRIM

AUTHOR'S PROFILE

Adlan Akram bin Mohamad Mazuki completed his studies for a Master in Materials Science at Universiti Sains Malaysia in 2011, where he developed a keen interest in polymer composites. Currently, Adlan Akram is a PhD candidate at the Faculty of Applied Science, UiTM, specializing in precious metal measurement methods. His doctoral research, titled "Optimising the Accuracy of Energy Dispersive X-Ray Fluorescent (EDXRF) Method for Gold Alloy Purity Measurements," explores enhancing the accuracy of the Energy Dispersive X-Ray Fluorescence (EDXRF) technique for measuring the purity of gold alloys. The goal of his research is to optimize these parameters, including instrument settings and sample handling, to enhance the precision and reliability of gold alloy purity measurements. He was funded by SIRIM Berhad under staff scholarship from 2019-2025. He holds a strong belief that research plays a critical role in advancing humanity. Driven by curiosity and inquiry, it allows us to explore and understand the vast complexities of our world, thereby nurturing a spirit of continuous learning and discovery. Curiosity and research are essential for fostering progress and enhancing our collective experience. He envisions that his research contributions could potentially lead to positive outcomes and benefit society in the future.

LIST OF PUBLICATION:

1. **Mazuki, A. A. M.,** Mahat, M. M., Abdullah, S., Ramli, R., & Nor, F. M. (2023). Improving the accuracy of EDXRF results in gold alloy analysis by matrix effect correction. Spectrochimica Acta Part B: Atomic Spectroscopy, 201, 106629.
2. **Mazuki, A. A. M**., Mahat, M. M., Ramli, R., & Abdullah, S. (2021). Variation in the collimator beam size of energy-dispersive X-ray fluorescence spectroscopy for improved measurement of gold purity. Journal of Applied Spectroscopy, 88, 552-556.
3. Nor, F. M., & **Mazuki, A. A. M**. (2020, April). Verification of the hydrostatic weighing system with existing gold purity instruments. In IOP Conference Series: Materials Science and Engineering (Vol. 824, No. 1, p. 012007). IOP Publishing.

LIST OF CONFERENCES:

1. "Optimizing EDXRF Methods for Accurate Gold Alloy Purity Assessment" Oral presentation International Nuclear Science Technology and Engineering Conference 2024 (iNuSTEC2024) by 14 -16 October 2024, at Danau Golf Club UKM, Bandar Baru Bangi, Selangor, Malaysia
2. "Improvement of The Accuracy of Gold Purity Measurements: Energy Dispersive X-Ray Fluorescent (EDXRF) Spectrometry Approach" Oral presentation in Virtual Colloquium Series 2020–2021: Physics And Materials Science International Symposium 2021 (PhyMaS 2.0) by 27 January 2021, (Best Presenter Award)
3. "Enhancing the Accuracy of Non-destructive Gold Purity Measurements Using EDXRF Method" Oral Presentation in SIRIM Scholastic 2023 by 08-10 August 2023, Kuala Selangor.